STUDY OF CEMENT BASED COMPOSITES MANUFACTURED BY EXTRUSION, COMPRESSION MOLDING AND FILAMENT WINDING

by

Garrett James Haupt

A Thesis Presented in Partial Fulfillment
of the Requirements for the Degree
Master of Science

ARIZONA STATE UNIVERSITY

May 1997

STUDY OF CEMENT BASED COMPOSITES MANUFACTURED BY

EXTRUSION, COMPRESSION MOLDING AND FILAMENT WINDING

by

Garrett James Haupt

has been approved

May 1997

APPROVED:

_____, Chair

_____

_____

Supervisory Committee

ACCEPTED:

_____

Department Chair

_____

Dean, Graduate College

ABSTRACT

Various techniques for manufacturing fiber reinforced cement composites and analysis of mechanical properties are the basis for this study. Extrusion, compression molding and pultrusion processes were used to manufacture test specimen. Discontinuous and continuous fiber composites were tested for tensile, flexural, compressive and shear properties.

A filament winding system was used for the manufacture of continuous-fiber reinforced cement based composites. Improvements made to the existing system made it possible to achieve higher fiber volume composites and a greater variety of composite lay-ups. Alkali-Resistant (AR) Glass fibers were used for the continuous fiber composites which were tested using a closed-loop servo hydraulic system. Tests for tension, compression and shear were performed on the specimen. Tensile strengths of 50 MPa and ultimate strain capacities in excess of 1% were achieved. Using this system made it possible to attain compressive and shear strengths of 15 MPa and 10 MPa, respectively.

An extrusion and a compression molding were used for the study of the discontinuous fiber composites. Various fiber volumes using polypropylene, alumina and steel fibers were tested. The R-Curve approach was used for the analysis of these composites to describe the crack propagation and crack instability under loading conditions.

The experimental observations are compared to prior work in this area and show that this type of composite material has practical structural applications. These composites can be manufactured to serve any structural design problem by simply varying the lay-up orientation and fiber volume.

ACKNOWLEDGMENTS

I would like to first thank my advisor and committee chair Dr. Barzin Mobasher. Through his extensive knowledge and moral support, he has made it possible for me to achieve my goal of earning a Masters of Science Degree. I would also like to thank my committee members, Dr. Apostolos Fafitis and Dr. Subramaniam Rajan. Thanks go out to Henry Anderson, Peter Goguen and John Lang for their assistance. I would like to thank the entire Engineering Lab Service staff for their expertise and knowledge. Special thanks to the entire staff of the Civil Engineering office, especially Debbie Trimmels for keeping track of my progress even better than I was. Financial support of the National Science Foundation grant # MSM921 is greatly appreciated as well.

I would like to recognize those who got me to this point. To Mr. Johnson, my high school math teacher, who first developed my interest for math. To Dr. Wang and Dr. Buttry, my structures professors at the University of Wisconsin at Platteville, for developing my interest in structures. Thanks to all my past teachers and professors.

A very special thanks goes out to my family. Through their support and guidance I have been able to achieve my goals and meet all challenges that face me. They have always been available for me and have always kept me focused. Thank you!

TABLE OF CONTENTS

LIST OF TABLES

LIST OF FIGURES

Figures

Page

CHAPTER 1

Introduction

1.1 Overview

Concrete is the most widely used material in the construction industry today. Concrete's wide use is due to its desirable properties of compressive strength, stiffness, resistance to various environmental conditions and its forming properties.

However, concrete does have some undesirable properties that limit its structural applications. Concrete has a low tensile capacity and limited toughness making it quite brittle. The limited toughness and tensile capacity of concrete may be influenced by the existence of aggregates. The role of the aggregate is to redirect the discontinuous microcracks that form under a state of tensile stress and allow the material to dissipate a nominal amount of energy. But once the microcracks bridge the gap and connect they form a continuous crack along which the concrete will fail.

Through the use of fibers in cement based products a significant increase in ductility and tensile strength can be gained. Fibers are able to bridge the microcracks in the matrix material. This provides the concrete with significantly increased ductility and tensile strength making it appropriate for a wider variety of structural applications.

1.2 Statement of problem

This study will concentrate on fiber reinforced cement based composites. Research aspects are based on composite specimen preparation and mechanical property evaluation. A single cement paste will be used to maintain a control matrix and allow a

basis for comparison. Discontinuous polypropylene, steel and alumina fibers will be utilized for the extrusion and compression molding test specimen and these will be tested in flexure. Continuous Alkali Resistant glass fibers will be utilized for the pultrusion test specimen and these will be tested in tension, compression and shear.

A closed loop servo hydraulic system will be used to perform the tests. Three-point flexural tests will incorporate a single Linear Variable Differential Transformer (LVDT) for center point deflection measurement and a Crack Opening Displacement (COD) gage for Crack Mouth Opening Displacement (CMOD). The COD gage will be used as a feedback signal to control the test. Tension tests will use two LVDTs mounted on opposing surfaces of the specimen. For this test the LVDTs will be used as the feedback signal to control the test. Shear tests will use two LVDTs mounted on one surface of the specimen in a crossing pattern. These tests will be controlled by the stroke LVDT of the hydraulic ram.

1.3 Organization

Chapter 2 presents the techniques used to manufacture fiber reinforced cement based composites. The emphasis is placed on the techniques used to incorporate discontinuous and continuous fibers into the cement matrix. Discussion of three types of samples, namely extrusion, pultrusion and compression molding, will be discussed in detail. The calculation of the volume fraction and specimen preparation will also be discussed.

Chapter 3 presents the test procedures for the bending, tension, shear and compression tests. A description of the test setup and procedure are fully covered.

Chapter 4 presents the experimental results from testing and observations regarding mechanical properties.

Chapter 5 presents some conclusions and recommendations for further study into this area.

CHAPTER 2

Manufacture and specimen preparation of cement based fiber reinforced composites

2.1 Fiber properties

There are many different fibers on the market today and choosing an appropriate fiber type must be achieved with the final properties in mind. Factors to consider when choosing a fiber are the application and the cost. Since the use of the fibers is for tensile reinforcement, a high ultimate tensile strength is a primary concern. Also important are the modulus of elasticity (E), ultimate strain and the bond strength. These factors can determine the overall strength of the composite. Fibers with relatively high modulus of elasticity and good bond strength will present a more efficient means of transferring the stress from the concrete to the fiber. High ultimate strains will increase the composites ductility, especially in the post peak loading region (Bentur 1990).

Continuous alkali-resistant (AR) glass fibers were used in the manufacture of composites using the filament winding technique. A spool of fibers contains 30 fiber bundles per roving, with each fiber bundle containing 204 single fiber strands. The fibers have a Young's modulus of 70 GPa with a single fiber tensile strength of 3600 MPa and a strain at failure of 2%. The fiber strand tensile strength is 1450-1900 MPa. Microsilica (silica fume) is added to the cement matrix to reduce the effects of alkaline attack on the fibers. The silica fume is used as a pozzalon to combine with the $Ca(OH)_2$ and other alkali's reducing the chance for alkali attack (Dvorak 1986).

Discontinuous alumina, polypropylene (PP) and steel fibers were used in the composites made from the extrusion and compression molding. The high purity Kaolin based alumina-silicate fibers have a Young's modulus of 105 GPa with a tensile strength of 1725 MPa. The average length of the alumina fibers is 0.762 mm and the diameter is 2.5 μm. The polypropylene fibers have a Young's modulus of 8.5-12.5 GPa with a tensile strength of 340-500 MPa. The length of the PP fibers is 12.0 mm and the diameter is 35-250 μm (Li 1995).

The behavior of a structure is dependent on the characteristics of the fibers present in it. The aspect ratio, which is the ratio of the fiber length to its diameter, is an important parameter to consider. For the continuous fibers the aspect ratio approaches infinity and can therefore be disregarded. Aspect ratios are most important in the discontinuous fiber composites. The critical embedment length (l_c) is another important factor. It is necessary for the fiber length to be great enough to transfer all of the stress into the fiber. If the fibers are shorter than the transfer length (l_t) the fiber will not carry the maximum fiber stress and will reduce the stress capacity of the overall structure. If the fiber length is greater than the transfer length, the structure approaches that of continuous fiber composites (Agarwal 1990).

The spacing of fibers throughout the composite can influence the overall composite performance as well. Fiber spacing is dependent on fiber dimensions, amount of fiber impregnation and the fiber volume used. Fibers closely spaced increase first crack strength and provide a more uniform crack distribution (Mobasher 1990).

2.2 Manufacture process

Different techniques were used to introduce fibers to the control mortar matrix. These include extrusion, pultrusion and compression molded. To keep consistent results a control mortar mix was utilized. The control mortar is composed of Type I/II cement and silica fume with a weight proportion of 1:0.15. A water-to-cementious solids ratio of 0.4 was used for the extrusion and compression samples and a ratio of 0.35 was used for the pultrusion samples. The higher water/cement ratio for extrusion and compression samples was chosen to provide better workability through the forming dies. Depending on the batch size, approximately 25 ml of superplasticizer per 10,000 grams of portland cement was added to the mix to maintain as low of a w/c ratio as possible. The advantage of a low w/c ratio is a reduction in capillary voids produced by having excess water. This reduction in void space increases density and therefore increases strength (Mehta 1995).

The cement, silica fume, water and fibers are weighed out prior to mixing and placed in separate containers. A number of batches were weighed out and kept separate from one another. This pre-mix preparation saved time during the specimen preparation procedure.

2.2.1 Extrusion

Due to the high fiber content of the mixes a conventional drum mixer will not adequately disperse the fibers. This has been studied by Li (Li 1995). A high-energy Omni Mixer that utilizes a center mounted wobble plate was used instead. The wobble plate is mounted inside a deformable rubber tub which contributes to the mixing action.

A shorter mix time and the absence of blades reduces fiber damage that conventional drum mixers will cause (Garlinghouse 1972).

The water, superplasticizer and silica fume were first blended in a conventional food processor to produce a slurry. This breaks down the silica fume to provide better dispersion throughout the mix. The water/silica fume slurry that is produced is placed in the Omni mixer. The portland cement is added and the two are mixed for approximately one minute. This creates a very even cement paste to which the fibers were added and mixed for two minutes. The mix is checked to insure proper dispersion of the fibers. The mix was then transferred to the forming stations.

An extrusion system developed by Li (Li 1995) was utilized for the manufacture of the short fiber reinforced concrete composites. Figure 2.1 presents a schematic of the system used. The system consists of a one horse power inductive motor, a 50:1 gear reduction box, an auger, a plexiglass mold and a vacuum setup. The mix is poured into a hopper which feeds the rotating auger. Pressure is built up through a 20% reduction in volume along the length of the auger. The mix is forced out into a mold. The dimensions of the mold are 1 inch by 3 inches by 13 inches long. A vacuum pump attached to the mold, relieves built up pressure due to compaction of the air within the mold. Once the mold is entirely filled, the feed tube is sealed off and the concrete is allowed to cure overnight. Four specimen can be prepared at one time using this process. Having attained initial set, the specimen are taken out of the mold and placed in a water bath for 28 days.

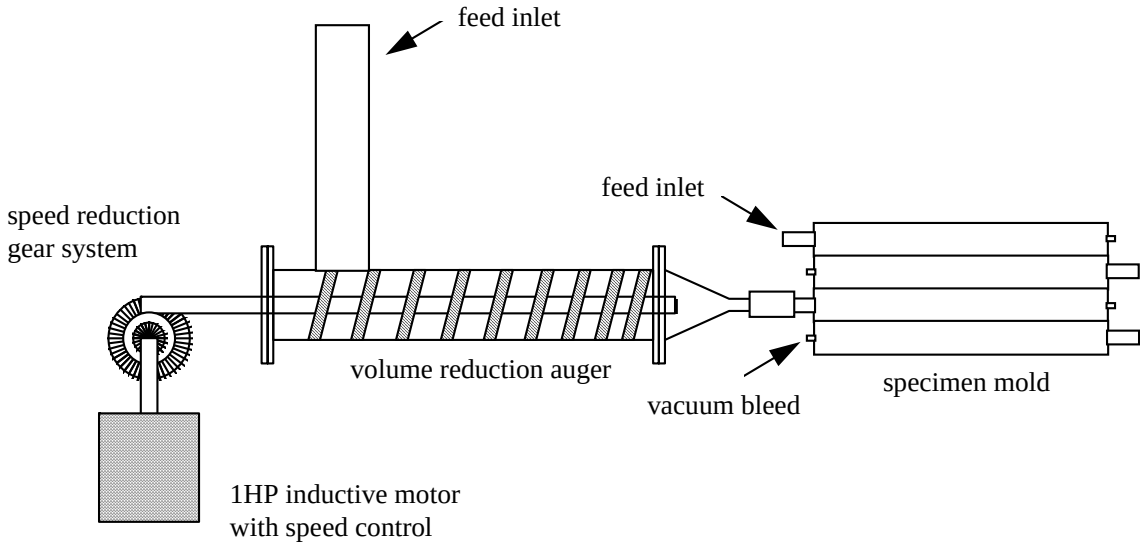

Figure 2.1 Schematic view of extrusion setup.

2.2.2 Compression molding

Concrete's strength can be influence by the water/cement ratio and the porosity. Since much of the water is used for fluidity and workability purposes, the w/c ratio is typically higher than desirable for maximum strength. Reducing the w/c ratio to the minimum poses the problem of not being able to work with the concrete. The concept behind the compression molding is to dewater the mix once it has been placed in the mold (Young 1995). Use of a compression molding to reduce the w/c ratio after the concrete has been placed eliminates the problem of low workability. The system was designed to have a feed hole on one side and bleed holes on the opposite side. Filter paper is placed on top of a #325 sieve mesh and placed between the bottom piece and the sides of the mold. This allows the water to seep out through the sides of the molding when pressure is applied for a continuous manufacturing process. The fiber mixture is forced in through the feed hole and the air escapes out the vacuum holes. This is done with the top in place but not secured tightly yet. It was found that for the manual batch type mixtures used in this study, it was easier to just cap the feed hole and vacuum holes and place the mixture in the mold with a trowel. With the mix in place the top piece is secured down. Figure 2.2 shows the compression molding and Figure 2.3 shows hydraulic pressure of 1000 psi being applied. A release agent is used to ease removal of the specimen.

Compression samples were made from the same mix as the extrusion samples and can therefore be done at the same time saving on sample preparation time. The mix which is described above is placed in the die and filled to approximately one eighth of an inch from the top. The top plate is then carefully placed on and the attachment screws

are hand tightened, initiating the dewatering process. Additional dewatering was done through the use of a hydraulic press. The die and specimen were weighed before and after dewatering in order to determine the new w/c ratio. Like the extrusion samples, these were allowed to cure over night and placed in a water bath for a 28 day cure.

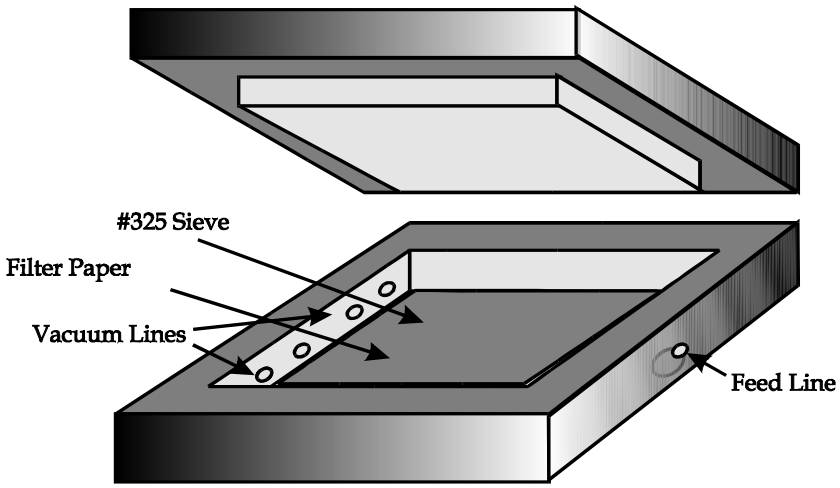

Figure 2.2 Schematic diagram of compression molding.

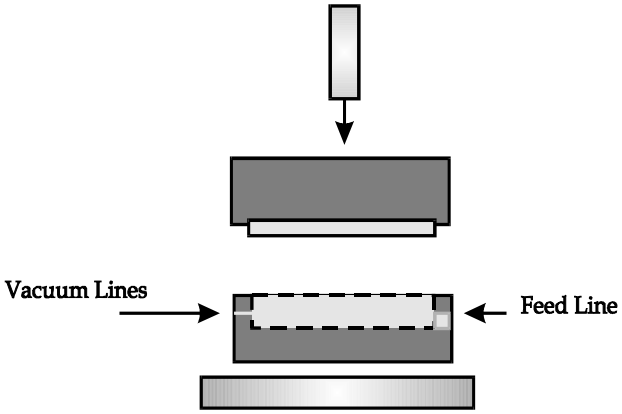

Figure 2.3 Compression molding under hydraulic pressure.

2.2.3 Pultrusion

The manufacture of the pultrusion samples is more involved than that of the extrusion and compression samples; therefore it is broken down into three parts: 1) preparation of the mix, 2) pultrusion setup and 3) calculation of the fiber volume.

2.2.3.1 Preparation of the mix

Like the extrusion and compression mixes, the water, silica fume and superplasticizer are blended in a food processor to make a slurry. A Hobart mixer was used to combine the slurry with the portland cement. Because of the time it takes to manufacture these samples, 4 ml of retarder was added to the mix to increase working time.

2.2.3.2 Pultrusion setup

The system used for the manufacture of the pultrusion samples is discussed in great detail by Pivacek in his study of FRC composites (Pivacek 1997). The process of making pultrusion samples remained quite similar to Pivacek's method with a few improvements to decrease time and labor. See Figure 2.4 for a schematic drawing of the pultrusion setup.

By pulling the fibers from the center of the roving, instead of unwinding them from the exterior, it was possible eliminate the continuous rotation of the fiber spool to release the rovings. Prior to doing this it was necessary to have a motor unwinding the roving just ahead of the fiber take up. The fibers easily pulled out of the center of the roving thereby eliminating the need for unwinding the roving. This reduced the chance

of the fibers getting caught and unexpectedly breaking however, there is a rotation of the roving as a result of this method.

The existing feeder tube required constant hand mixing in order to maintain an even coating of the fiber. With the application of a small vibrating motor to the tube this problem was eliminated and again reduced labor.

The existing method of rotating the plexiglass molding and winding on top of the previous layer becomes quite difficult and cumbersome as the lay-ups get more complicated and thicker. To eliminate this problem, individual layers were made one at a time and were cut from the mold and stacked on top of each other until the desired lay-up was complete. The first layer is placed on top of a square piece of plywood covered with clear plastic wrap. The plastic wrap acts in place of a release agent making removal of the cured sample quite simple.

Once the lay-up was complete, another layer of clear plastic wrap and a second piece of plywood were placed on top. The lay-up, which is sandwiched between the two pieces of plywood, was then placed in a hydraulic press. Pressing the samples ensured a smooth surface, with an even thickness throughout, as well as slightly dewater the sample. The sample is compressed for 2 hours after which time it is placed in a steam cure room for 24 hours. The sample is removed from the plywood and clear plastic wrap and placed in a calcium hydroxide water bath for 28 days.

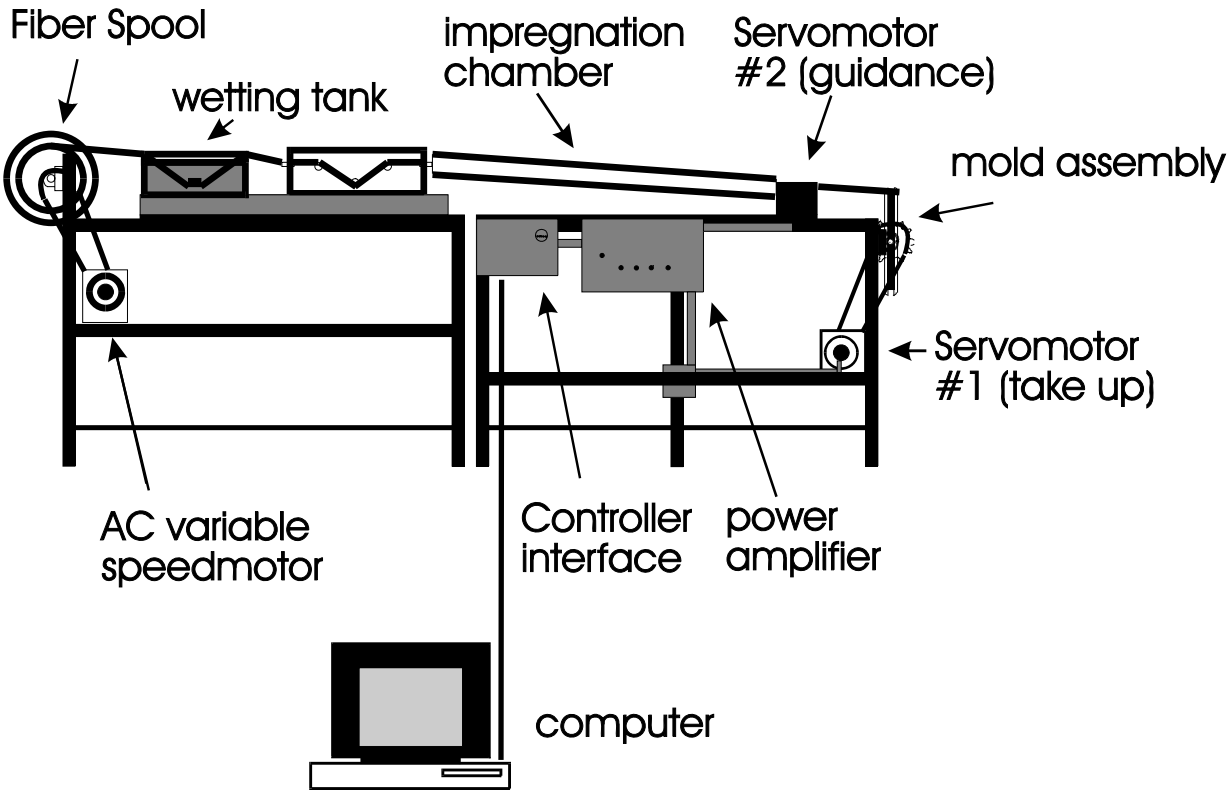

Figure 2.4 Schematic side view of the filament winding setup.

2.2.3.3 Calculation of fiber volume (V_f)

The calculation of the fiber volume of each specimen is calculated according to the following formula

$$V_{fiber} = A_{fiber} / A_{composite}$$

where

$$A_{fiber} = N * \pi * r^2 * \eta_1 * \eta_2$$

with

N = the total number of windings or mold revolutions in constructing the sample (464)

r = the average radius of the single glass fiber (6μm)

η_1 = the number of fiber bundles in the roving (30)

η_2 = the number of single stands in a bundle (204)

and

$$A_{composite} = \int z * dx = [z_i * w_i]$$

where

z_i = the thickness of the specimen taken at various points (1.08 cm)

w_i = the weight given to the point (here all equal to one)

The thickness of the material was averaged over the sample area to arrive at the total area of the composite.

$$A_{fiber} = 464 * \pi * (6\ \mu m)^2 * 30 * 204 = 3.23E\text{-}4\ m^2$$

$$A_{composite} = 1.08\ cm * 46.99\ cm * (m / 100\ cm)^2 = 5.08E\text{-}3\ m^2$$

$$V_{fiber} = 0.063 \approx 6\%$$

2.3 Test specimen preparation

2.3.1 Extrusion/Compression molding

Preparation of the extrusion and compression molding specimen required the same steps. The specimen were removed from the water bath after curing for 28 days and allowed to surface dry. A center mark was placed along one of the long edges of each specimen. A water-cooled diamond blade tile saw was used to make cuts in each sample. Twenty extrusion samples were prepared in this way; ten with a cut of 3/4 inch and ten with a cut of 1 inch. Eight compression molding samples were prepared with a cut of 1/2 inch. All specimen were allowed to dry at least 24 hours prior to testing.

2.3.2 Pultrusion

2.3.2.1 Tension

The sample, measuring approximately 18 inches by 18 inches, was removed from the water bath and allowed to surface dry. The diamond blade saw was used to cut the individual specimen to the test size of 12 inches long by 3 inches wide. Because of the uneven edges left after curing, the sample is first cut along one edge parallel to the fibers. For the samples with fibers at 45^0 angles on the outer surface, a drafters triangle was used to mark off the proper cut line. Once the first edge was cut, a tee-square was used to mark off the other sides at right angles. The sample was then ready to be cut into individual specimen. The thickness was taken at numerous spots and averaged out over the entire specimen.

The tensile specimen were cut into a dogbone shape in order to concentrate the stress and ensure failure over the gage length. A steel template and a marker were used

to trace a line to be cut along. A table mounted router was used to cut the specimen into the dogbone shape as shown in Figure 2.5.

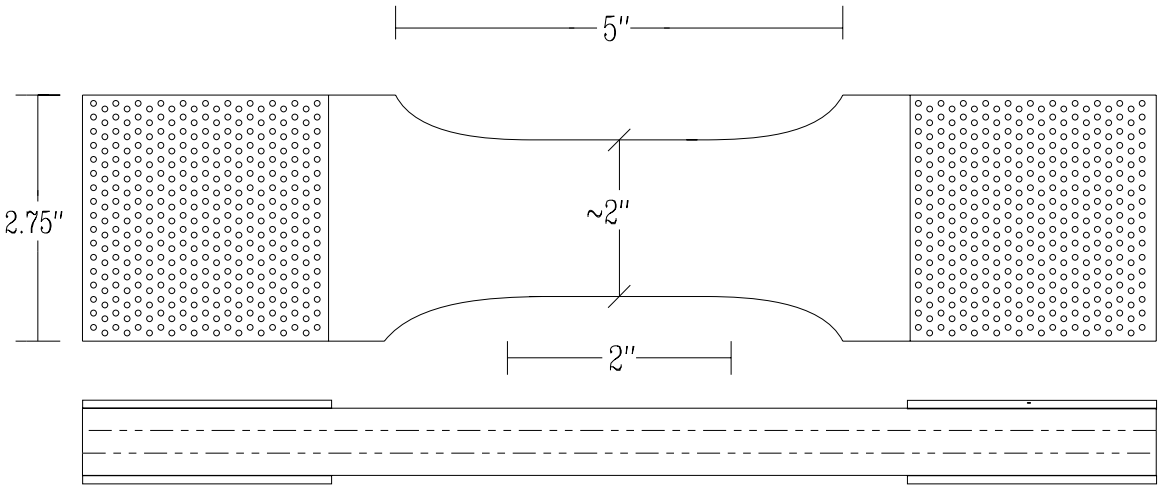

Figure 2.5 Tension specimen cut into a dogbone shape.

Perforated 1/16 inch steel plates were epoxied to both sides of the top and bottom gripping faces of the specimen. The plates provide an even distribution of the gripping force and served as a durable and ductile medium. Two-Ton epoxy was used to secure the steel plates to the specimen. Steel weights were placed on top of the epoxied steel plates to maintain a proper cure with minimal thickness variance. Paper was placed directly between the specimen and the weights to prevent them from attaching to each other. The specimen was allowed to cure overnight with the weights in place.

2.3.2.2 Shear

Like the tension specimen, the sample was removed from the water bath and allowed to surface dry. The diamond blade saw was used to cut the individual specimen

similarly to the tension specimen. The final shear specimen size was 16 inches long by 8 inches wide and again the thickness is dependent on the lay-up.

Pieces of U-channel steel were epoxied along the 16 inch length on top and bottom. The U-channels were cut from a 1 inch by 3 inch piece of 16 gauge tube steel. A high strength epoxy with a bond strength of 2350 psi and a tensile strength of 7200 psi was used. The ends of the U-channel were closed off using duct taped. This created a trough approximately 7/8 inches by 1 3/8 inches by 16 1/2 inches long. The epoxy and hardener were mixed in a 1:1 ratio by volume and placed in the bottom of the trough. The depth of the epoxy depended on the thickness of the specimen and how much volume it would displace. Then the bottom edge of the shear specimen was placed in the trough and carefully aligned and centered. Using cinder blocks to keep the sample upright and in the correct position for full cure, the sample was allowed to cure for 24 hours. The process was repeated for the top edge of the sample as well and the duct tape was removed after the epoxy had cured.

CHAPTER 3

Experimental setup

3.1 Experimental scope

Bending, tension, shear and compression tests were performed in the Graduate Structures Laboratory at Arizona State University. The three-point bending tests were performed on a closed-loop servohydraulic controlled MTS 810 material test system with a load capacity of 100 kN (20 kip). The tension tests were performed on a closed-loop servohydraulic controlled INSTRON model A484-92 test system with a load capacity of 225 kN (50 kip). The shear tests were performed on a closed-loop servohydraulic controlled MTS model 204.71 material test system with a load capacity of 250 kN (55 kip). The compression tests were performed on a closed-loop servohydraulic controlled Structural Behavior Engineering Laboratories, Inc. (SBEL) model CT-110-S test system with a load capacity of 500 kN (110 kip). Test Star software was used to carry out the feedback-controlled closed-loop testing. Two LVDTs were used for the tension and compression tests as the feedback signal. A COD gage was used for the three-point bending test as the feedback signal. The stroke LVDT of the MTS model 204.71 was used as the feedback signal for the shear tests. A 12 bit resolution data acquisition system was used to collect the test data. Video capture equipment and a PULNiX camera were used to take digital pictures of the shear, compression and tension specimen.

3.2 Test procedures

3.2.1 Three-point bending

Extrusion and compression specimen were prepared for testing by first fastening the fixtures for the LVDT, with a range of ±5.08 mm (±0.2 in), and the COD, with a range of ±1.5 mm (±0.06 in). Figure 3.1 shows a schematic view of specimen mounted in the load frame. The specimen, with all fixtures superglued in place, was positioned in the test apparatus with no applied force. The LVDT and COD were adjusted so that each would have its maximum range available for the test. Testware software was used to run the test. See Table 3.1 for testing details. A pre-load was applied to the specimen, under load control, to ensure proper contact at all points. The specimen was loaded using a constant CMOD rate and unloaded using a constant load controlled rate. Through the duration of the test, the data acquisition system recorded the time, actuator stroke, force, CMOD, and deflection.

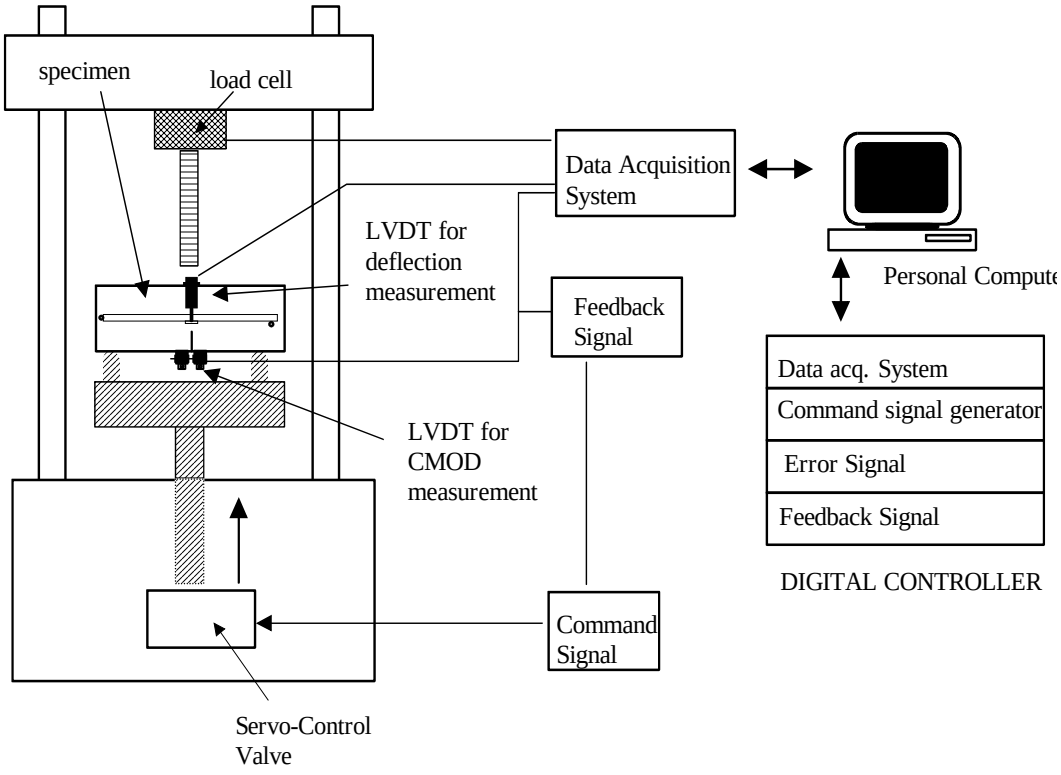

Figure 3.1 Schematic of three-point bend test.

Table 3.1 Testware details.

Fiber type	pre-load (lbf)	loading rate (mm/sec)	# of loops
Steel	10	0.005	19
Polypropylene	10	0.0025	19
Alumina	5	0.0002	15

3.2.2 Tension

Specimen were tested using INSTRON's 500 kN hydraulic grips with serrated jaw-faces. The specimen were placed in the hydraulic grips and a force of 1000 psi was used to hold them in place. Figure 3.2 shows the dogboned specimen in the grips as well as a schematic view of the testing apparatus. As discussed by Pivacek (1997), the specimen were tested with fixed end conditions due to the hydraulic grips.

Two LVDTs, with a range of ±1.27 mm (±0.05 in), were secured on either face of the specimen. A gage length of 60 mm was used to monitor specimen elongation. The signal from the LVDTs was averaged and used as the feedback control for the closed-loop system. A 3/8 inch rod was placed in the LVDT mounts and a 60 mm template was placed between them to ensure proper alignment and spacing of the LVDTs. The mounts were then glued to the specimen using Superglue. The testing procedure was run using a constant strain rate of 0.0005 mm/sec. The data acquisition system recorded the stroke, force and LVDT displacement.

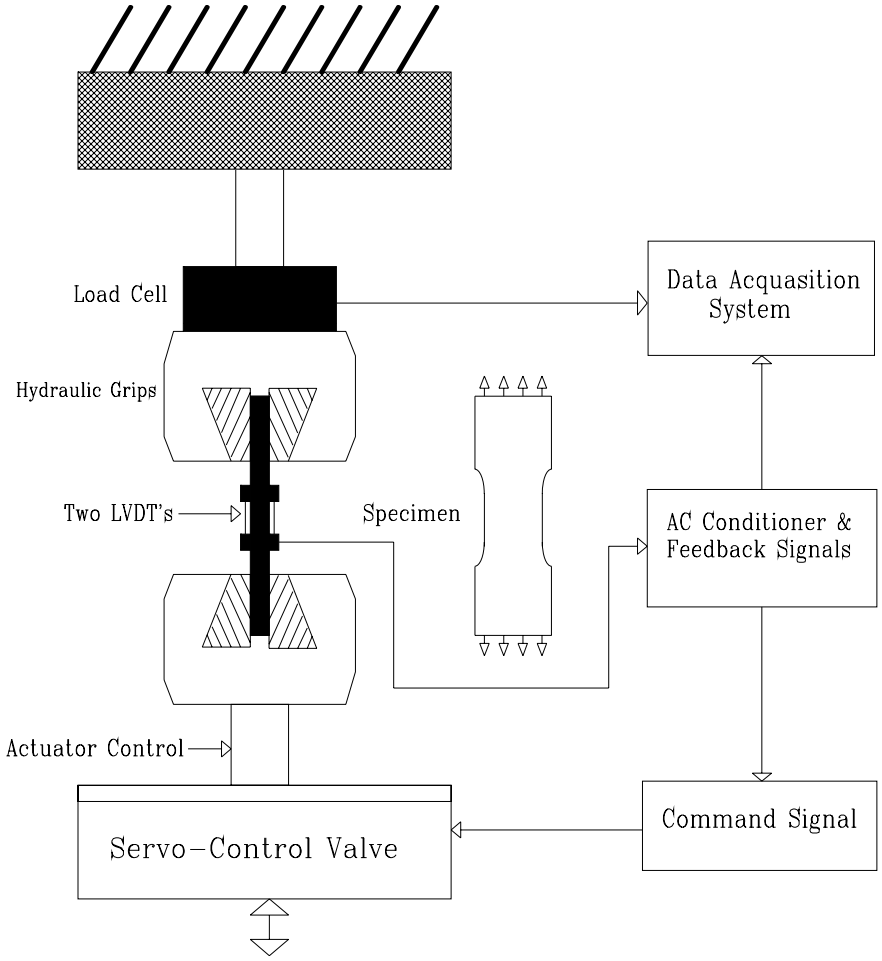

Figure 3.2 Dogbone tension specimen in hydraulic grips.

3.2.3 Shear

A load frame as shown in Figure 3.3 for shear testing was developed. Two LVDTs, with a range of ±5.08 mm (±0.2 in), measure the specimen deformation across the two diagonals. The stroke displacement, applied force and specimen displacement are recorded through the data acquisition system.

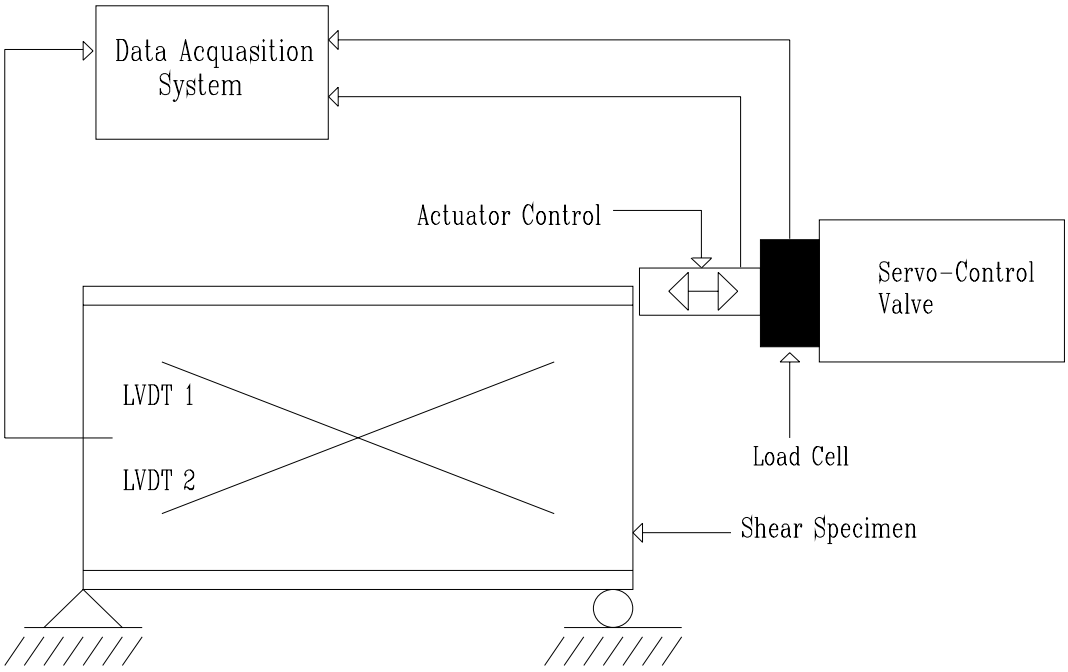

Figure 3.3 Schematic of shear test setup.

Fixtures for the LVDTs were developed for this test. The fixtures allow for rotation of the LVDTs as the sample displaces. This maintains proper alignment and accurate readings. The fixtures are superglued to the specimen at a spacing of 14 inches by 3 inches. The specimen is placed in the loading frame and secured to mounts which are free to slide in the direction of the loading. The slides are not permitted to move in

any direction other than along that of the loading are secured to the floor by 1-1/2 inch bolts. To resist the force applied, an I-beam was mounted to the floor with a pivoting joint attached. The joint is propped against the specimen and because it is free to rotate does not transmit any torsional force. To prevent any overturning moments from crushing the sample instead of shearing them, a top bar was mounted just in front of the applied load. With the specimen securely mounted in the loading frame, the LVDT's were put in place. Each LVDT was set to it's midpoint to allow for possible deflection in either direction. A digital volt meter was used to set the LVDT's to zero. Testware software was used to run the test under actuator stroke control. A constant rate of 0.005 in/sec (0.127 mm/sec) was used for all tests. The data acquisition system recorded the stroke, force and both LVDT's individually.

3.2.4 Compression

Compression tests were performed using a Structural Behavior Engineering Laboratories, Inc. (SBEL) 110 kip (500 kN) capacity test system. The specimen used were prepared the same way as the shear samples. The specimen size was 8 inches by 8 inches. Elastomeric pads were placed under the specimen to provide an even distribution of the applied force to the steel U-channel which in turn provided even distribution of the force throughout the specimen. A ball-and-socket compression head was used to provide free-end loading conditions and remove the possibility for unwanted torsional forces to be introduced. Figure 3.4 shows a schematic view of the compression test setup.

Two LVDTs, with a range of ±1.27 mm (±0.05 in), were used for the compression test. A gage length of 90 mm was used. The test was run at a constant strain rate of

0.0015 mm/sec with the two LVDTs averaged together and used as the feedback control signal. The data acquisition system recorded the stroke, force and LVDT displacement.

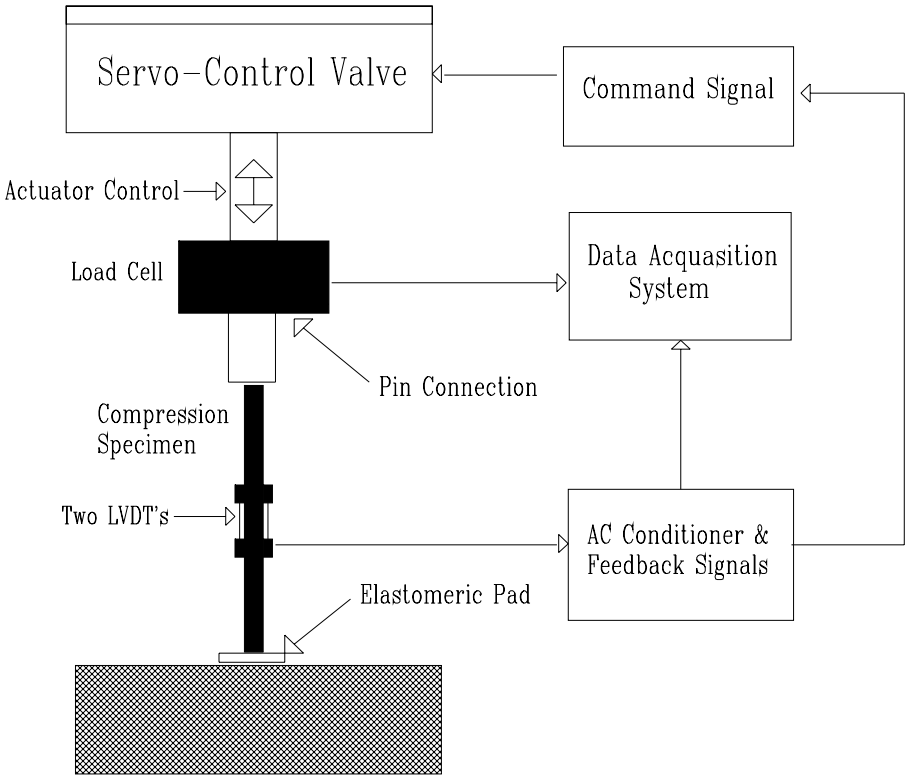

Figure 3.4 Schematic view of compression test setup.

CHAPTER 4

Discussion of experimental results

4.1 Three-point bending

Three-point bending tests were performed on 20 extrusion specimen and 9 compression molding specimen. The specimen type and results from testing are tabulated in Table 4.1. Three types of fibers were investigated.

4.1.1 Load versus CMOD

Test data is first manipulated in View Point where it can be cleaned up and easily plotted. Graphs of the load versus CMOD were generated and the compliance, which is the inverse of the slope in the loading region, were calculated. Figures 4.1-4.4 are the load versus CMOD graphs generated for some of the extrusion specimen. The compliance and the initial crack length were used to calculate the initial modulus of elasticity, E_c'. An effective crack length was calculated using E_c' and the compliance from the next loading cycle.

Table 4.1 Three-point bend test data.

Specimen	Fiber type	W/C	V_f (%)	Notch size (mm)	E (GPa)	Peak load (N)	Peak CMOD (mm)	Peak defl. (mm)
CC2A*	alumina	0.30	2	12.7	15.43	382.5	0.017	0.042
CC2B*	alumina	0.30	2	12.7	12.10	319.3	0.019	0.045
CC2C*	alumina	0.26	2	12.7	18.65	405.8	0.015	N/A
CC2D*	alumina	0.35	2	12.7	16.19	452.5	0.019	N/A
CC2P2B*	alumina/pp	0.23	2/2	12.7	7.35	568.6	0.508	N/A
CC4A*	alumina	0.4	4	12.7	10.86	342.6	0.021	0.051
CC6A*	alumina	0.35	6	12.7	16.39	541.5	0.023	0.087
CP2A*	pp	0.30	2	12.7	11.44	757.9	0.428	0.688
EC2A1	alumina	0.40	2	25.4	7.27	219.1	0.030	0.077
EC2B1	alumina	0.40	2	25.4	12.46	442.6	0.026	0.022
EC2G	alumina	0.40	2	19.05	11.18	345.5	0.016	0.066
EC2H	alumina	0.40	2	19.05	11.84	666.3	0.025	0.061
EC2P2A	alumina/pp	0.40	2/2	19.05	7.31	338.7	0.037	0.115
EC2P2A1	alumina/pp	0.40	2/2	25.4	9.26	317.4	0.037	0.108
EC2P2B	alumina/pp	0.40	2/2	19.05	6.03	286.1	0.043	0.102
EC2P2B1	alumina/pp	0.40	2/2	25.4	8.04	258.1	0.037	0.101
EC4B	alumina	0.40	4	19.05	10.89	566.9	0.020	N/A
EC4C	alumina	0.40	4	19.05	14.30	711.4	0.021	0.131
EP2A1	pp	0.40	2	25.4	5.56	466.5	1.005	1.858
EP2B1	pp	0.40	2	25.4	5.78	253.6	0.846	1.595
EP2C	pp	0.40	2	19.05	4.58	309.1	1.024	1.882
EP2D	pp	0.40	2	19.05	2.60	407.0	0.527	0.982
EPA1	mortar	0.40	N/A	25.4	8.97	311.5	0.022	0.075
EPB1	mortar	0.40	N/A	25.4	9.00	277.8	0.019	0.074
ES5A1	steel	0.40	5	25.4	14.18	1419.2	0.285	0.564
ES5A2	steel	0.40	5	25.4	22.28	2816.2	0.474	1.271
ES5B	steel	0.40	5	19.05	10.78	2387.3	0.605	1.311

* denotes compression molding specimen

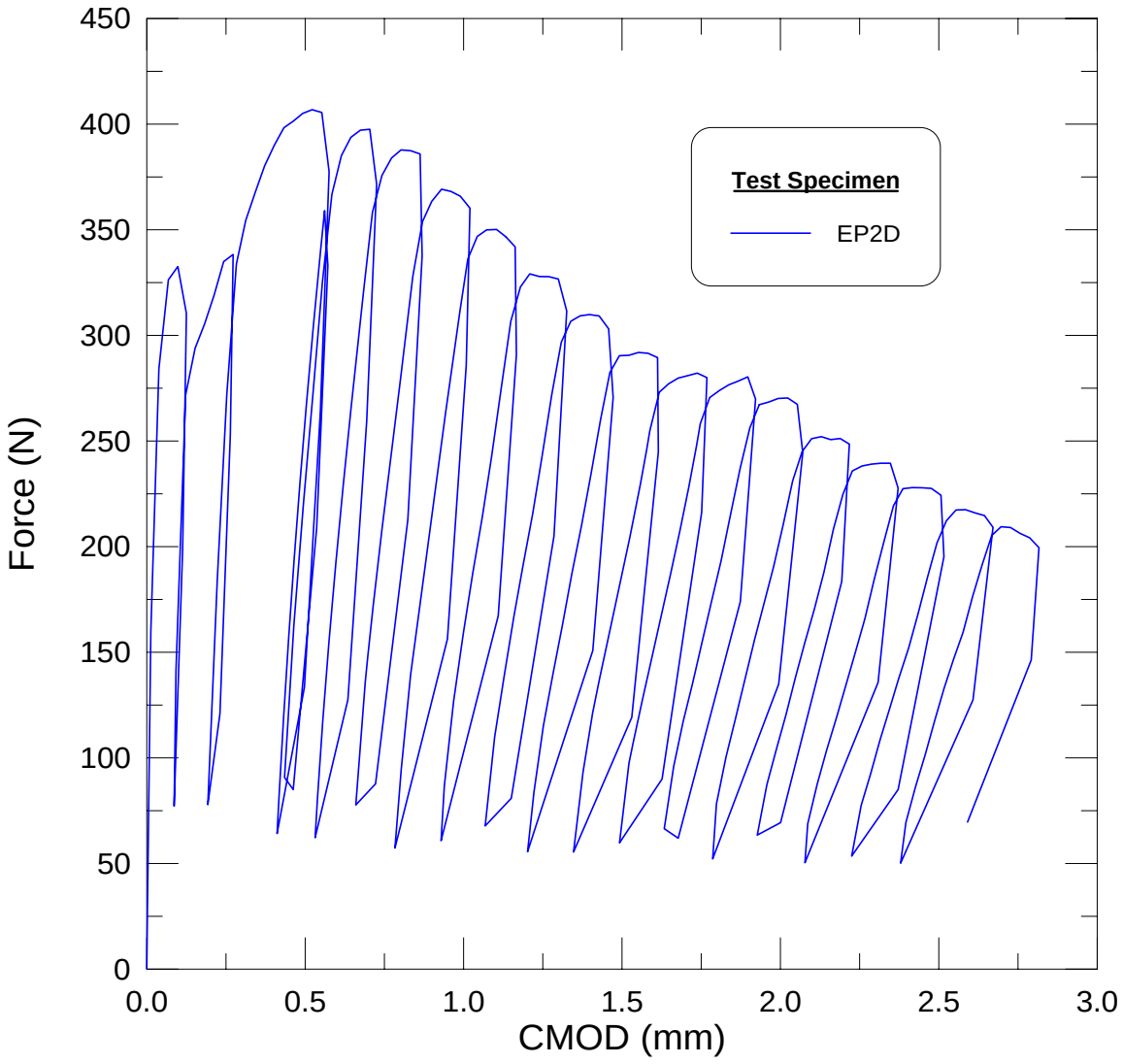

Figure 4.1 Load versus CMOD graph for test specimen EP2D.

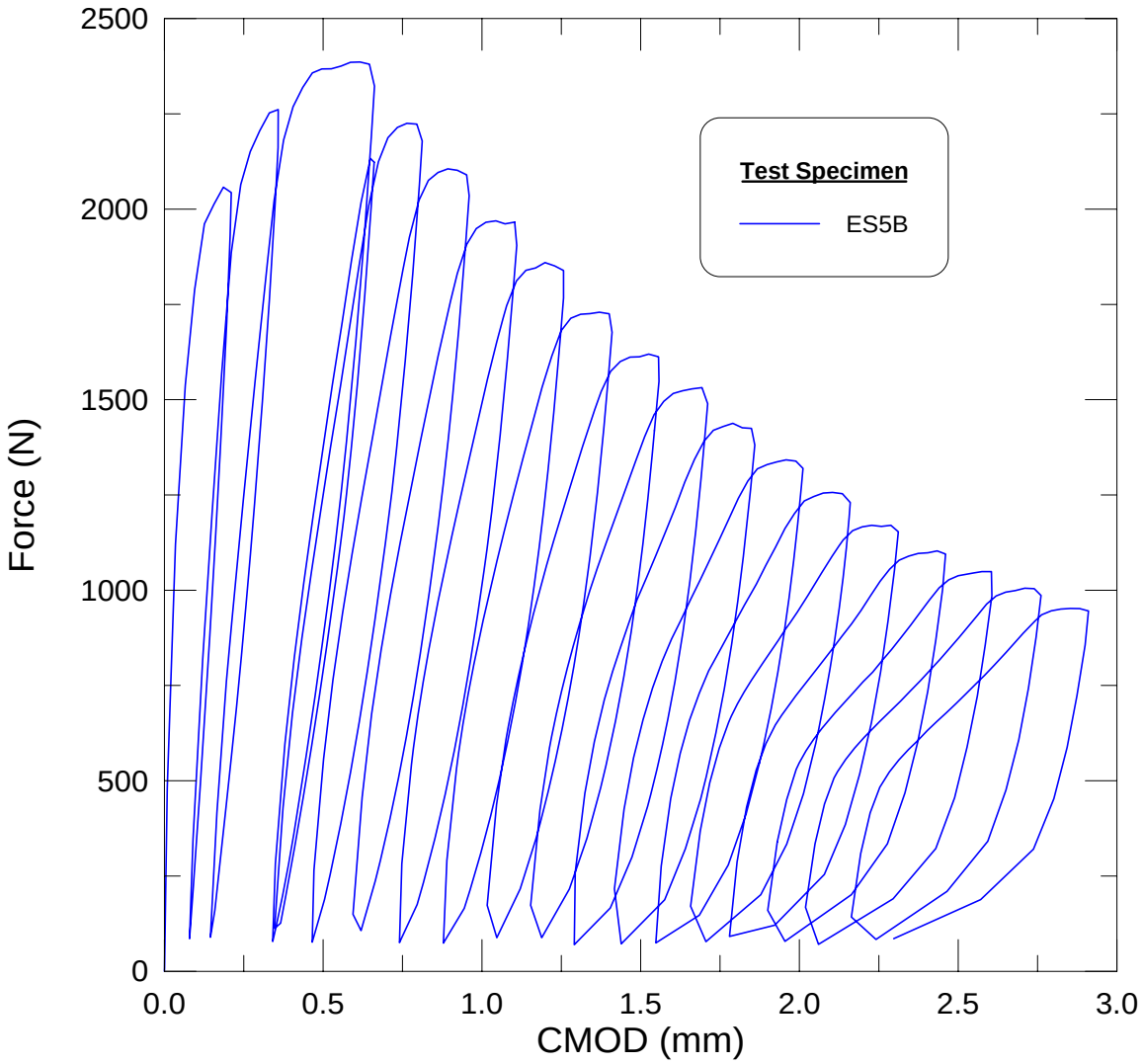

Figure 4.2 Load versus CMOD graph for test specimen ES5B.

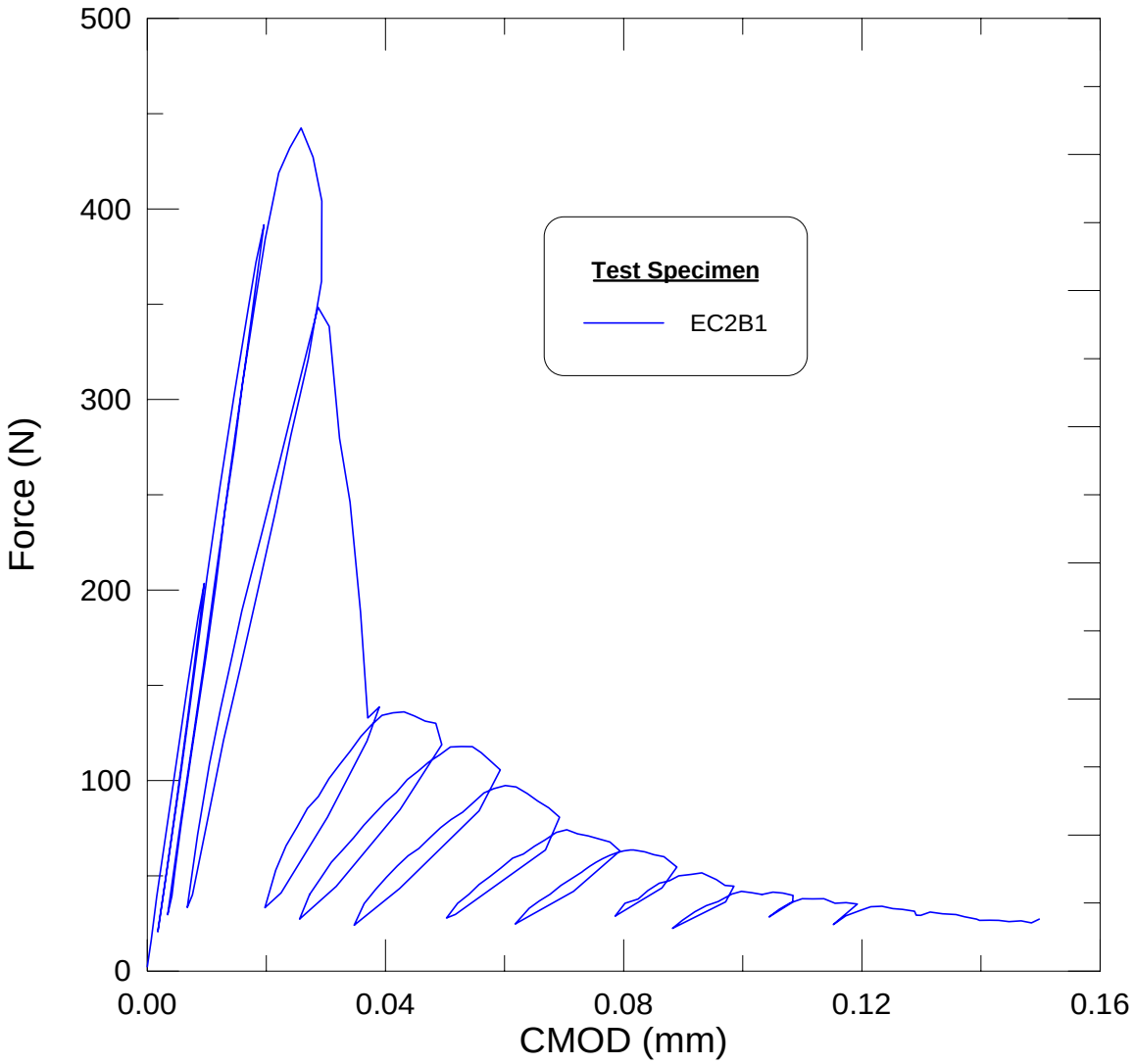

Figure 4.3 Load versus CMOD graph for test specimen EC2B1.

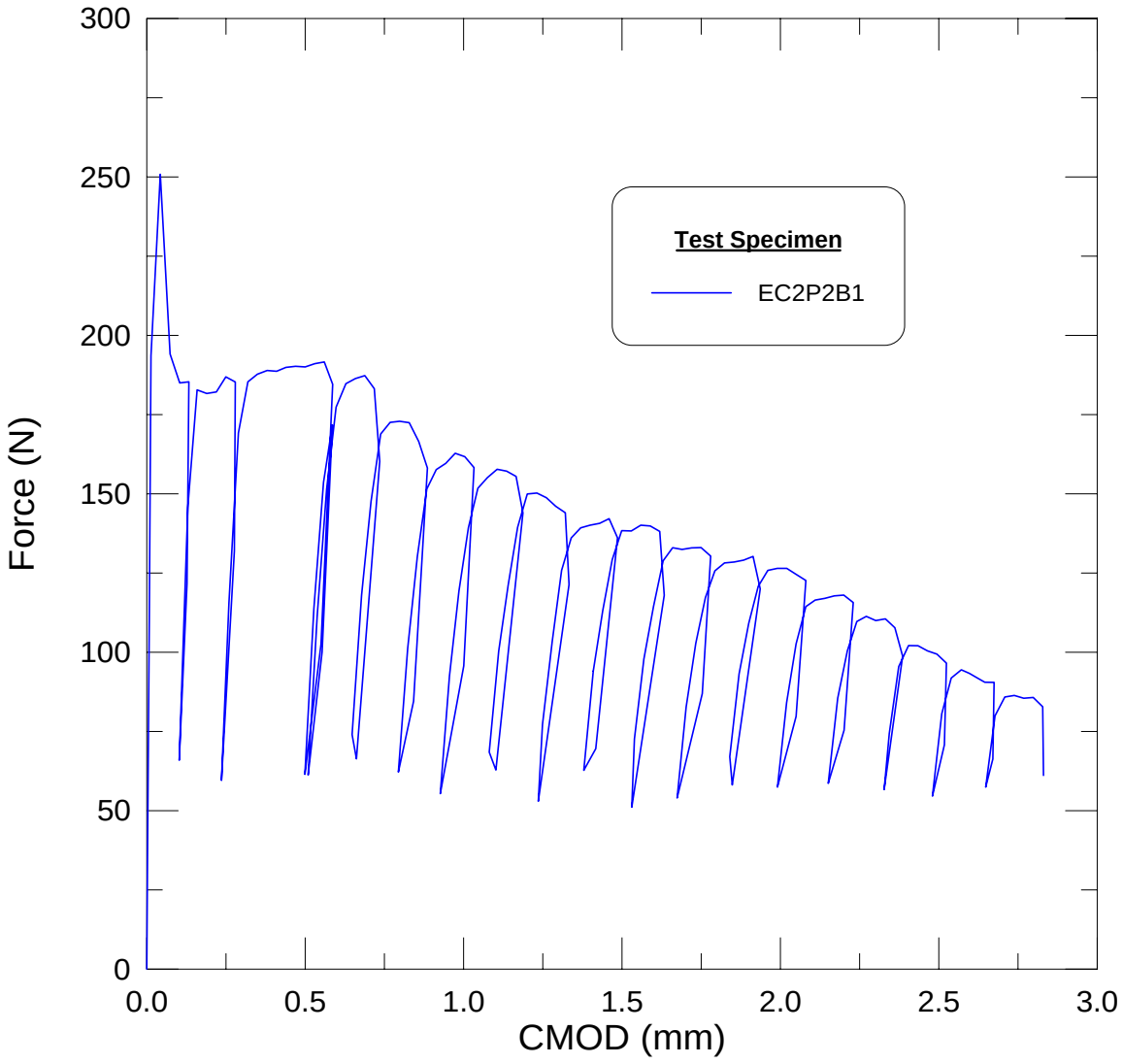

Figure 4.4 Load versus CMOD graph for test specimen EC2P2B1.

4.1.2 R-Curves

Analysis of the three-point bending test results is based on measurement of fracture toughness of the specimen. R-Curves make it possible to study the process of fracture and the brittle-ductile transition in materials with varying composition, size and geometry (Mobasher 1995). The R-Curve is generated by plotting fracture toughness, K_{1C}, as a function of crack extension. R-Curve analysis has been studied in depth by Li (Li 1995) which describes the procedure for computation of the R-Curve based on three-point bending loading-unloading tests.

Figure 4.5 illustrates the increase in toughness and crack extension through the addition of fibers. The plain mortar specimen has a toughness of K_{1C} = 17.1 MPa $mm^{1/2}$ and a crack extension of 1.2 mm; this shown by a single data point. By adding 4% alumina fibers the toughness increases to K_{1C} = 27.8 MPa $mm^{1/2}$ and the crack extension remains close at 1.7 mm. With the addition of 2% polypropylene fibers and 2% alumina fibers the toughness increases to K_{1C} = 50 MPa $mm^{1/2}$ and an increase in crack extension of 40 mm. This illustrates the effect of different fibers. The alumina fibers increase the toughness by bridging the microcracks but once cracking reaches beyond this stage they are unable to resist further crack growth. The polypropylene fibers are able to bridge the microcracks as well as larger cracks and therefore increase the crack extension and specimen ductility.

Figure 4.6 represents a comparison of notch lengths for the 2% polypropylene extrusion specimen. The notch represents an initial crack length in the specimen. R-

Curves are a material property and are independent of geometry and size. This plot illustrates that the R-Curves for these specimen are independent of the initial crack.

Figure 4.7 illustrates the R-Curves for compressed (w/c = 0.23) and non-compressed (w/c = 0.4) specimen containing 2% polypropylene and 2% alumina fibers. As a result of the de-watering process the specimen porosity is decreased which accounts for the increased toughness. The compressed specimen is more notch sensitive and brittle then the non-compressed specimen. A higher energy release rate is required to propagate cracking in the compressed specimen.

Figure 4.8 illustrates the effect of alumina fibers. The addition of 4% alumina fibers slightly increased the toughness and greatly increased the crack extension while the addition of 6% alumina fibers greatly increased both toughness and crack extension.

Figure 4.9 represents the extrusion and compression molding specimen containing 2% alumina fibers. All four extrusion specimen displayed a toughness ranging between 12 - 16 MPa $mm^{1/2}$. However, the specimen with an initial notch length of 25 mm displayed a more stable crack growth. The compression molding specimen displayed a toughness twice that of the extrusion specimen and a crack extension similar to the 25 mm notched extrusion specimen.

Figure 4.10 represents a comparison between specimen containing 2% polypropylene fibers and specimen containing both 2% polypropylene and 2% alumina fibers. The specimen with only the polypropylene fibers exhibited greater toughness of the order 70 - 100 MPa $mm^{1/2}$ while the other specimen were on the order of 40 - 50 MPa $mm^{1/2}$. The specimen containing both fibers exhibited an increased crack extension.

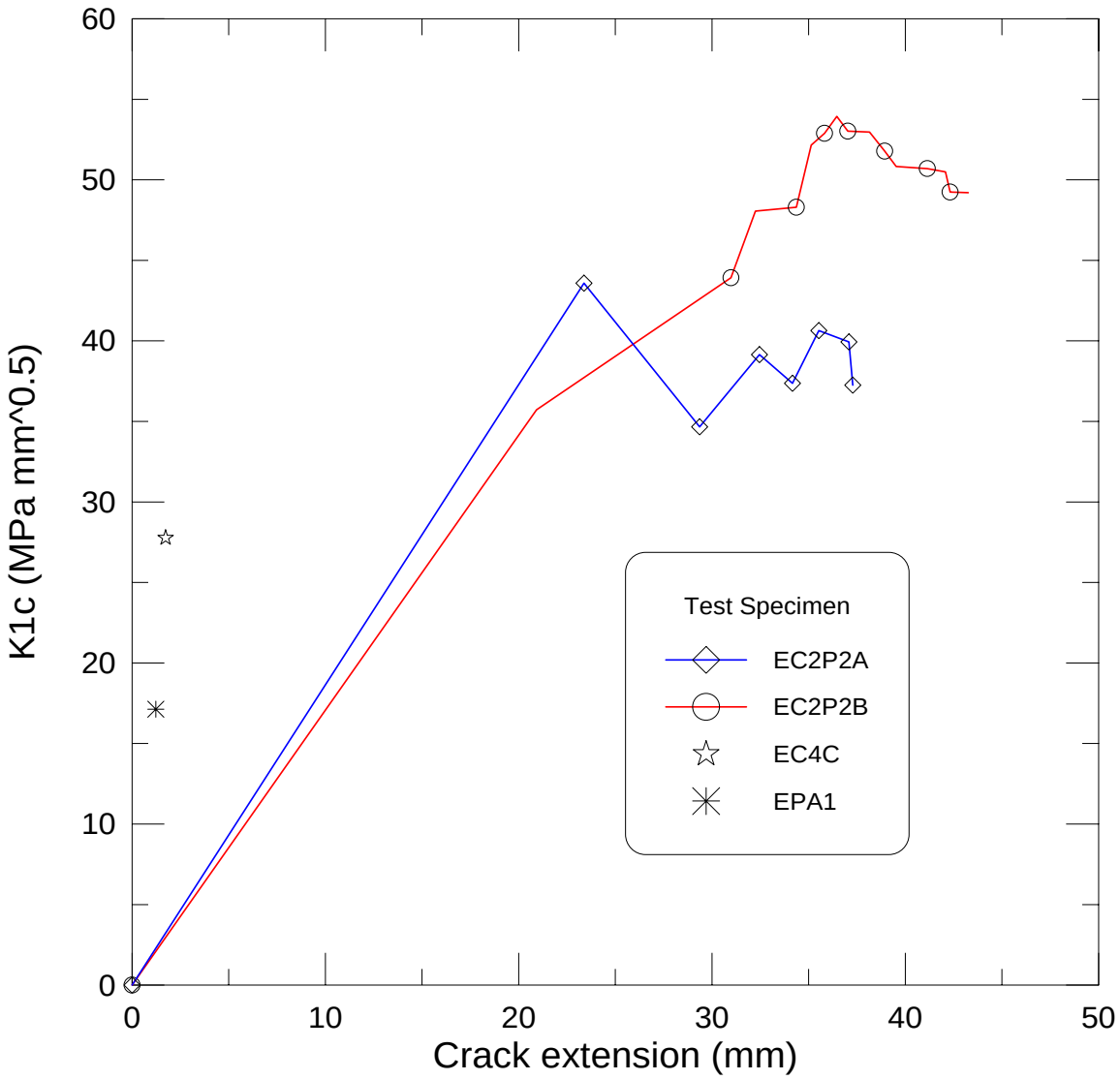

Figure 4.5 R-Curves for 2% alumina and 2% pp, 4% alumina and paste specimen.

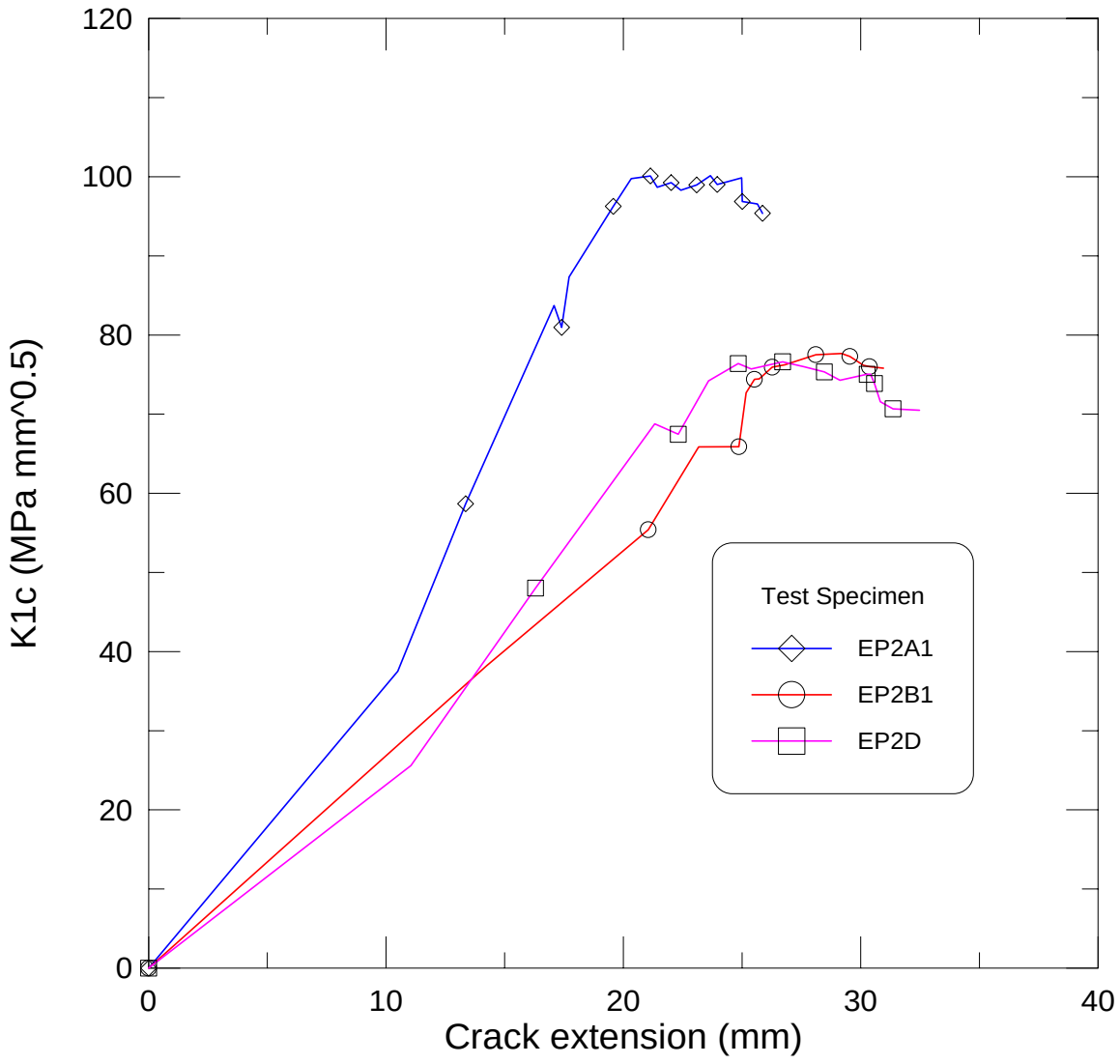

Figure 4.6 R-Curves for 2% pp specimen.

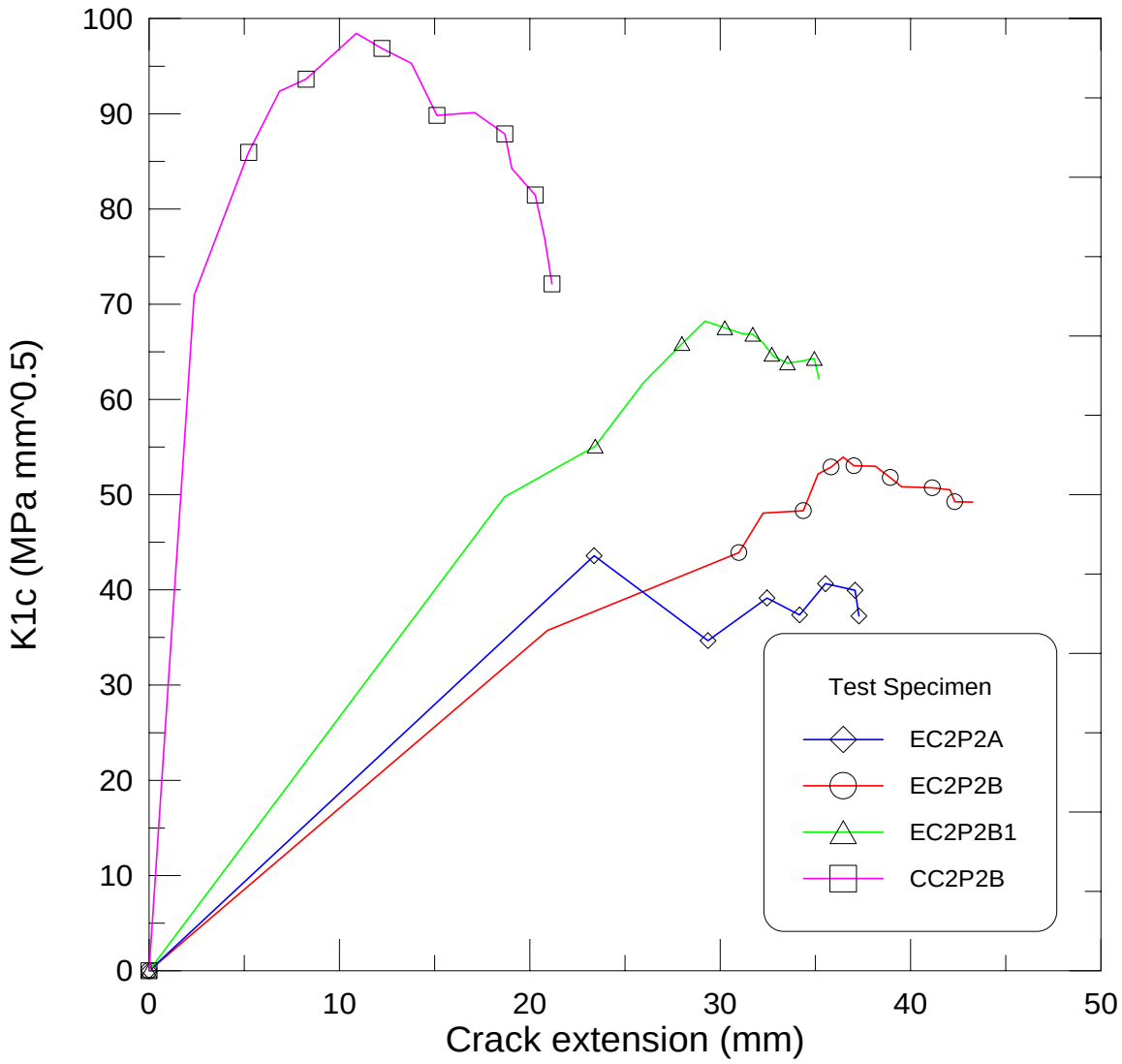

Figure 4.7 R-Curves for 2% alumina and 2% pp specimen.

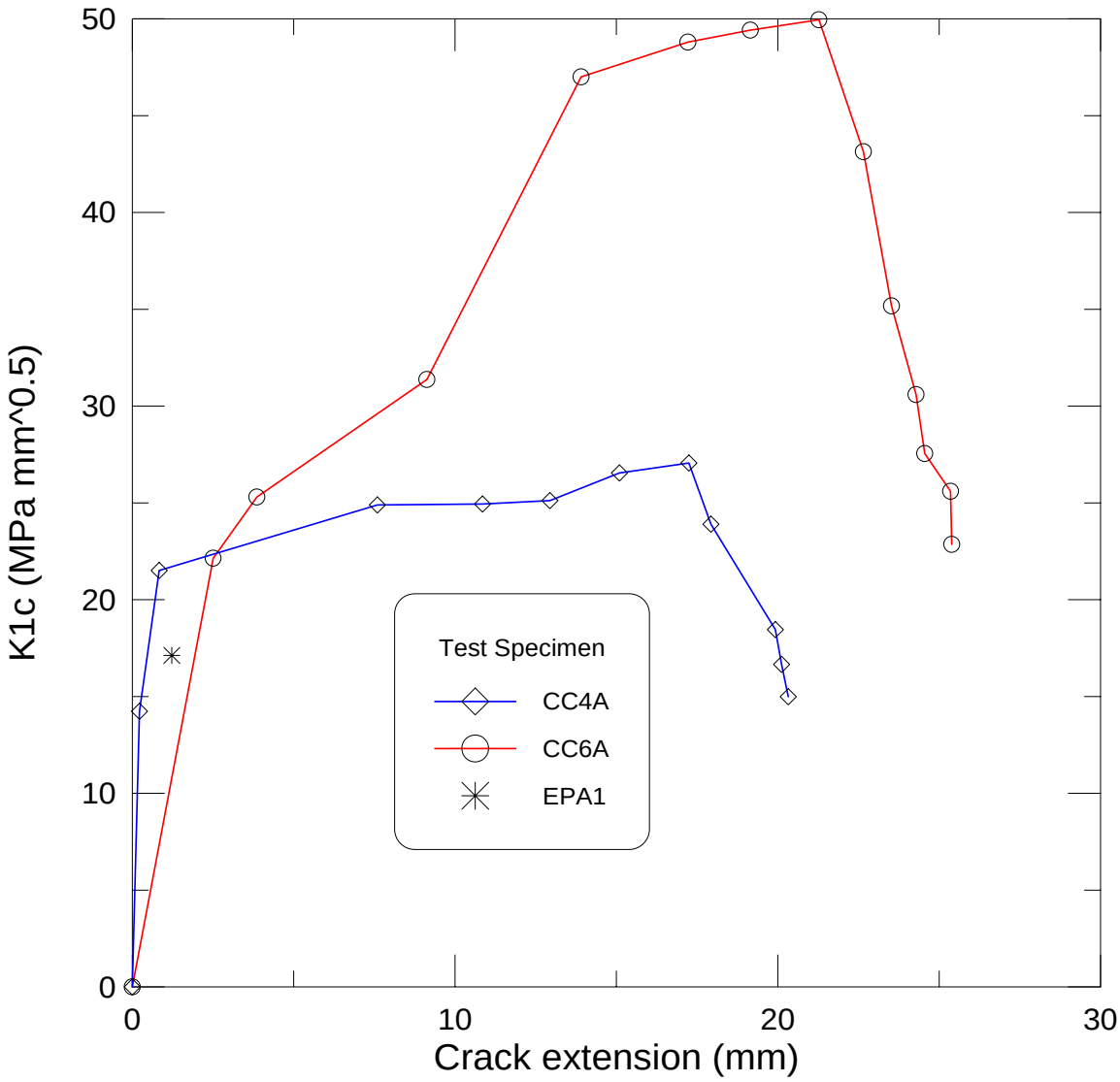

Figure 4.8 R-Curves for 4% and 6% alumina and paste specimen.

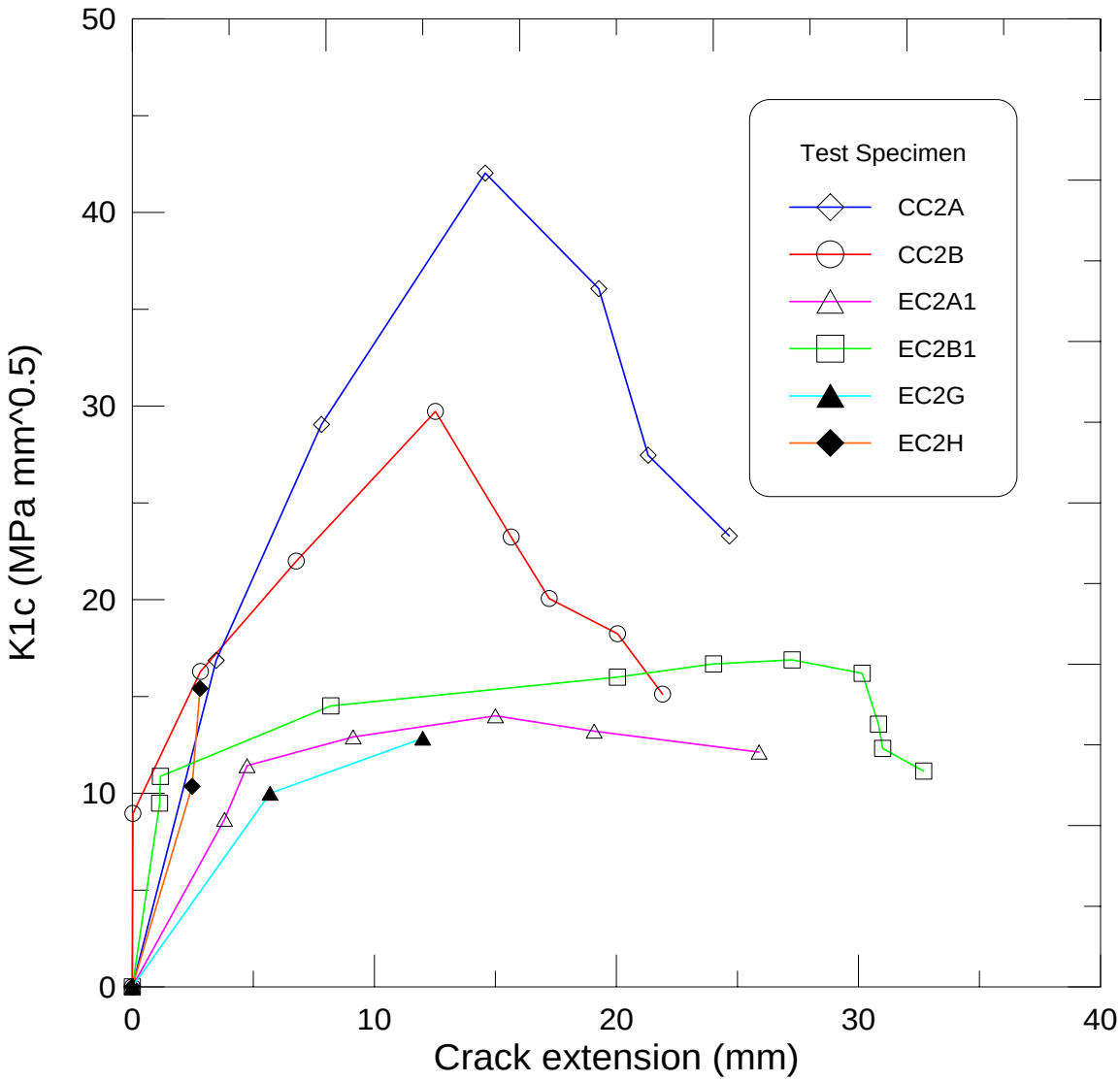

Figure 4.9 R-Curves for 2% alumina specimen.

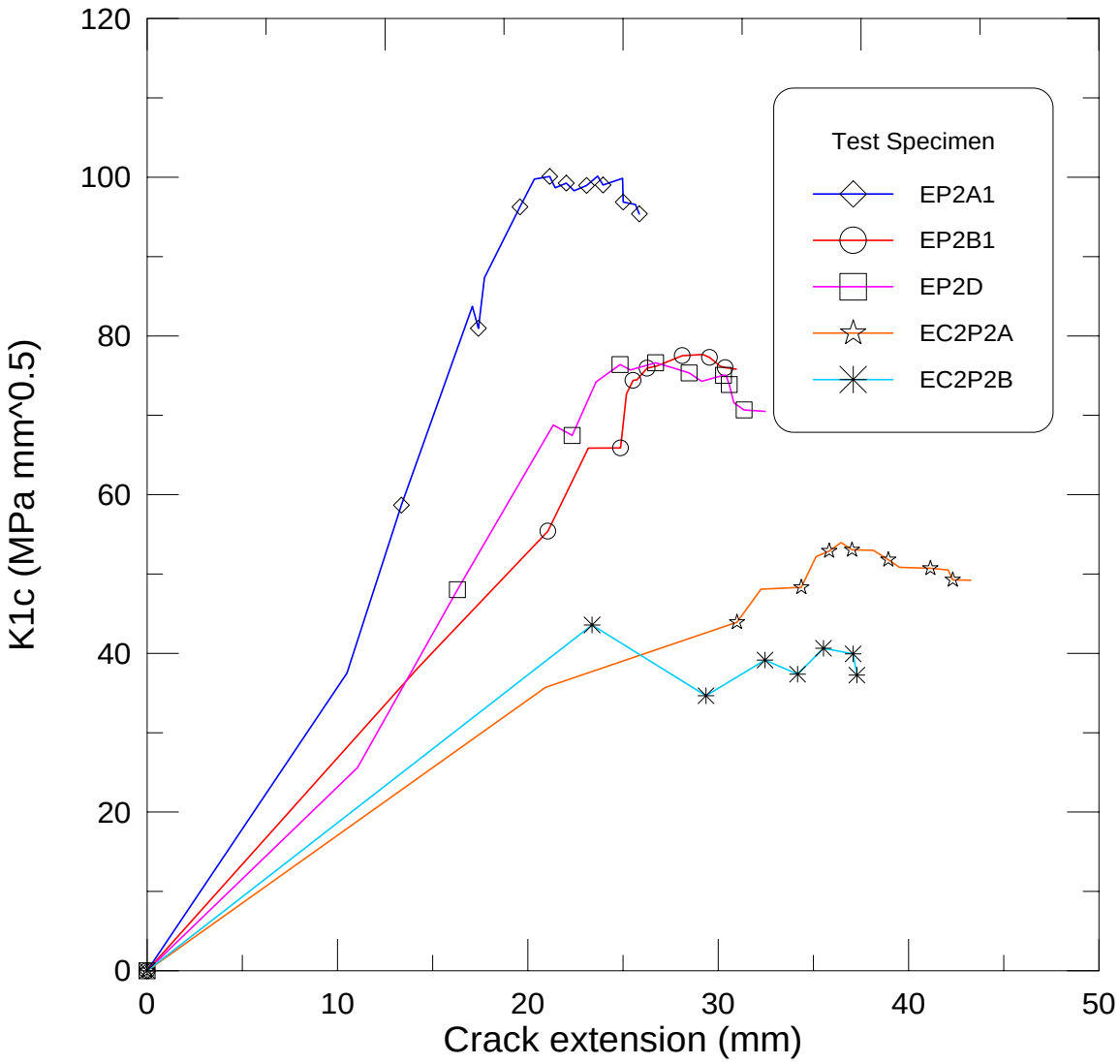

Figure 4.10 R-Curves for 2% pp specimen versus 2% alumina and 2% pp specimen.

4.2 Tension

Uniaxial tension tests were performed on 9 samples and the results are tabulated in Table 4.2. The parameters used in the analysis of the tensile response included the modulus of elasticity (E), bend over point (BOP or proportional limit) stress and strain, and the ultimate stress and strain.

Table 4.2 Tension test results.

Specimen	V_f (%)	$E_{initial}$ (MPa)	$\sigma_{ultimate}$ (MPa)	$\varepsilon_{ultimate}$ (%)	σ_{BOP} (MPa)	ε_{BOP} (%)
$[45/-45]_S$						
D1	9.6	2362	1.48	0.108	1.09	0.043
D2	9.6	507	0.236	1.11	0.046	0.127
D3	9.6	1194	1.42	0.227	1.17	0.118
average		1354	1.045	0.482	0.769	0.096
std. dev.		938	0.702	0.547	0.627	0.046
$[0/45/-45]_S$						
H1	5.6	15755	38.4	1.19	5.54	0.042
H2	5.6	14064	46.8	1.14	4.81	0.034
H3	5.6	12859	47.4	1.71	5.7	0.043
average		14226	44.2	1.35	5.35	0.040
std. dev.		1455	5.03	0.316	0.474	0.0049
$[0/-45/45/90]_S$						
O1	8.8	14154	52.5	1.57	7.94	0.022
O2	8.8	25402	51.45	1.085	15.14	0.094
O3	8.8	11865	47.01	1.008	6.05	0.052
average		17140	50.32	1.22	9.71	0.056
std. dev.		7246	2.91	0.305	4.80	0.036

Figure 4.11 represents the tensile response of the [0/45/-45]s test specimen. The initial portion of the response is quasi-linear and provides an average experimental modulus of elasticity of 14.2 GPa. Beyond 25 MPa the response becomes nonlinear

which suggests cracking. Each of the three specimens demonstrate peak strengths in the range of 35-45 MPa and strains of 1.1-1.7 %.

Figure 4.12 represents the tensile response of the [0/-45/45/90]s test specimen. The initial portion of the response is quasi-linear and consistent with the initial response of the [0/45/-45]s test specimen. The average experimental modulus of elasticity was 17.1 GPa. An average peak strength of 50.3 GPa was found to be greater while an average peak strain of 1.22 % remained nearly the same. A comparison of the two figures shows the addition of the transverse layer increased the post-peak response of the specimen by providing a weak layer to distribute the cracks and increase the strain response.

Figure 4.13 represents the tensile response of the [45/-45]s test specimen. Test data from specimen GPD1 was discarded due to premature caused by test equipment malfunction. The initial response of GPD2 and GPD3 provide an experimental modulus of elasticity of 1.2 GPa and 2.4 GPa. The average ultimate strength of the two specimens was 1.5 MPa, which is on the range of 50 times less than either of the other lay-ups. The average ultimate strain from the two specimen was 0.17 % which is an order of magnitude less than the other lay-ups. The low peak stress and strain can be attributed to the shear failure of the matrix phase and inability of the fibers to bridge the matrix cracks.

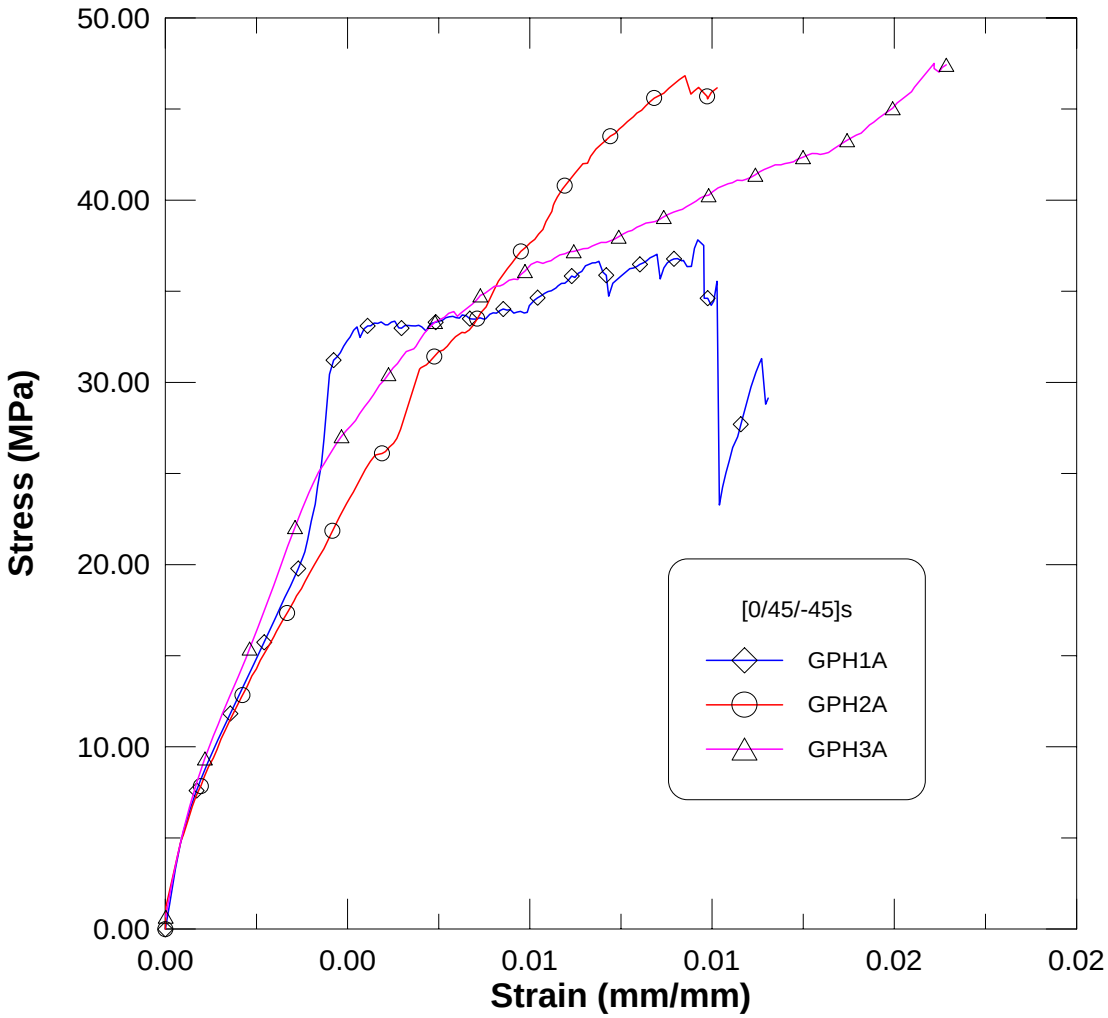

Figure 4.11 Tensile stress-strain response of [0/45/-45]s.

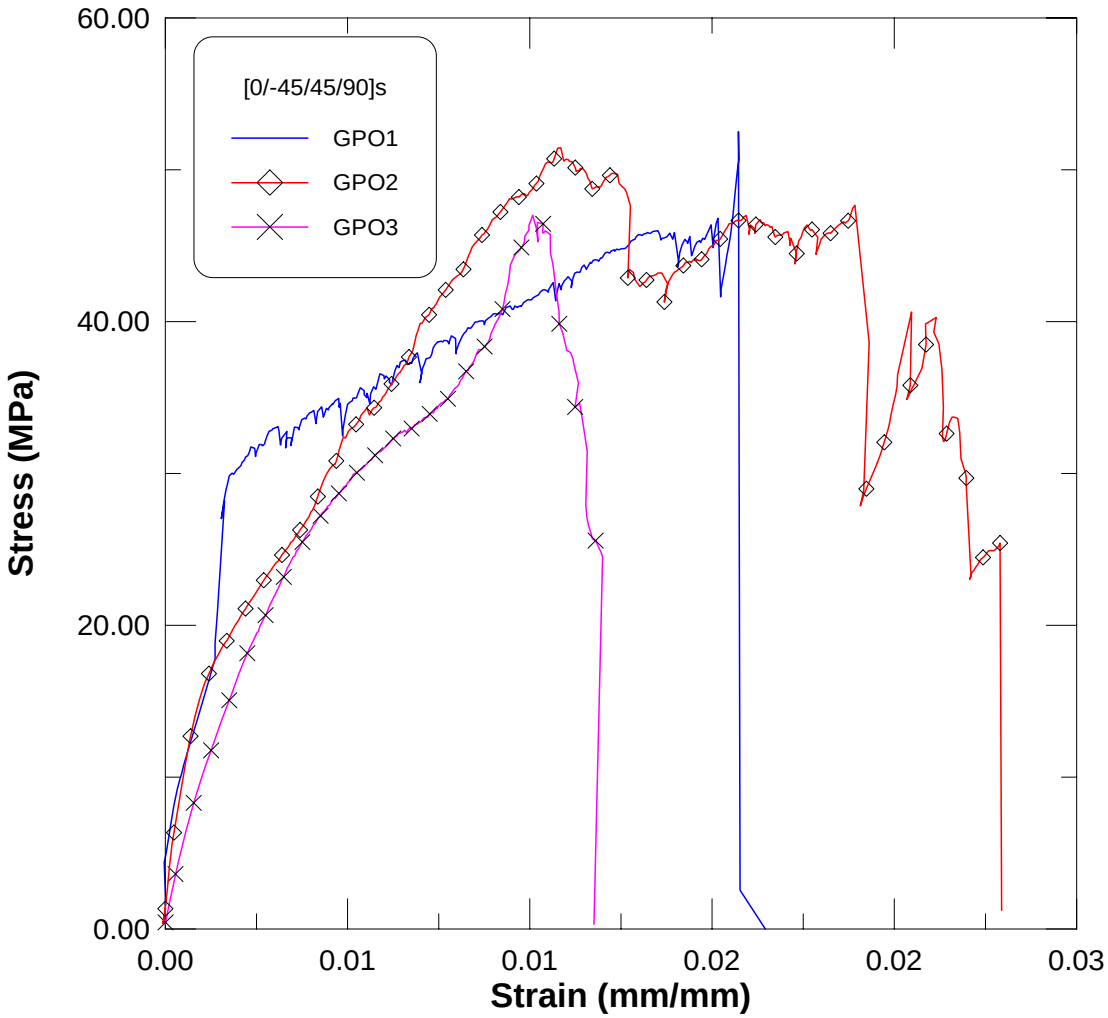

Figure 4.12 Tensile stress-strain response of [0/-45/45/90]s.

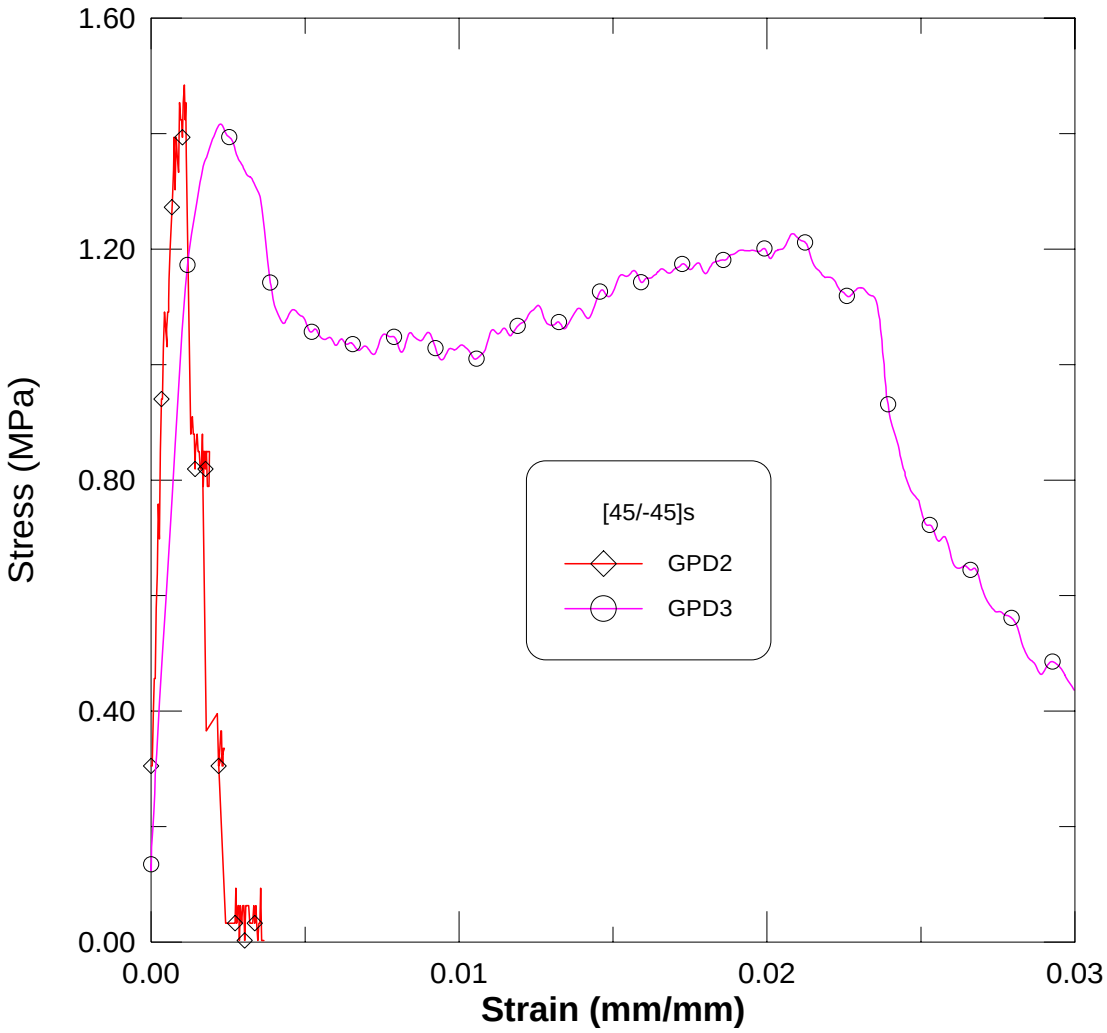

Figure 4.13 Tensile stress-strain response of [45/-45]s.

4.3 Shear

In order to verify the assumptions used in the analysis of the test results, finite element method was employed to check the validity of the proposed methodology. GS-USA was used to do a finite element analysis of a homogenous specimen having dimensions of 1 inch by 8 inches by 16 inches. A unit load of 1000 lbf was applied to the specimen allowing for simple relative comparisons. The specimen used in the FE analysis with the LVDT orientation is shown in Figure 4.14. The shear stress across the longitudinal axis of the specimen was plotted for comparison purposes, see Figure 4.15. Figure 4.16 is a plot of shear stress versus shear strain for various modulus of elasticity's using FEM and one experimental modulus of elasticity.

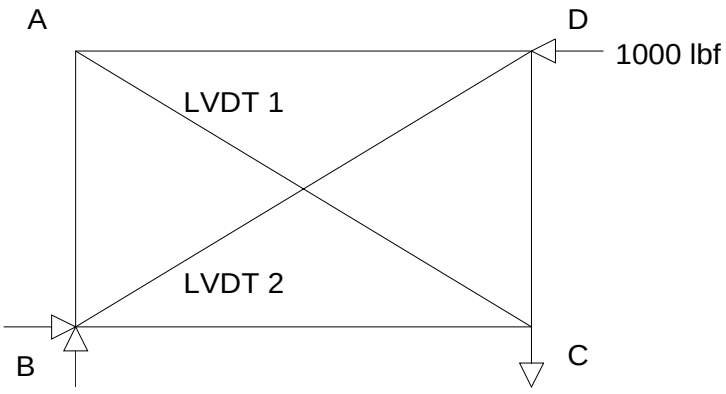

Figure 4.14 Schematic of LVDT layout.

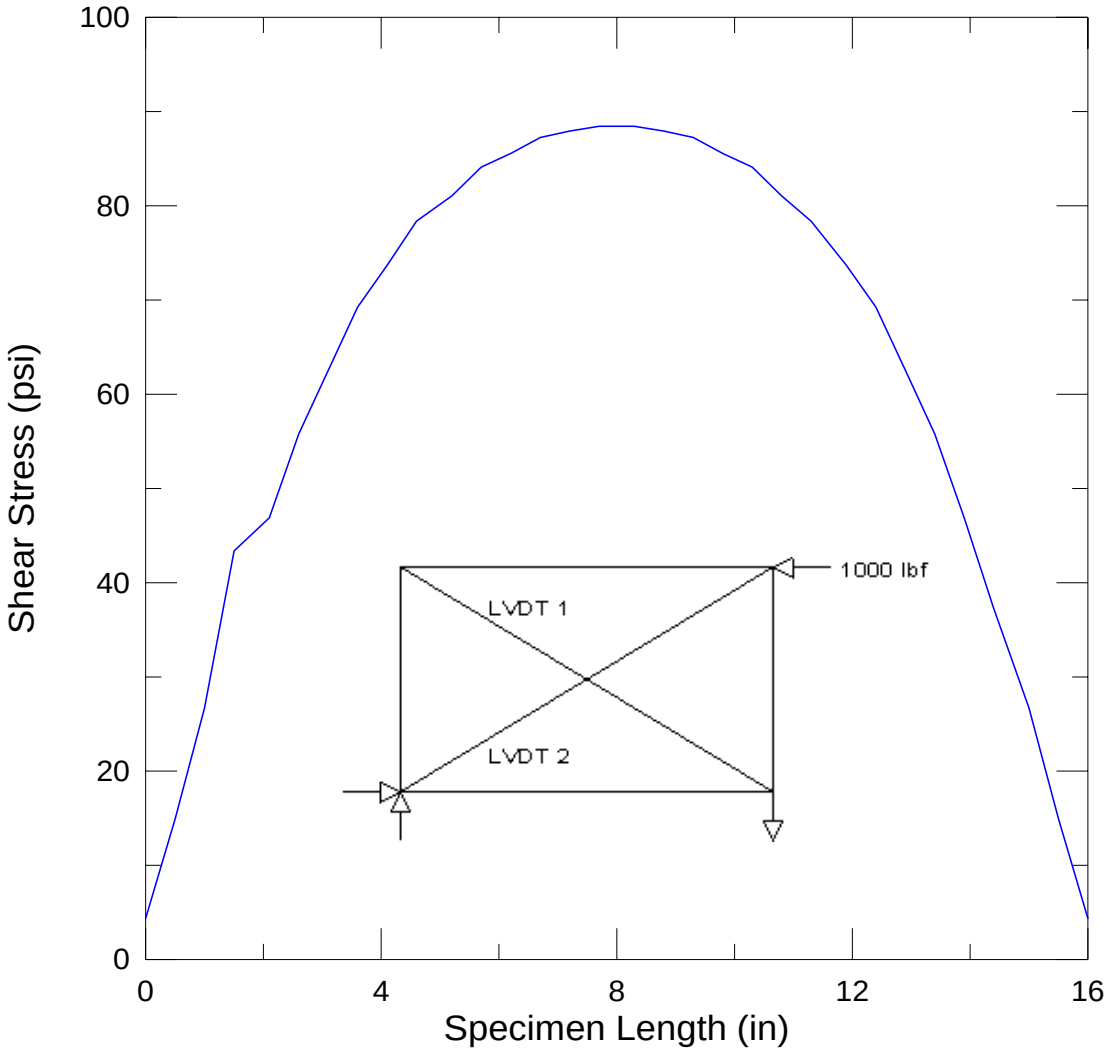

Figure 4.15 Finite Element analysis of shear stress distribution.

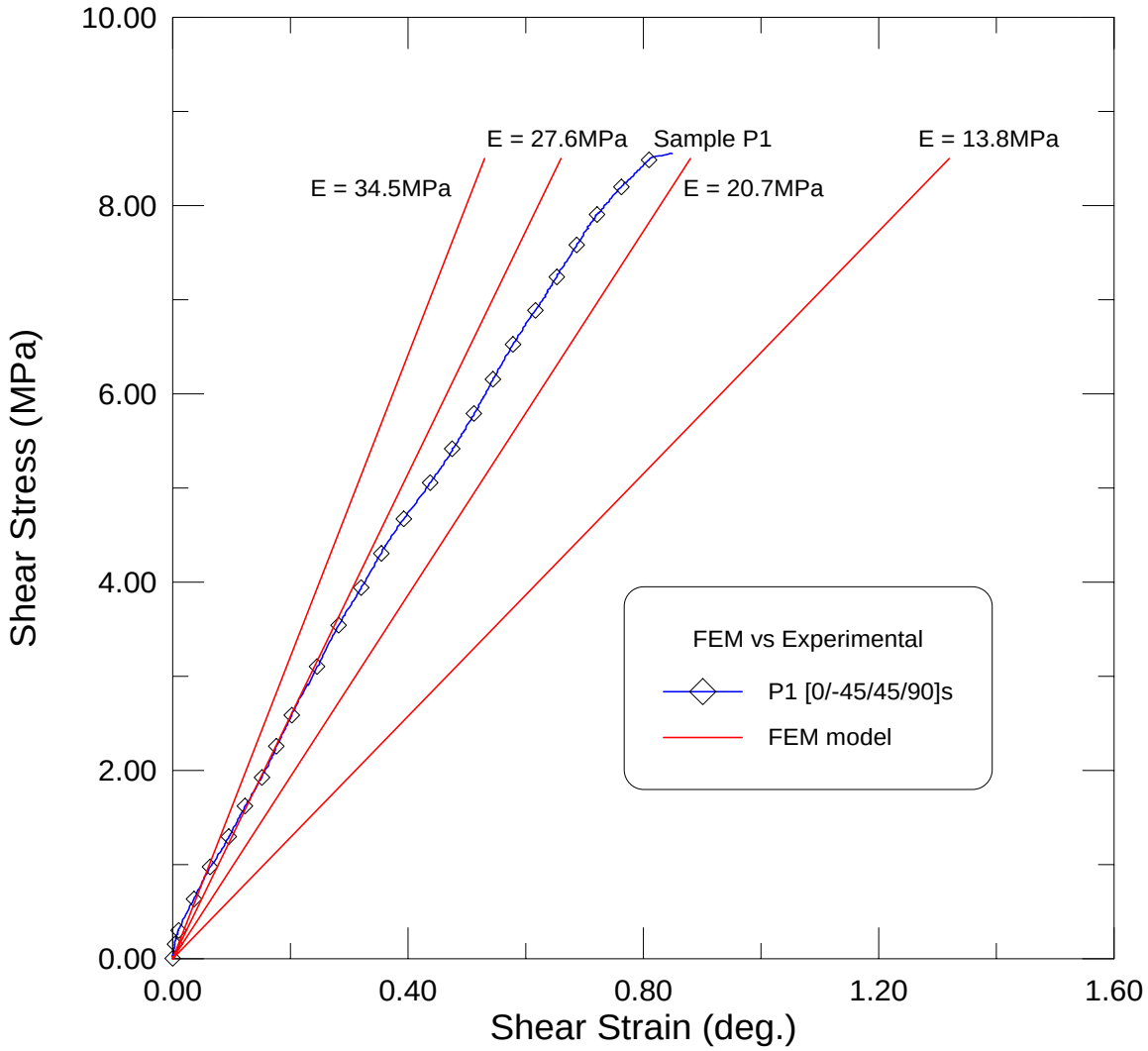

Figure 4.16 FEM modeling of sample P1 for various E's.

Direct shear tests were performed on 12 specimen. The experimental data is tabulated in Table 4.3. The parameters used in the analysis of the tensile response included the shear modulus (G), modulus of elasticity (E), bend over point (BOP or proportional limit) stress and strain, and the ultimate stress and strain. Data is collected as follows: force (lbf), time (sec), actuator stroke (in) and two LVDT displacements (in). The shear modulus is calculated as the slope of the shear stress versus shear strain graph. The modulus of elasticity can then be calculated using the relation $G = E/[2(1+\nu)]$. The modulus of elasticity data tabulated in Table 4.3 are elastically equivalent values and should be used only for comparison purposes. Figure 4.17 and Figure 4.18 are plots of the LVDT displacement versus time and force versus total LVDT displacement, respectively. Each plot displays the LVDT orientation in reference to the applied force and the resisting forces. The data from the two LVDTs are added together and converted to shear strain (γ) to get the entire specimen displacement. The applied force is converted to metric units and normalized to represent the elastically equivalent shear stress (τ). The equations used follow.

$$\tau = (V*Q)/(I*t) = (1.5*V)/A$$

where

V = the applied force

$Q = \int A*y*dA = (d/2)*t*(d/4)$

A = cross-sectional area

y = distance to centroid

I = moment of inertia = (t*d^3)/12

t = specimen thickness

d = specimen length

$$\gamma = 90 - \alpha$$

The derivation for this equation is as follows:

$$\tan(\alpha/2) = a/b$$

where

α = deformed angle (now is less than 90^0)

$a = (d^2 + h^2)^{1/2} + \delta_1$

$b = (d^2 + h^2)^{1/2} + \delta_2$

d = specimen length

h = specimen height

δ_1 = LVDT 1 displacement

δ_2 = LVDT 2 displacement

therefore

$\alpha = 2*\tan^{-1}\{[(d^2 + h^2)^{1/2} + \delta_1] / [(d^2 + h^2)^{1/2} + \delta_2]\}$

Table 4.3 Shear test results.

Specimen	V_f (%)	G (MPa)	E (MPa)	τ_{BOP} (MPa)	γ_{BOP} (deg.)	$\tau_{ultimate}$ (MPa)	$\gamma_{ultimate}$ (deg.)
[0/90]s							
E4	4.4	9.27	21.87	1.03	0.076	4.13	0.456
[0/45/90]s							
G5	6.3	11.98	28.28	2.16	0.100	4.68	0.302
[0/-45/90]s							
C1	6.3	10.28	24.26	3.57	0.206	7.23	0.527
C2	6.3	10.65	25.13	5.33	0.300	6.90	0.460
average		10.47	24.70	4.45	0.253	7.07	0.494
std. dev.		0.26	0.62	1.24	0.066	0.23	0.047
[0/45/-45]s							
I6	5.0	23.42	55.27	5.74	0.340	8.10	0.488
I7	5.0	23.67	55.86	5.43	0.252	10.60	0.636
J1	4.9	20.69	48.83	5.85	0.522	6.85	0.746
J3	4.9	22.48	53.05	4.55	0.430	7.21	0.776
average		22.57	53.25	5.39	0.386	8.19	0.662
std. dev.		1.35	3.19	0.59	0.116	1.69	0.130
[45/-45]s							
L2	4.2	30.24	71.37	2.90	0.146	5.76	0.198
L3	4.2	33.07	78.05	4.10	0.091	5.74	0.387
average		31.66	74.71	3.50	0.118	5.75	0.293
std. dev.		2.00	4.72	0.84	0.039	0.01	0.134
[0/-45/45/90]s							
F1	4.9	26.61	62.80	3.52	0.169	7.06	1.180
F2	4.9	27.77	65.54	3.56	0.237	9.07	1.000
P1	7.3	7.70	18.17	4.48	0.371	8.54	0.843
P2	7.3	23.37	55.20	3.56	0.164	9.66	0.967
average		21.37	50.43	3.78	0.235	8.58	0.998
std. dev.		9.30	21.94	0.47	0.096	1.11	0.139

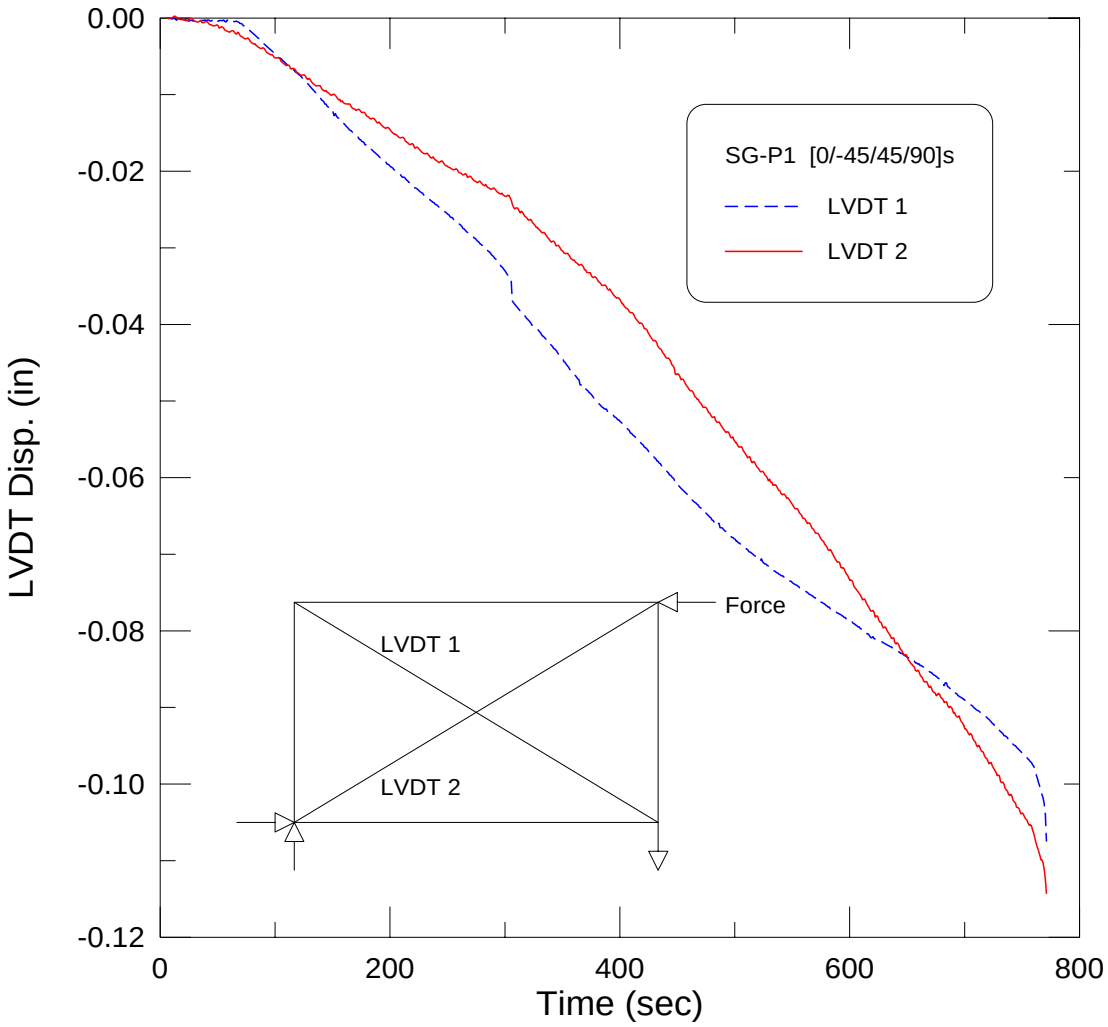

Figure 4.17 LVDT displacement versus time.

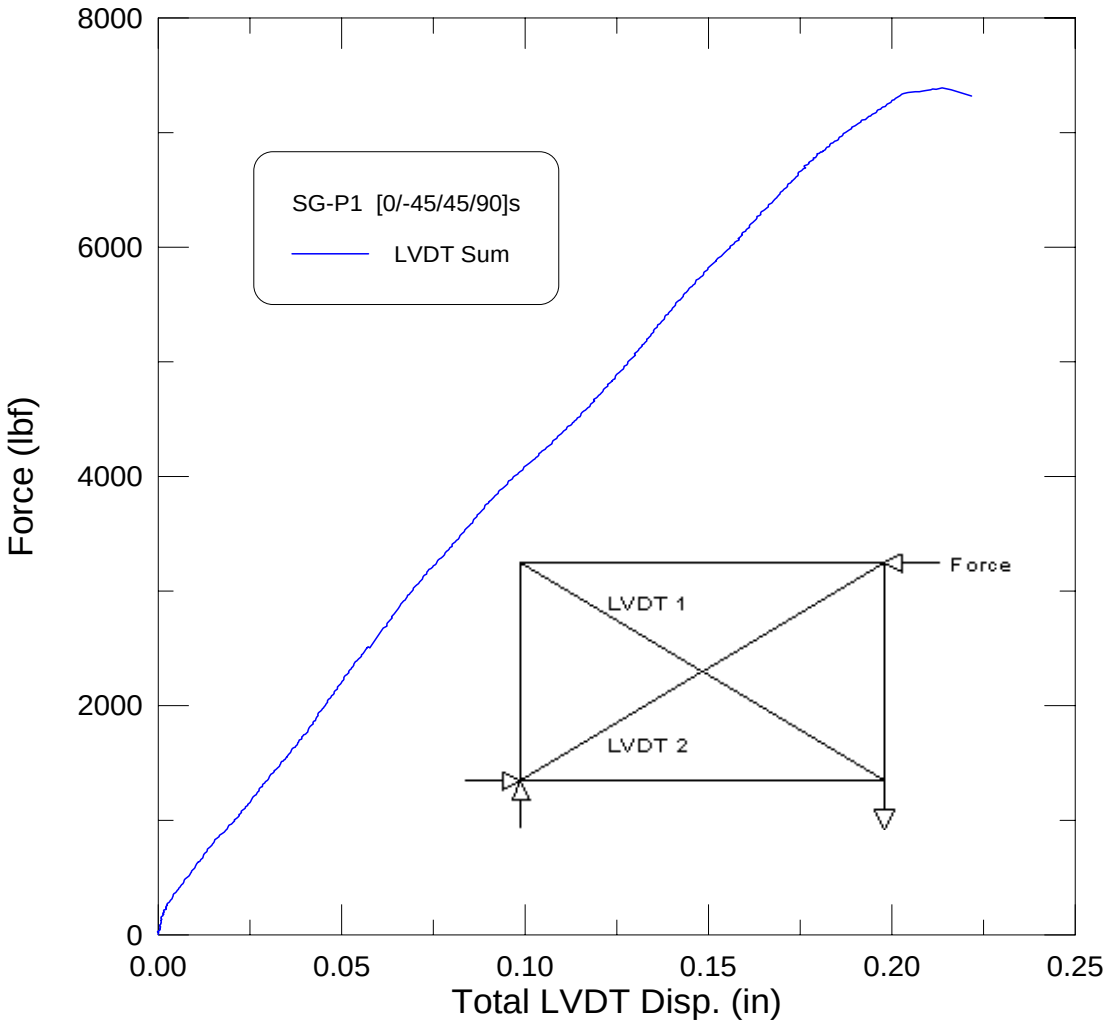

Figure 4.18 Force versus total LVDT displacement.

Figure 4.19 represents the shear response of the [0/90]s test specimen. The initial response is quasi-linear having a modulus of elasticity of 22 MPa. Initial cracking takes place around 3.50 MPa. The peak shear stress is 4.13 MPa at a shear strain of 0.46^{o}.

Figure 4.20 represents the shear response of the [0/45/90]s and [0/-45/90]s test specimen. Both specimen display a quasi-linear initial response with a modulus of elasticity of 24-28 MPa. As expected, the peak shear stress and peak shear strain for the [0/-45/90]s specimen (6.9-7.2 MPa and $0.46\text{-}0.53^{o}$) were greater than that for the [0/45/90]s specimen (4.7 MPa and 0.30^{o}). The addition of the cross layer adds to the distribution of cracking and therefore increasing the stress and strain capacity over that of the [0/90]s. The increase in peak stress and strain in the [0/-45/90]s over the [0/45/90]s can be attributed to the forces being directed in a tensile manner along the 45^{o} fibers instead of a compressive manner.

Figure 4.21 represents the shear response of the [0/45/-45]s test specimen. The initial response gives a modulus of elasticity of 49-56 Mpa, more than twice the stiffness obtained for specimen without the 45^{o} layer. Peak shear stresses were on the order of 8.2 MPa and shear strains on the order of 0.66^{o}. The first signs of cracking occur at around 6.5 MPa. The addition of an extra cross layer has given the composite increased stress and strain capacity.

Figure 4.22 represents the shear response of the [45/-45]s test specimen. Initial modulus of elasticity for these specimen are on the order of 75 MPa. Both specimen had a peak shear stress of 5.75 MPa ,however, the shear strains for the specimen were quite different. Specimen L2 displayed a brittle characteristic and failed suddenly at a shear

strain of 0.20^{o} while specimen L3 displayed some post-peak response and failed at a shear strain of 0.39^{o}.

Figure 4.23 represents the shear response of the [0/-45/45/90]s test specimen. This composite proved to be the optimum of all the specimen tested. A modulus of elasticity of approximately 50 MPa was observed. Only the [45/-45]s had a higher modulus of elasticity, which can be attributed to the absence of non load bearing layers. The average peak shear stress was 8.58 MPa and the average ultimate shear strain was 1.00^{o}. The first signs of cracking occurred around 4 MPa.

Figure 4.24 represents a comparison between the different specimen orientations. The [45/-45]s specimen displayed the highest resistance to shear strain up to 4.5 MPa. The [0/-45/45/90]s, [0/-45/90]s, [0/45/-45]s and [0/90]s specimen show similar strain resistance up to 4 MPa, beyond this point the response varies for each sample due to the orientation effects. The [0/90]s specimen is quite brittle and reaches its peak at 4 MPa. The [0/-45/45/90]s, [0/-45/90]s and [0/45/-45]s specimen attain similar peak shear stresses of 7-8.5 MPa. The [0/-45/45/90]s specimen reached a peak shear strain of 0.8 degrees, nearly twice that of all the other specimen.

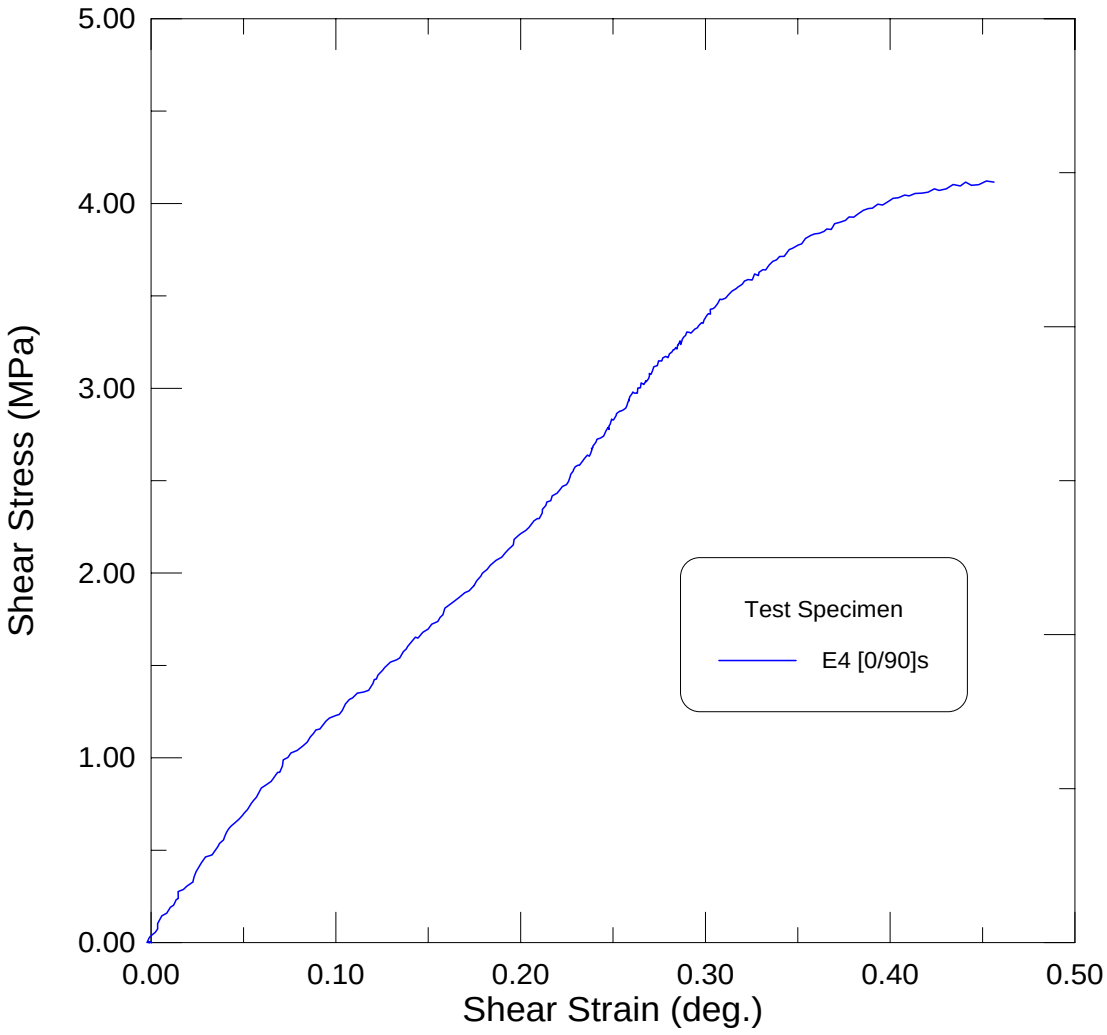

Figure 4.19 Shear stress-strain response of [0/90]s.

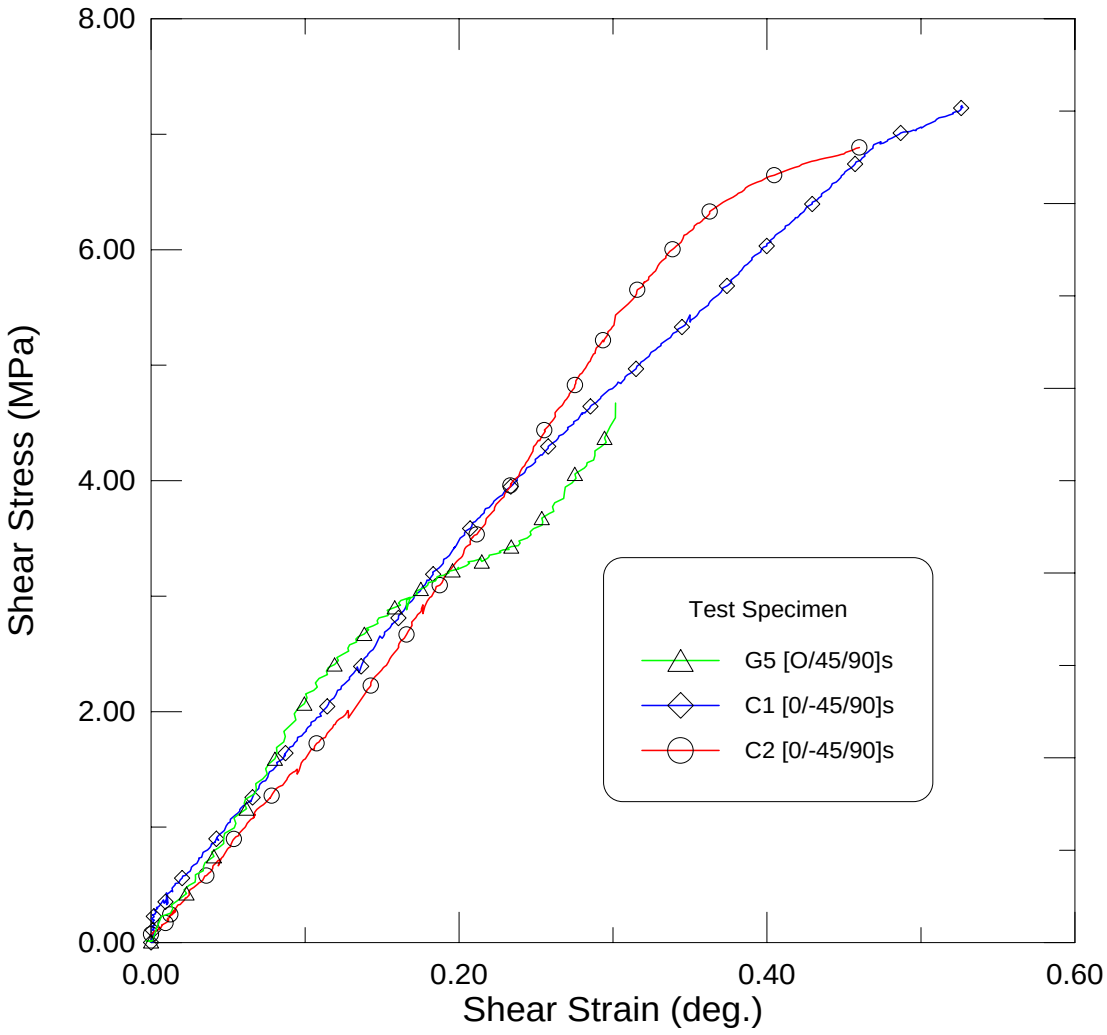

Figure 4.20 Shear stress-strain response of [0/45/90]s and [0/-45/90]s.

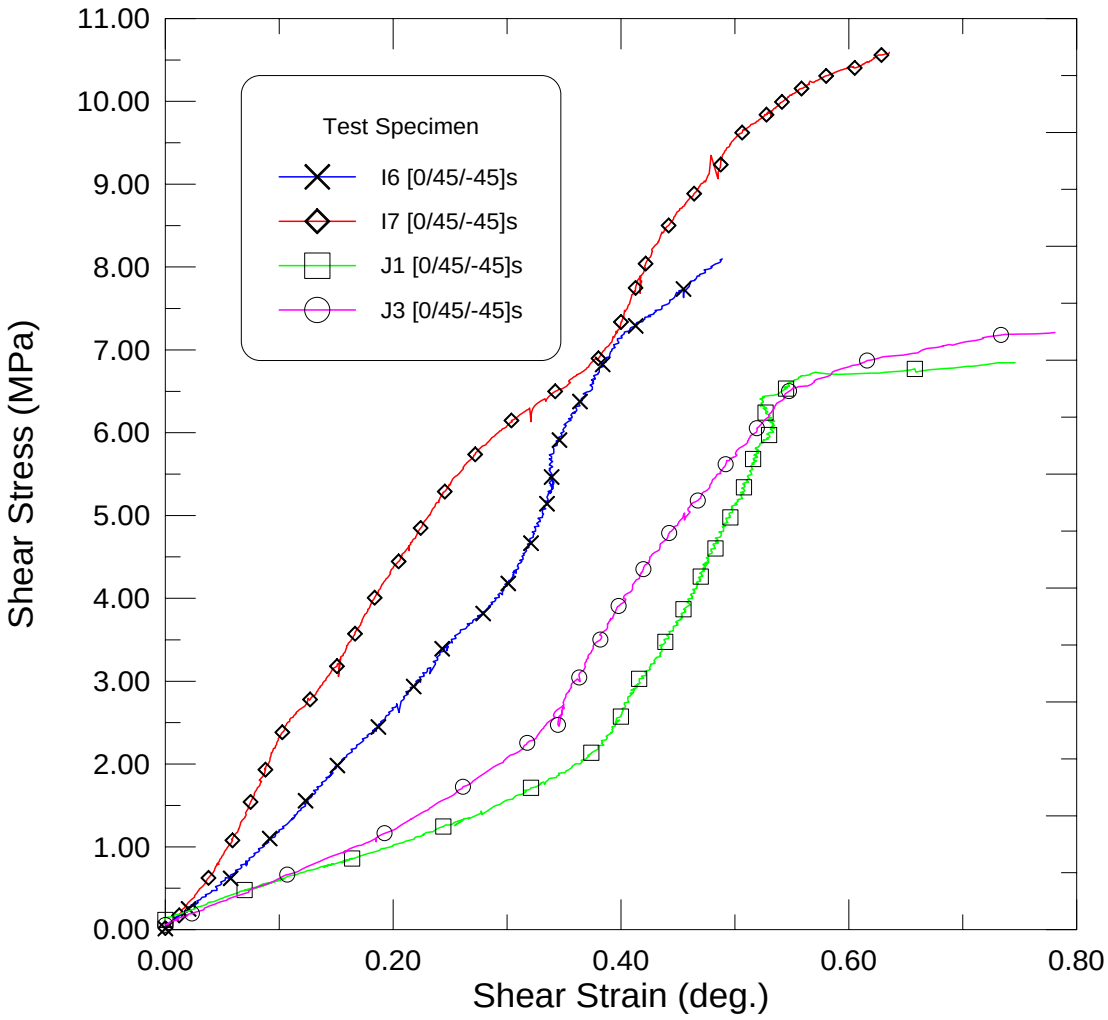

Figure 4.21 Shear stress-strain response of [0/45/-45]s.

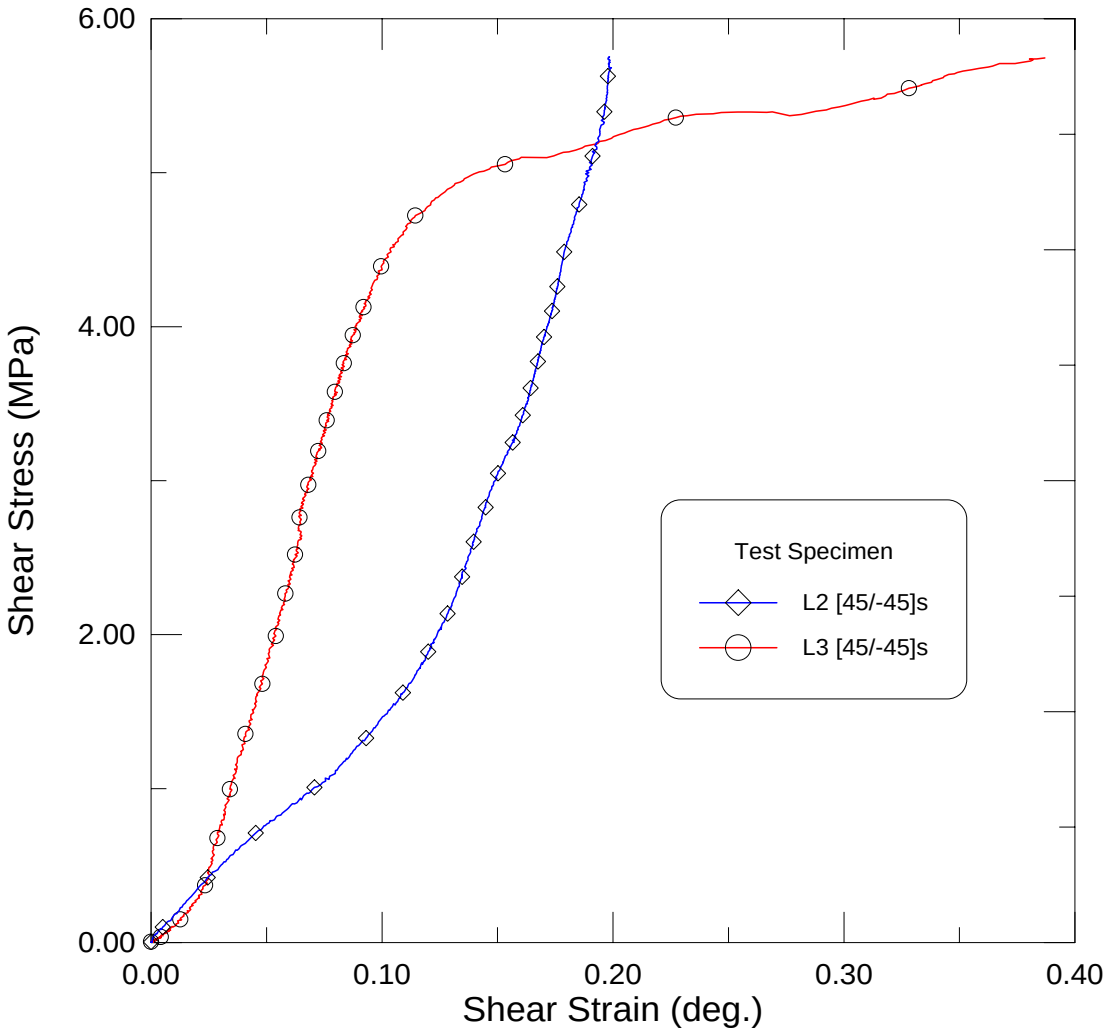

Figure 4.22 Shear stress-strain response of [45/-45]s.

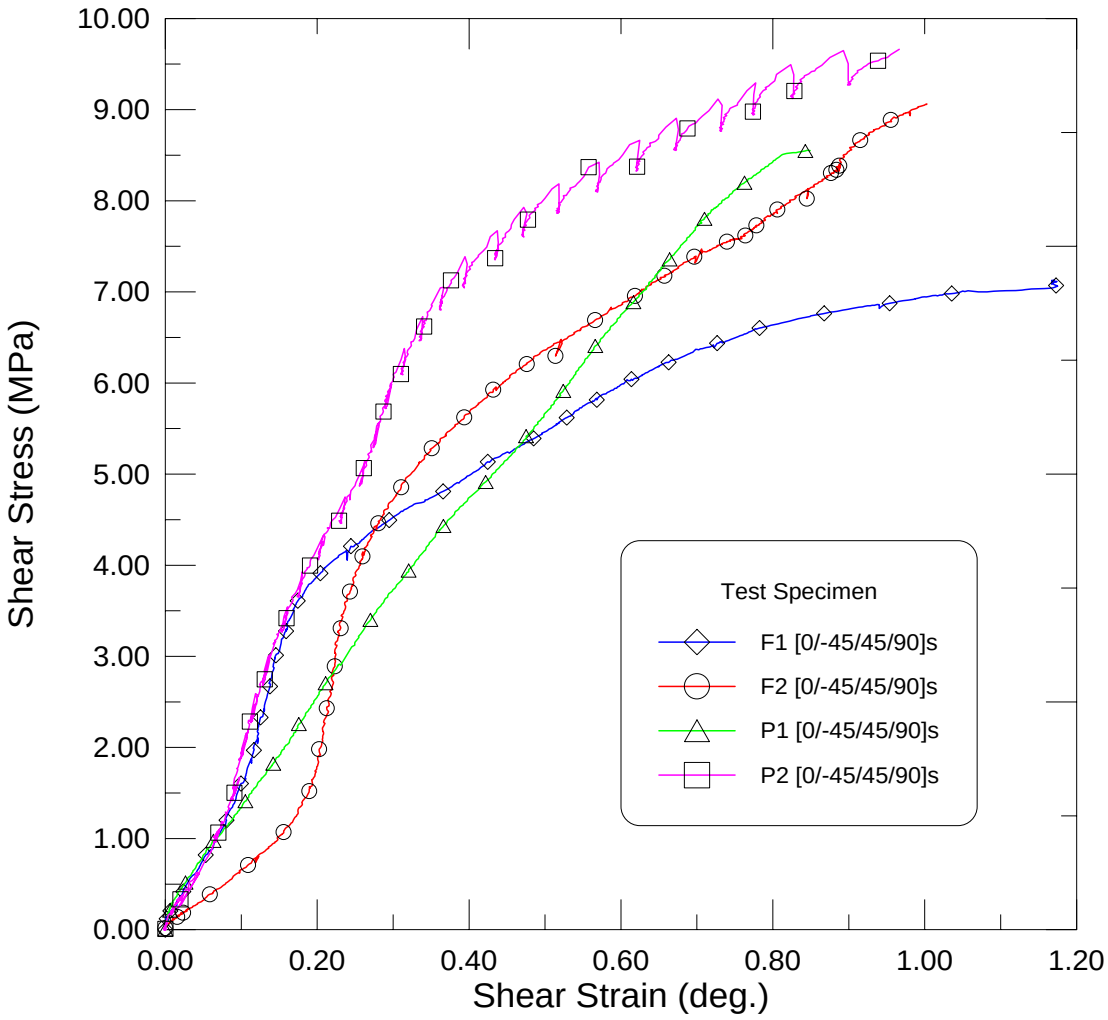

Figure 4.23 Shear stress-strain response of [0/-45/45/90]s.

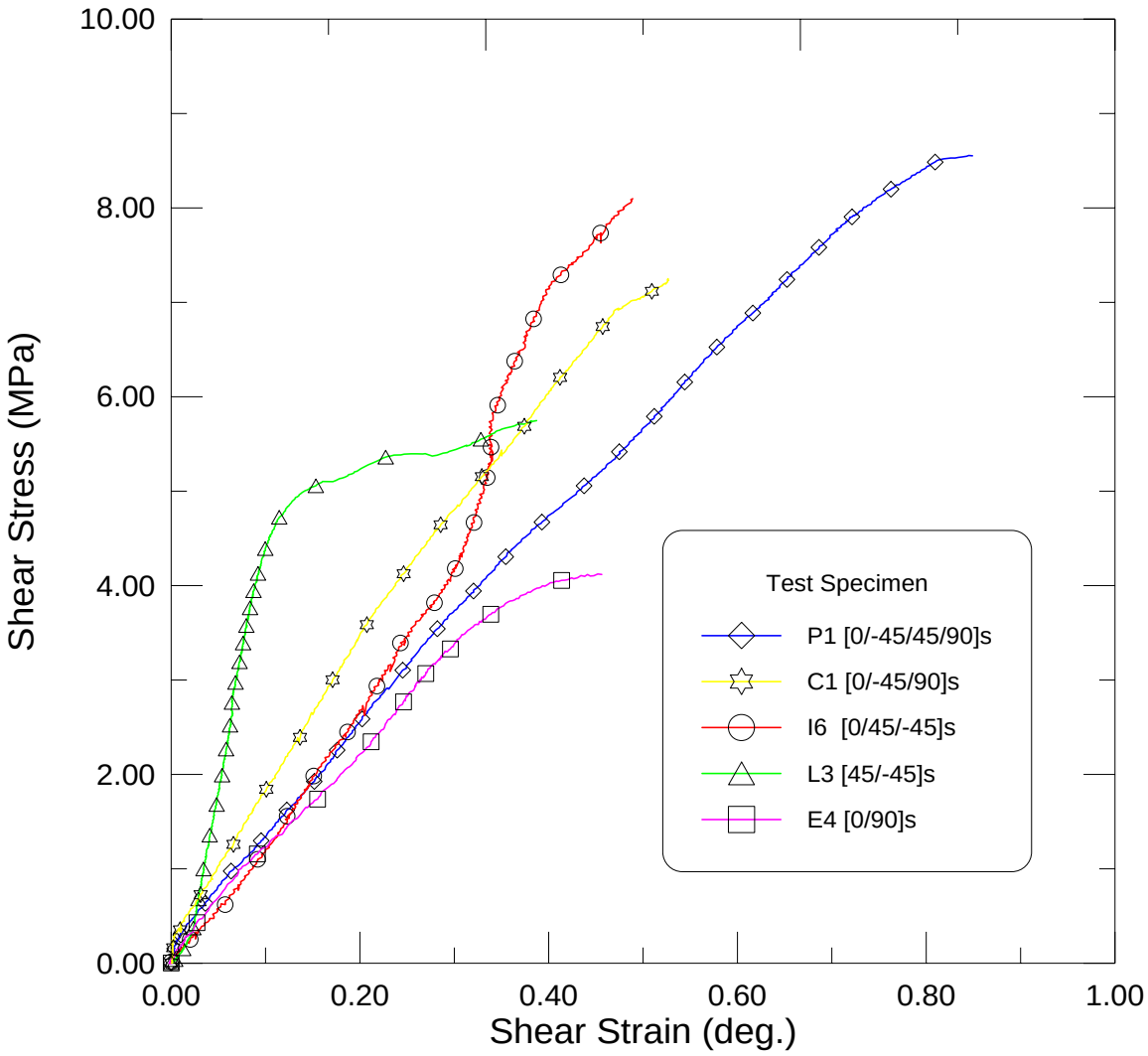

Figure 4.24 Comparison of shear specimen orientation.

4.4 Compression

Compression tests were performed on two [45/-45]s and two [0/-45/45/90]s specimen. The experimental results are tabulated in Table 4.4.

Table 4.4 Test results from compression testing.

Specimen	V_f (%)	Stress (MPa)	Strain (%)	E (GPa)
[45/-45]s				
K1	5.3	11.47	0.128	24.15
K2	5.3	10.32	0.110	21.68
[0/-45/45/90]s				
N1	7.9	14.46	0.180	11.09
N2	7.9	12.95	0.152	11.10

Figure 4.25 represents the compressive response of the [0/-45/45/90]s test specimen. The initial portion of the response is quasi-linear and provides an experimental modulus of elasticity of 11.09 GPa and 11.10 GPa. At approximately 8 MPa the specimen experience some initial cracking causing the response to become nonlinear. Peak strengths of 14.5 MPa and 13.0 MPa and peak strains of 0.18% and 0.15% were observed.

Figure 4.26 represents the compressive response of the [0/45/-45]s test specimen. The initial response of specimen K1 is quasi-linear but the response of K2 was somewhat erratic. This would suggest early cracking and fiber debonding of the specimen. Experimental modulus of elasticity were found to be 24.15 GPa and 21.68 GPa. Peak strengths of 11.47 MPa and 10.32 MPa and peak strains of 0.13% and 0.11% were observed.

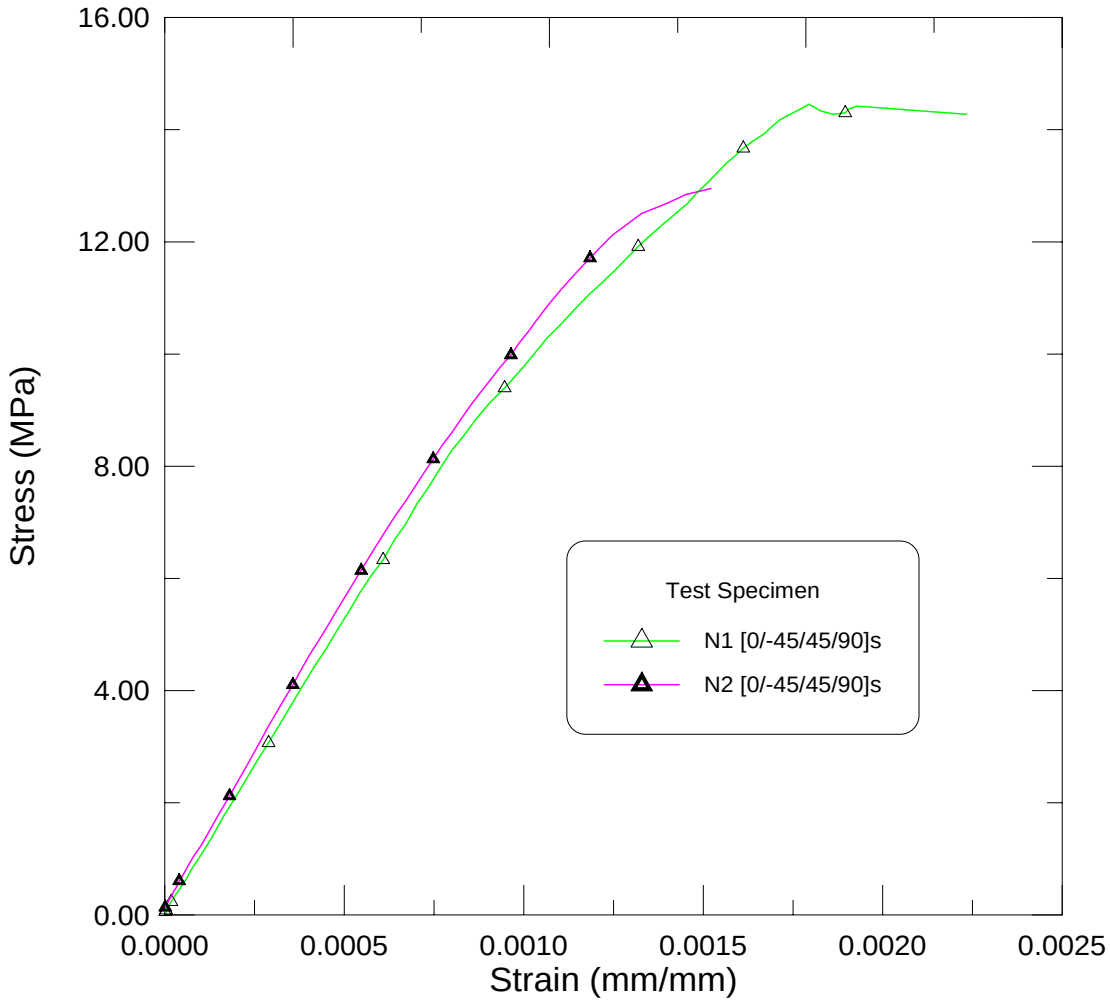

Figure 4.25 Compressive stress-strain response of [45/-45]s.

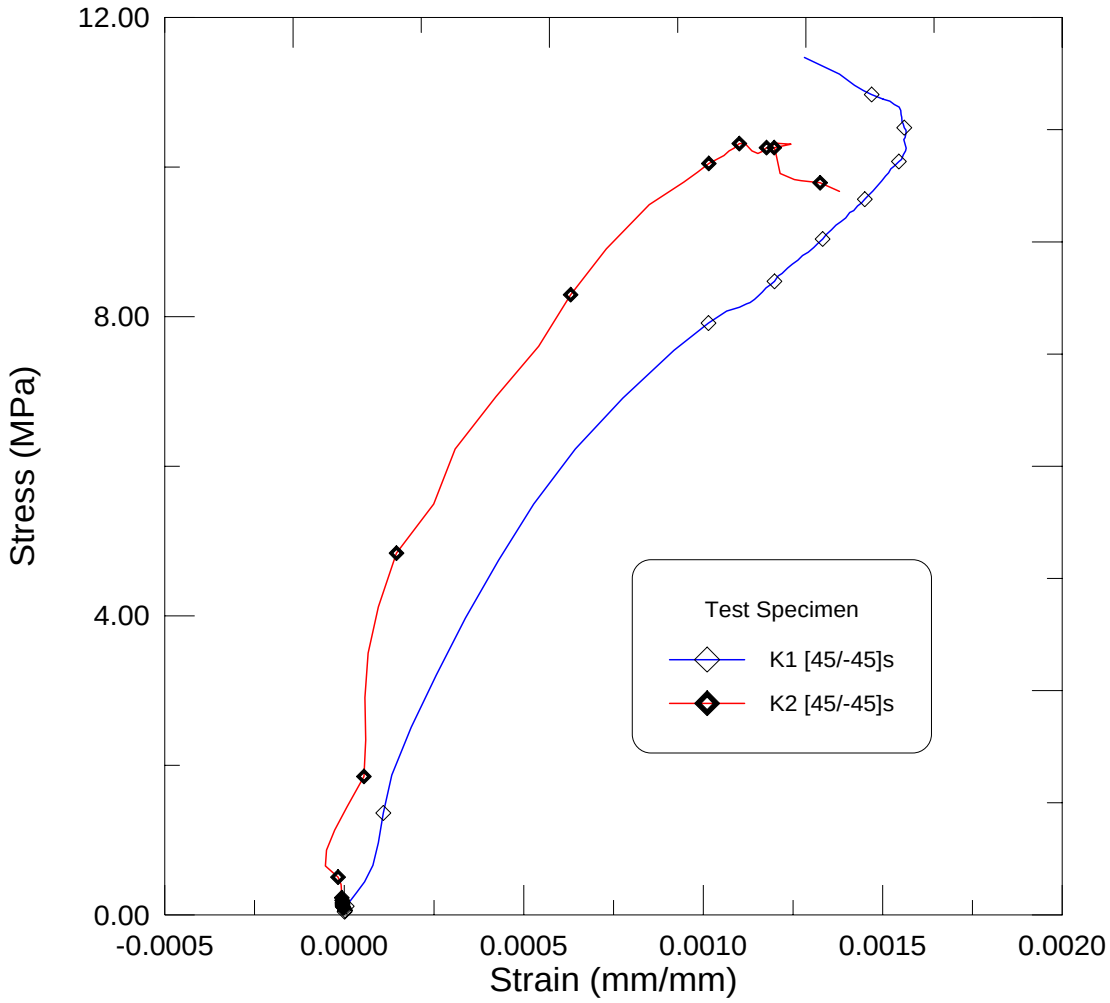

Figure 4.26 Compressive stress-strain response of [0/-45/45/90]s.

CHAPTER 5

Conclusion and recommendations for future research

5.1 Conclusion

Cement based composites were manufactured using pultrusion, extrusion and compression molding techniques. A variety of laminate orientations were manufactured with continuous AR-Glass fiber volumes of up to 9% using the pultrusion method. Discontinuous alumina, polypropylene and steel fiber composites were manufactured using the extrusion and compression molding methods. A reduction in the water/cement ratio from 0.40 to 0.25 was attained using the compression mold.

Mechanical tests for tension, compression and shear were performed on the pultrusion composites. Tensile strengths of 50 MPa, compression strengths of 14 MPa and shear strengths of 9 MPa were obtained from [0/-45/45/90]s laminates.

Three-point bending tests were performed on the extrusion and compression molding composites. Introducing alumina fibers to mortar increased the composite toughness but did not increase the ductility of it. The addition of polypropylene fibers was able to greatly increase composite ductility as well as increase the toughness. Using the compression molding to decrease specimen porosity through a reduction of the water/cement ratio increased the toughness of the specimen.

5.2 Future recommendations

It is hoped that this study will encourage further research into the development of fiber reinforced cement based composites. The development of high strength fiber composites could have a significant role in the retrofit and new construction industry.

Experimental results have shown that high tensile strengths and moderate compressive and shear strengths can be achieved with the addition of continuous and discontinuous fibers. Extending testing and Finite Element Analysis of more complex laminates may show significant improvements in shear and compression strengths of continuous fiber composites. Further study of the compression molding composites could also be attempted.

REFERENCES

Agarwal, B. D. and Broutman, L. J., Analysis and Performance of Fiber Composites, John Wiley & Sons, Inc., Second Edition, 1990.

Bentur, A. and Mindness, S. Fiber Reinforced Cementitious Composites, Elsevier Science Publishers LTD, 1990.

Dvorak, G. J. and Laws, V., "Analysis of First Ply Failure in Composite Laminates," *Engineering Fracture Mechanics,* Vol. 25, Numbers 5/6, 1986, Pergamon Press Ltd., pp. 763-770.

Garlinghouse, L. H. and Garlinghouse, R. E., "The Omni Mixer–A New Approach to Mixing Concrete," *ACI Journal,* April 1972.

Gettu, R., Mobasher, B., Carmona, S. and Jansen, D. C., "Testing of Concrete Under Closed-Loop Control," Elsevier Science Inc., 1996.

Gopalaratnam, V. S. and Shah, S. P., "Softening Response of Plain Concrete in Direct Tension," *ACI Journal,* May-June 1985.

Li, C., "Mechanical Behavior of Cementious Composites Reinforced with High Volume Content of Fibers," Doctoral Dissertation, Arizona State University, May 1995.

Mehta, P. K. and Monteiro, P. J. M., CONCRETE, Prentice Hall, Second Edition, 1993.

Mobasher, B., "Reinforcing Mechanism of Fibers in Cement Based Composites," Doctoral Dissertation, Northwestern University, June 1990.

Mobasher, B., and Li, C. Y., and Arino, A., "Experimental R-Curves for Assessment of Toughening in Micro-Fiber Reinforced Hybrid Composites," American Concrete Institute, ACI SP-155-5, pp. 93-114, 1995.

Mobasher, B., Pivacek A., and Haupt, G. J. "A Filament Winding Technique for Manufacturing Cement Based Cross-Ply Laminates," manuscript in review, Journal of Advanced Cement Based Materials, Feb. 1997.

Mobasher, B., Stang, H. and Shah, S. P., "Microcracking in Fiber Reinforced Concrete," *Journal of Cement and Concrete Research,* Vol. 20, 1990, pp. 665-676.

Pivacek, A., "Development of a Filament Winding Technique for Manufacturing Cement Based Materials," Masters Thesis, Arizona State University, May 1997.

Young, W. and Chiu, C., "Study on Compression Transfer Molding," *Journal of COMPOSITE MATERIALS*, Vol. 29, No. 16, 1995.

APPENDIX A

Three-point bending test results

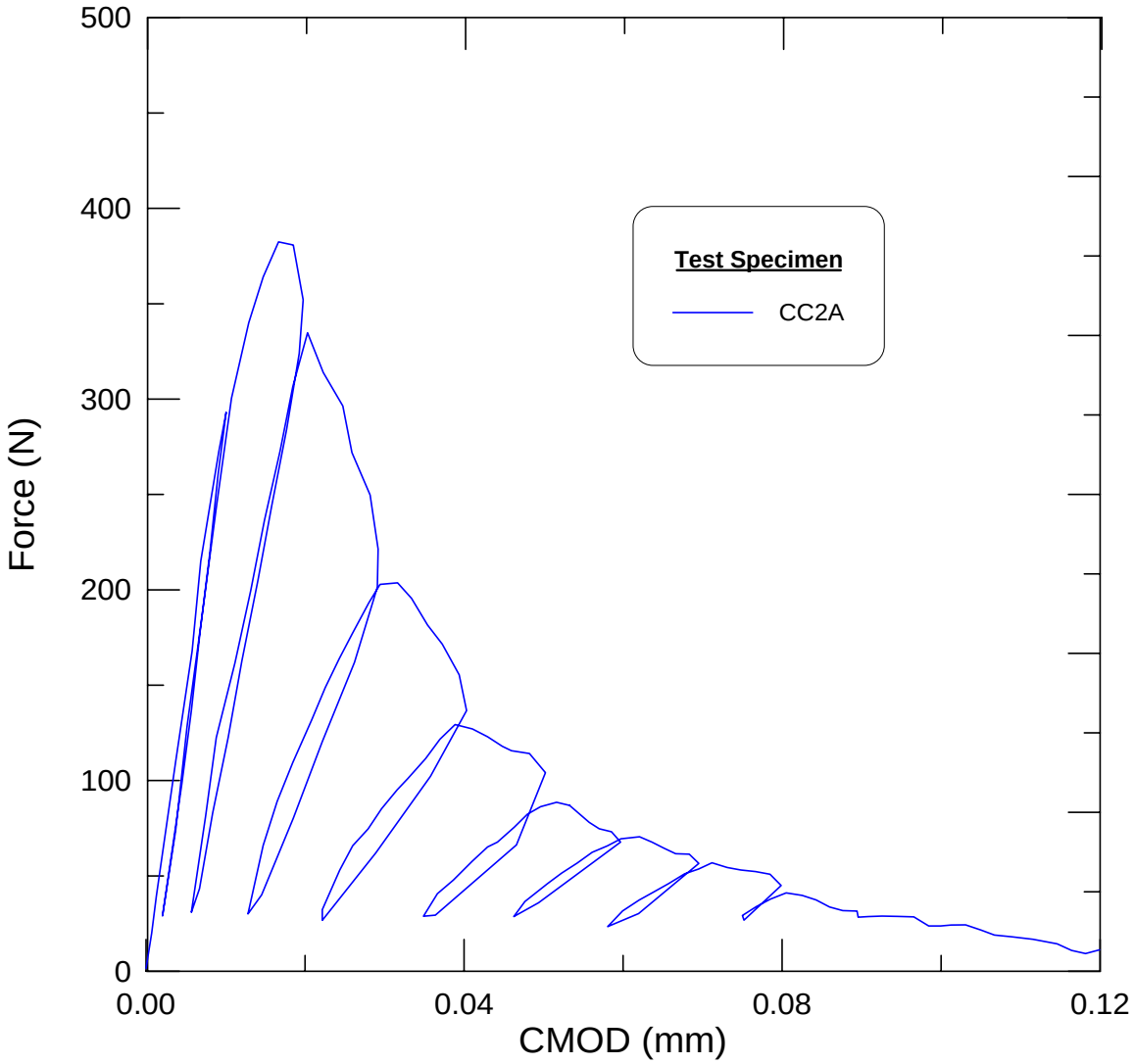
500
400
300
200
100
0
Force (N)
0.00
0.04
0.08
0.12
CMOD (mm)
Test Specimen
CC2A

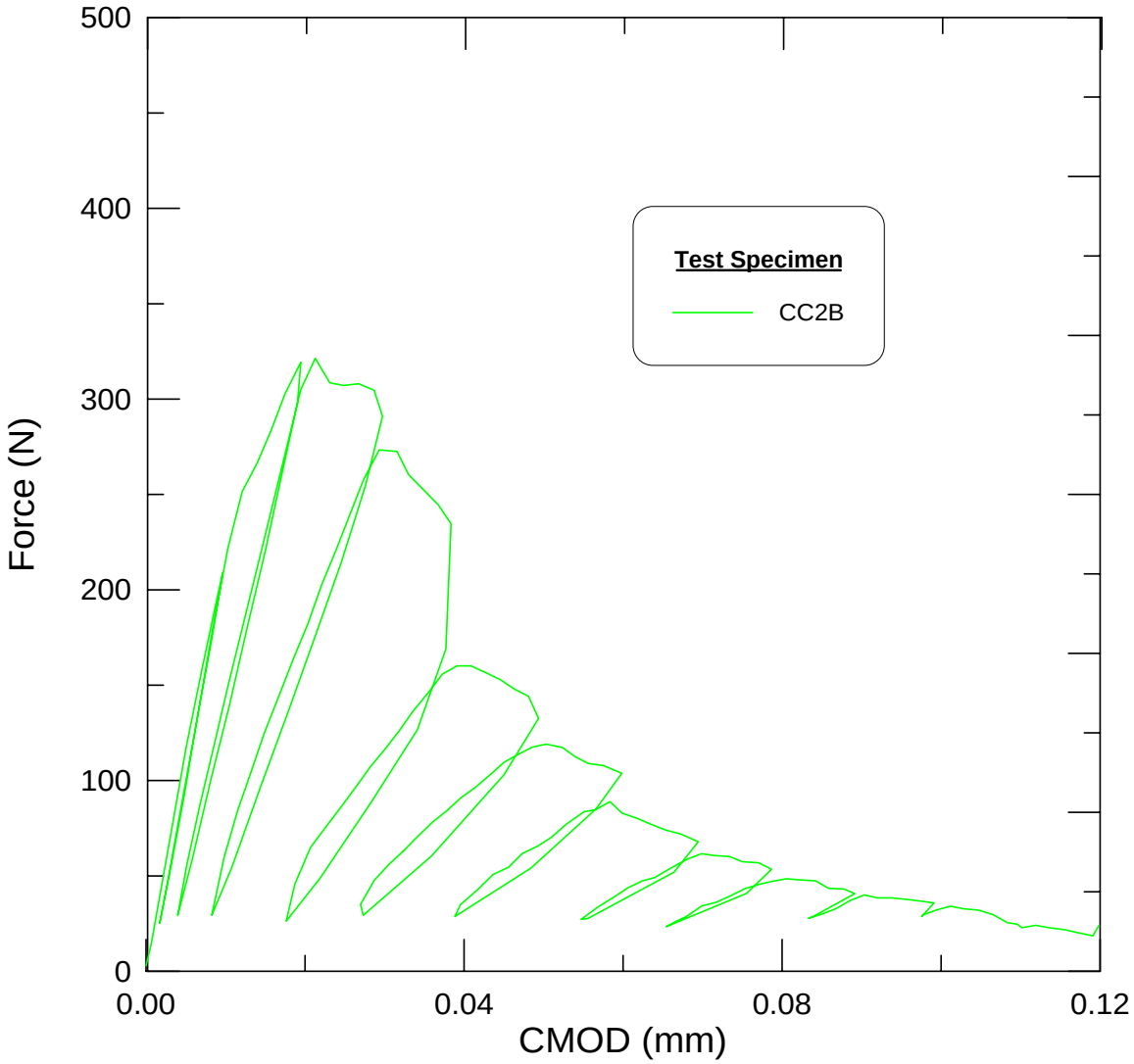
500
400
300
200
100
0
Force (N)
0.00
0.04
0.08
0.12
CMOD (mm)
Test Specimen
CC2B

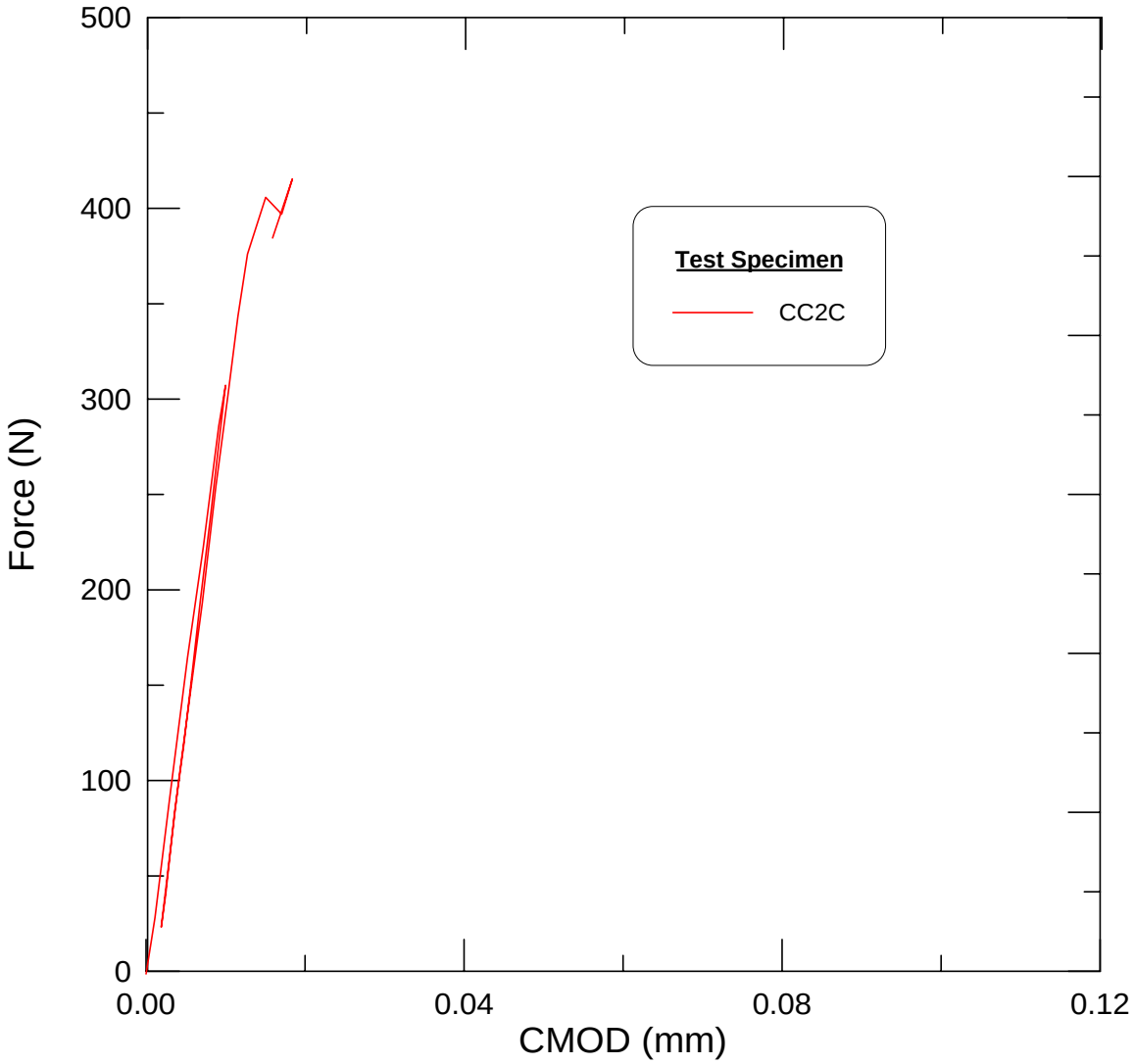
500
400
300
200
100
0
Force (N)
0.00
0.04
0.08
0.12
CMOD (mm)
Test Specimen
CC2C

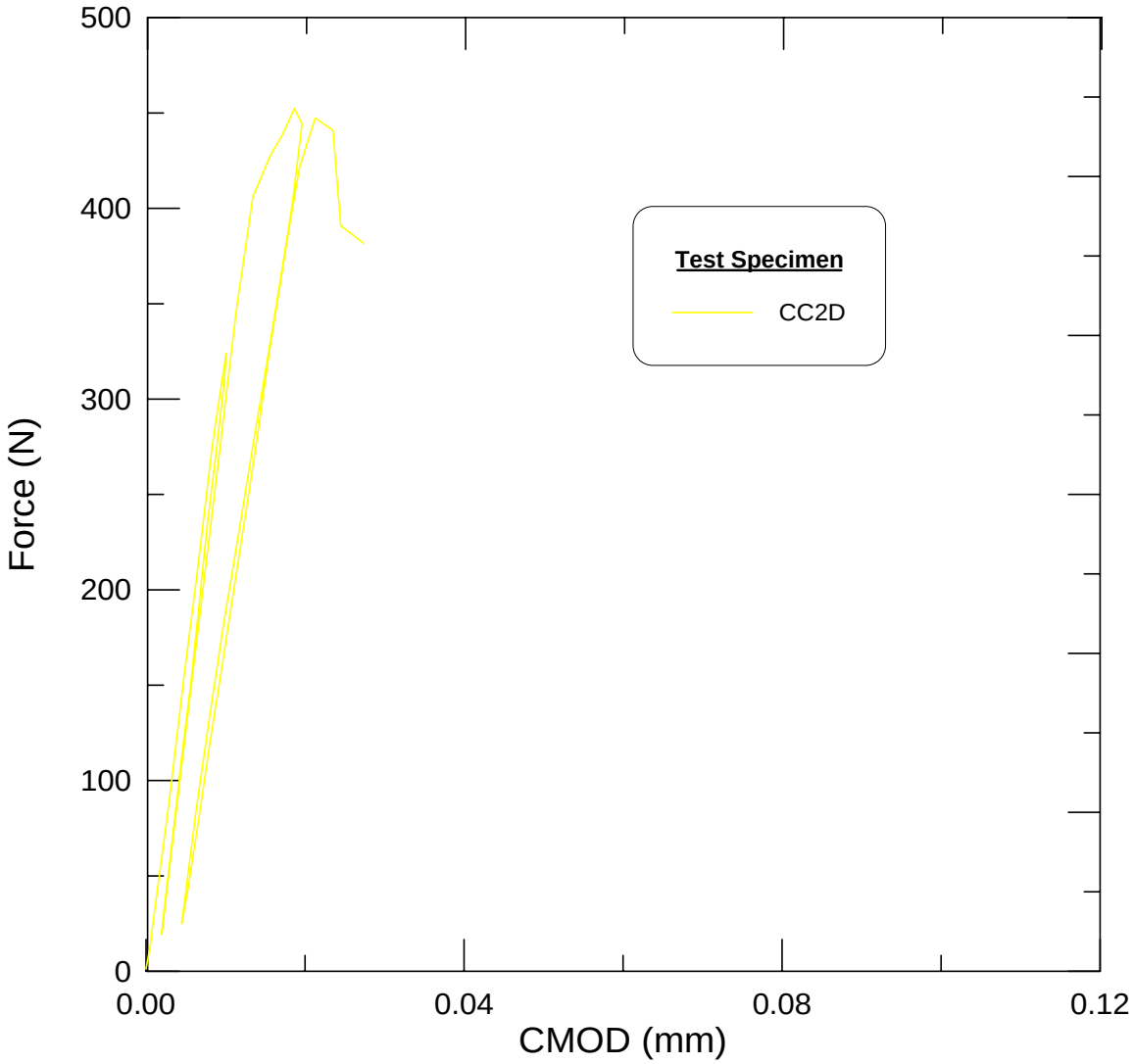
500
400
300
200
100
0
Force (N)
0.00
0.04
0.08
0.12
CMOD (mm)
Test Specimen
CC2D

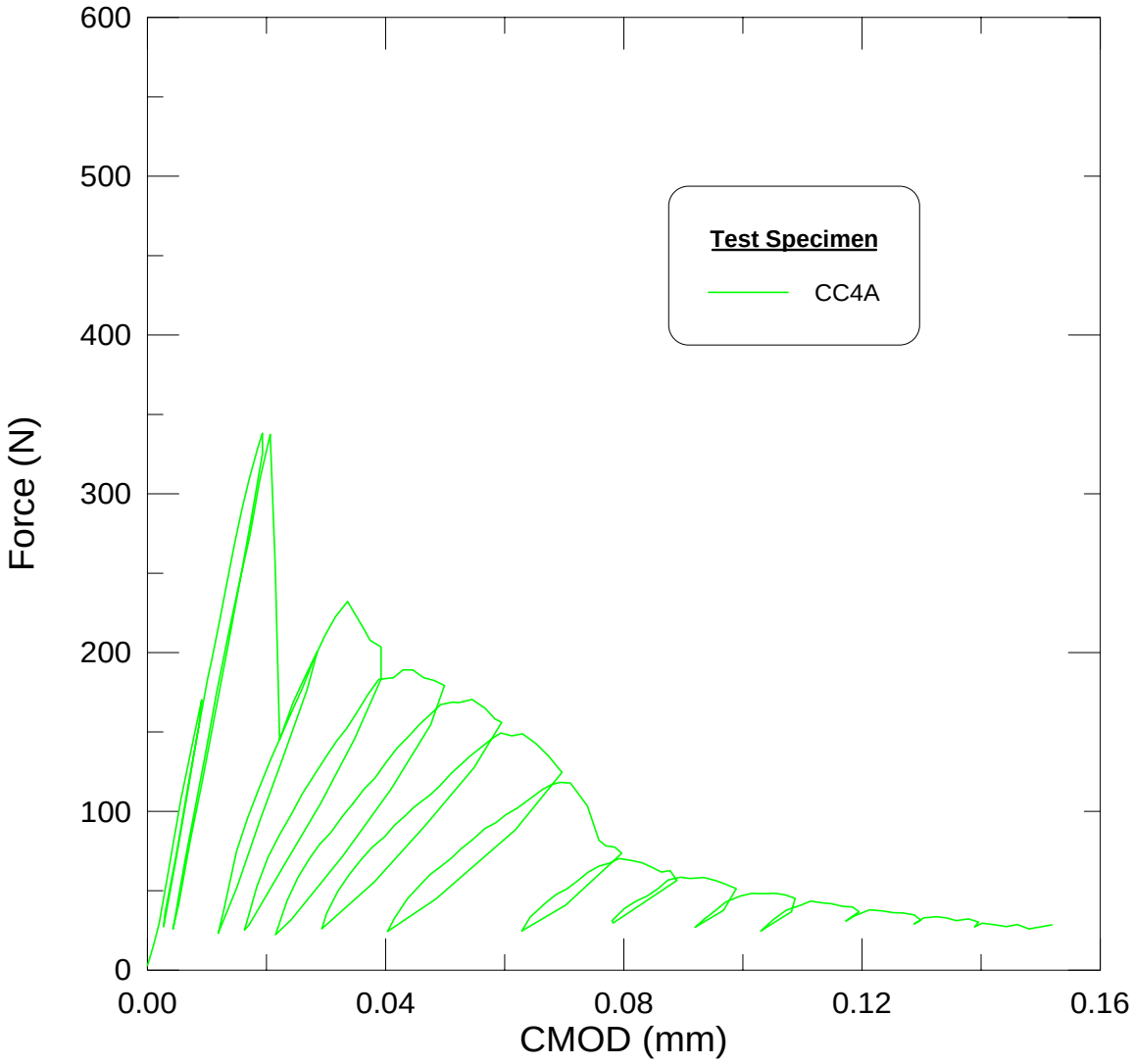
600
500
400
300
200
100
0
Force (N)
0.00
0.04
0.08
0.12
0.16
CMOD (mm)
Test Specimen
CC4A

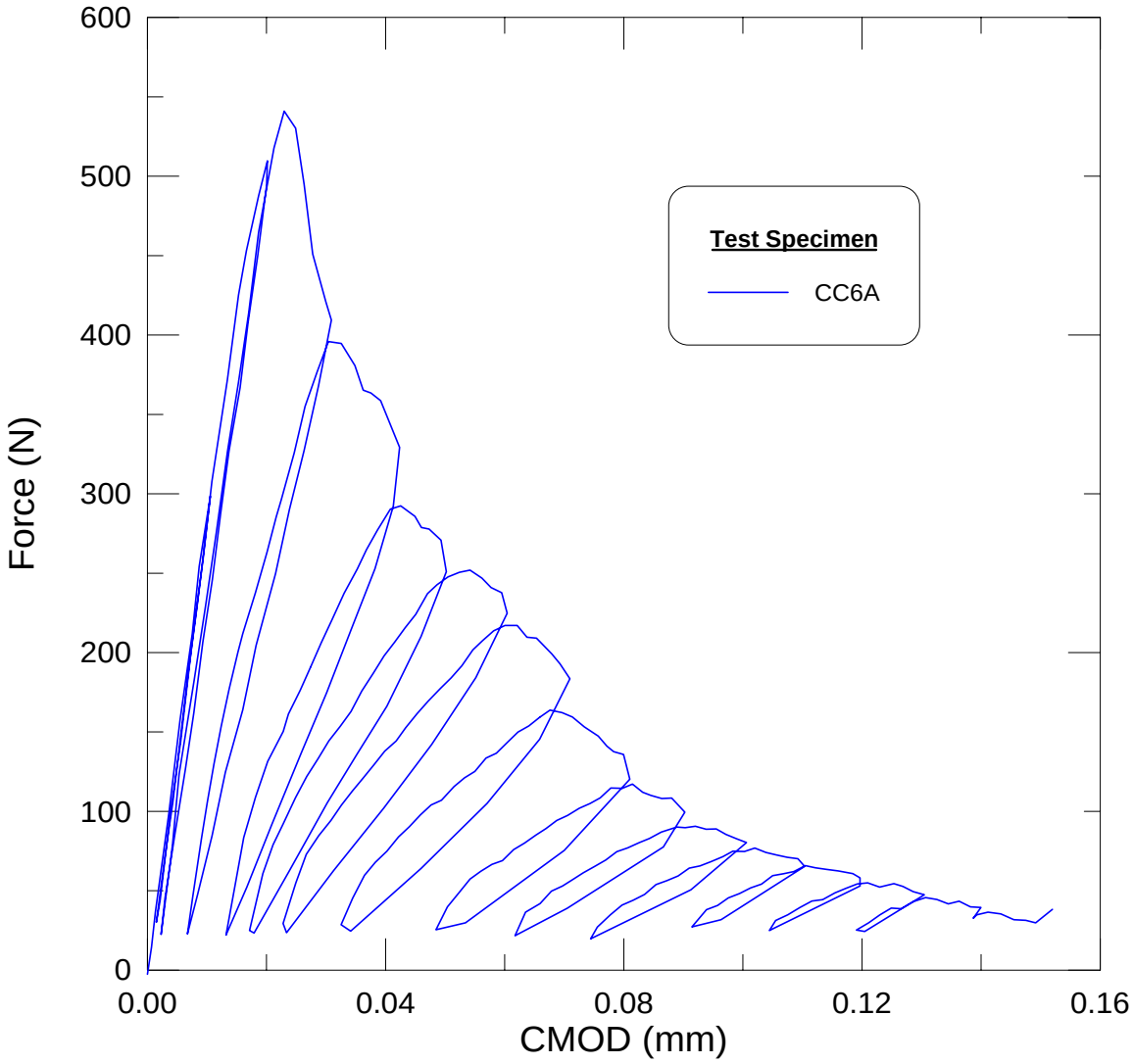
600
500
400
300
200
100
0
Force (N)
0.00
0.04
0.08
0.12
0.16
CMOD (mm)
Test Specimen
CC6A

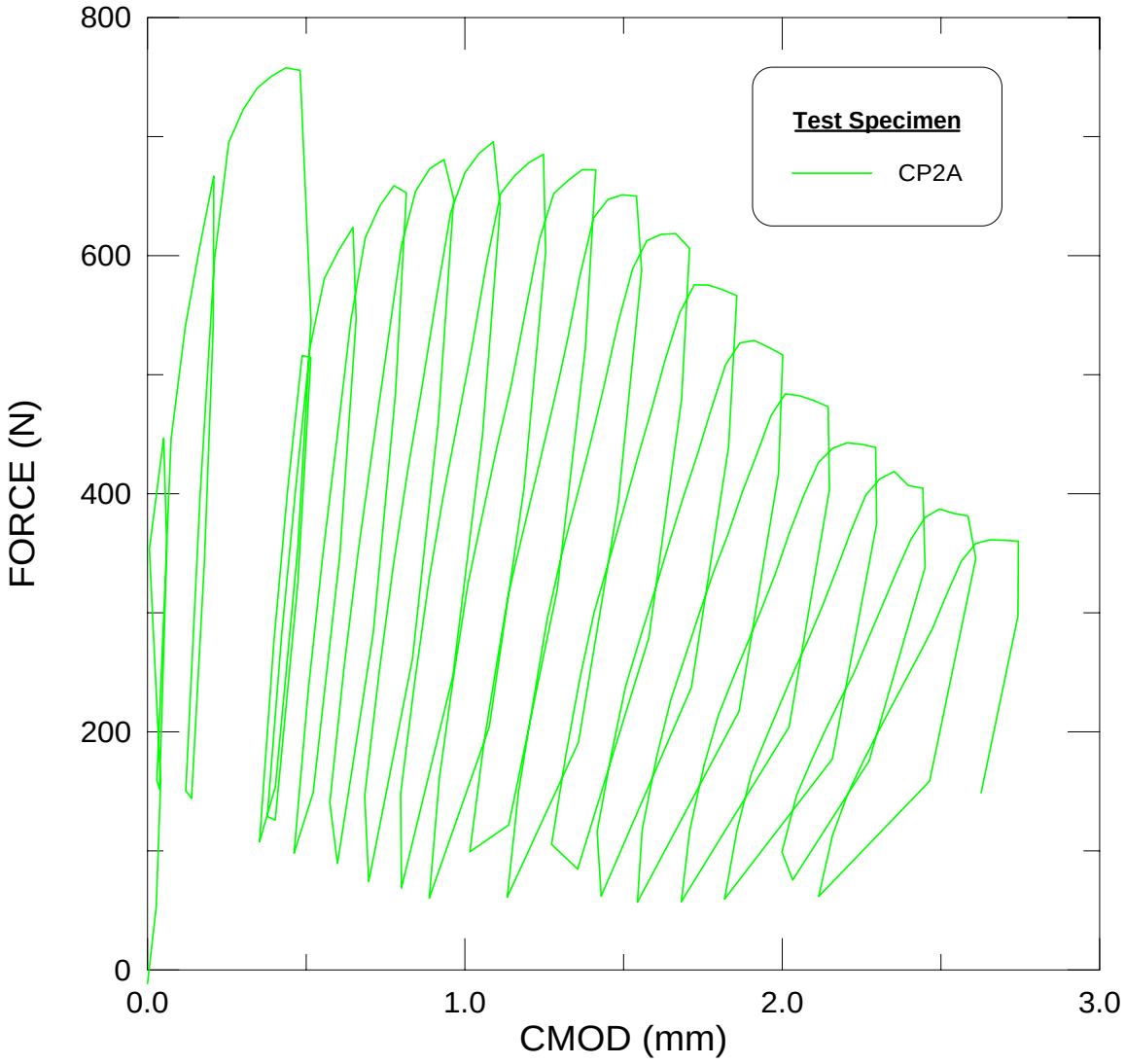
800
600
400
200
0
FORCE (N)
0.0
1.0
2.0
3.0
CMOD (mm)
Test Specimen
CP2A

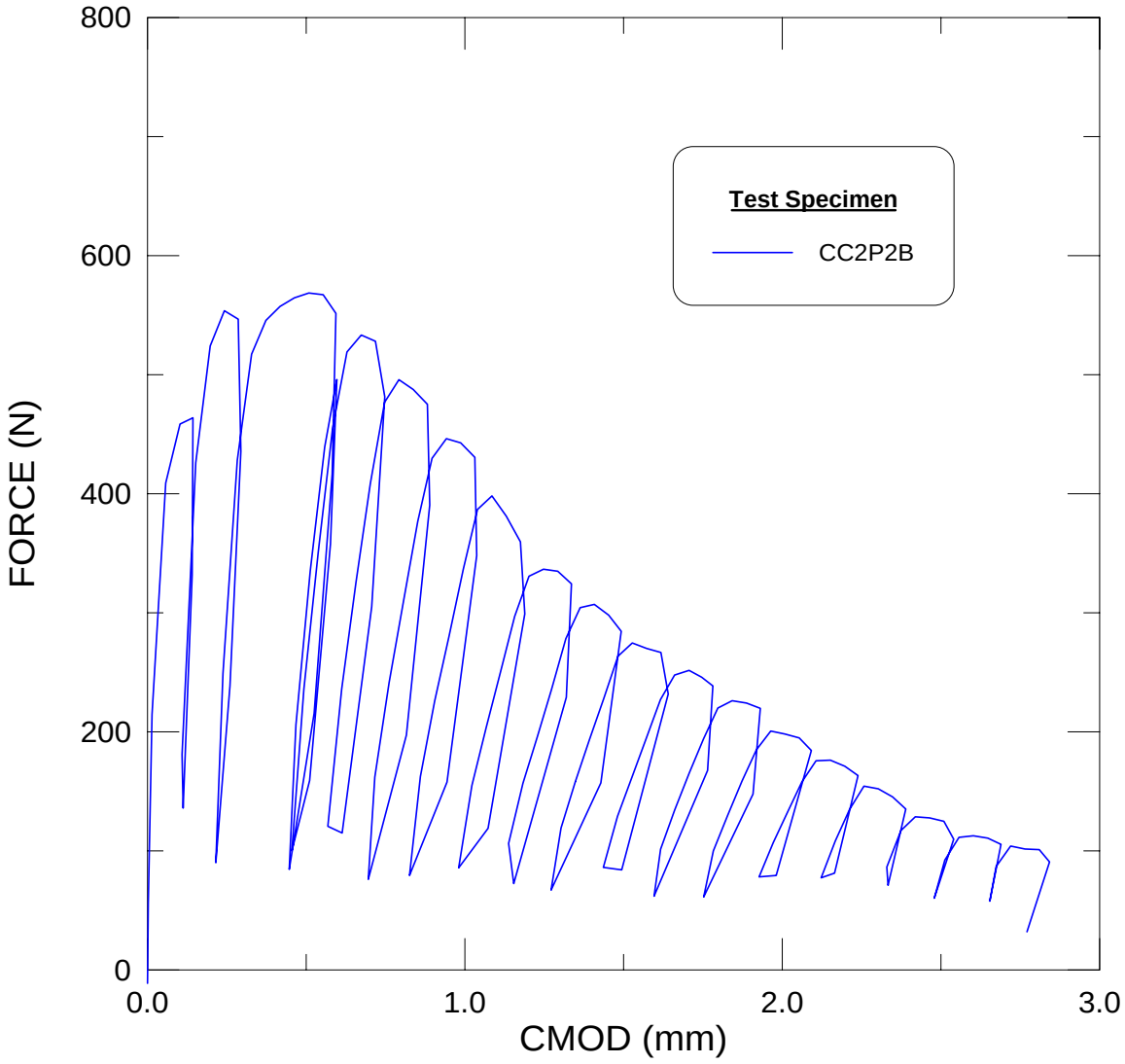
800
600
400
200
0
FORCE (N)
0.0
1.0
2.0
3.0
CMOD (mm)
Test Specimen
CC2P2B

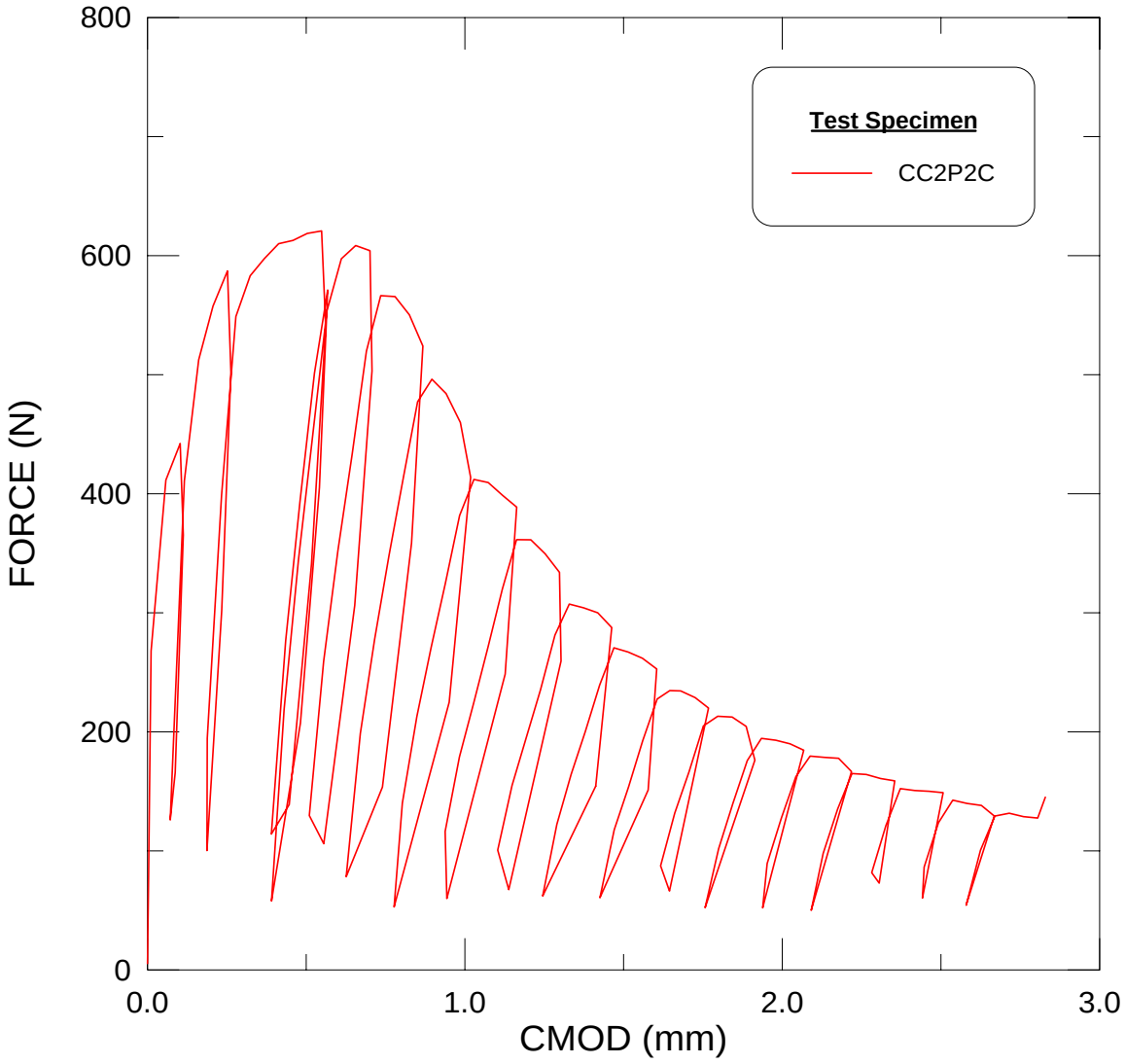
800
600
400
200
0
FORCE (N)
0.0
1.0
2.0
3.0
CMOD (mm)
Test Specimen
CC2P2C

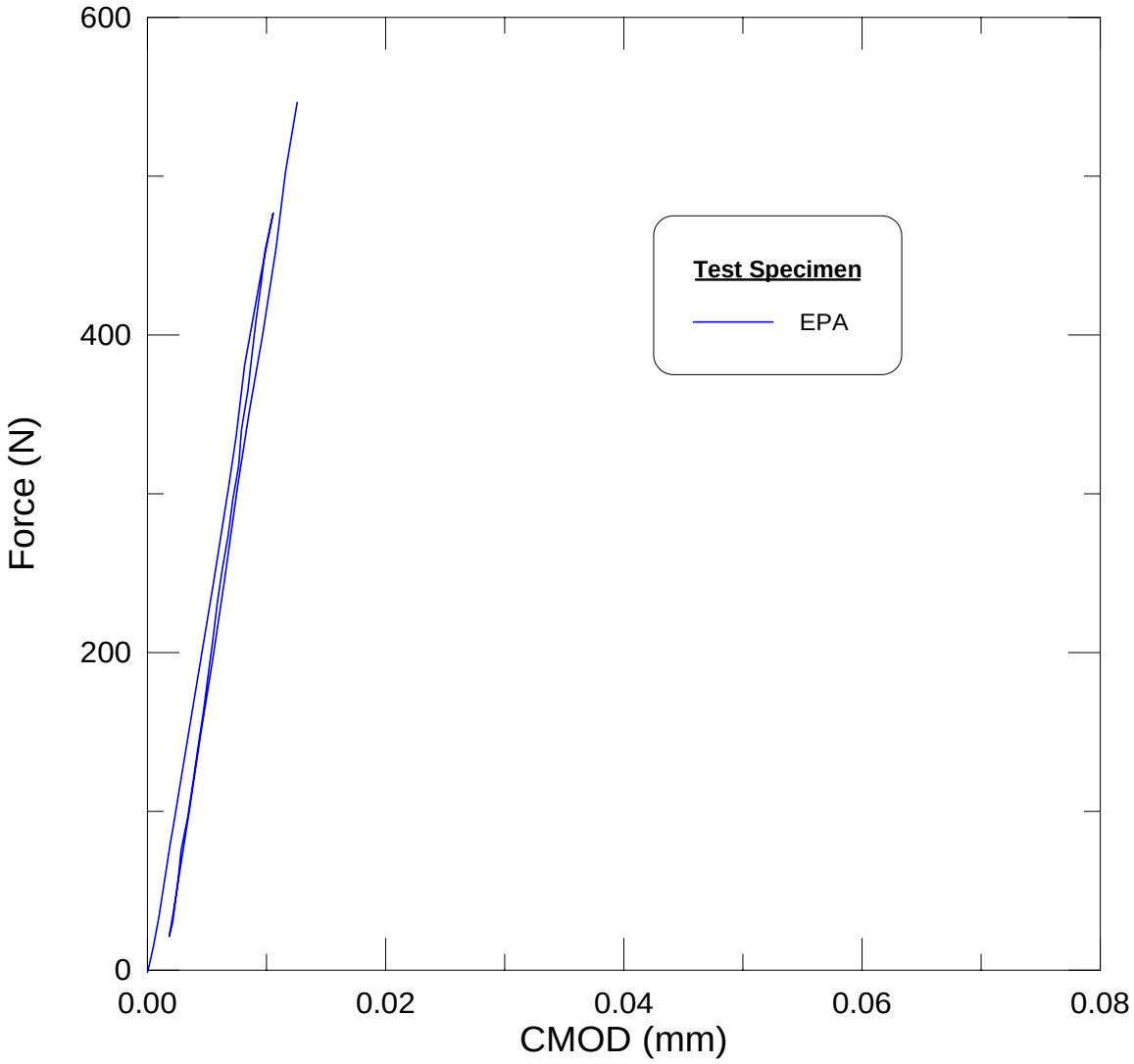
600
400
200
0
Force (N)
0.00
0.02
0.04
0.06
0.08
CMOD (mm)
Test Specimen
EPA

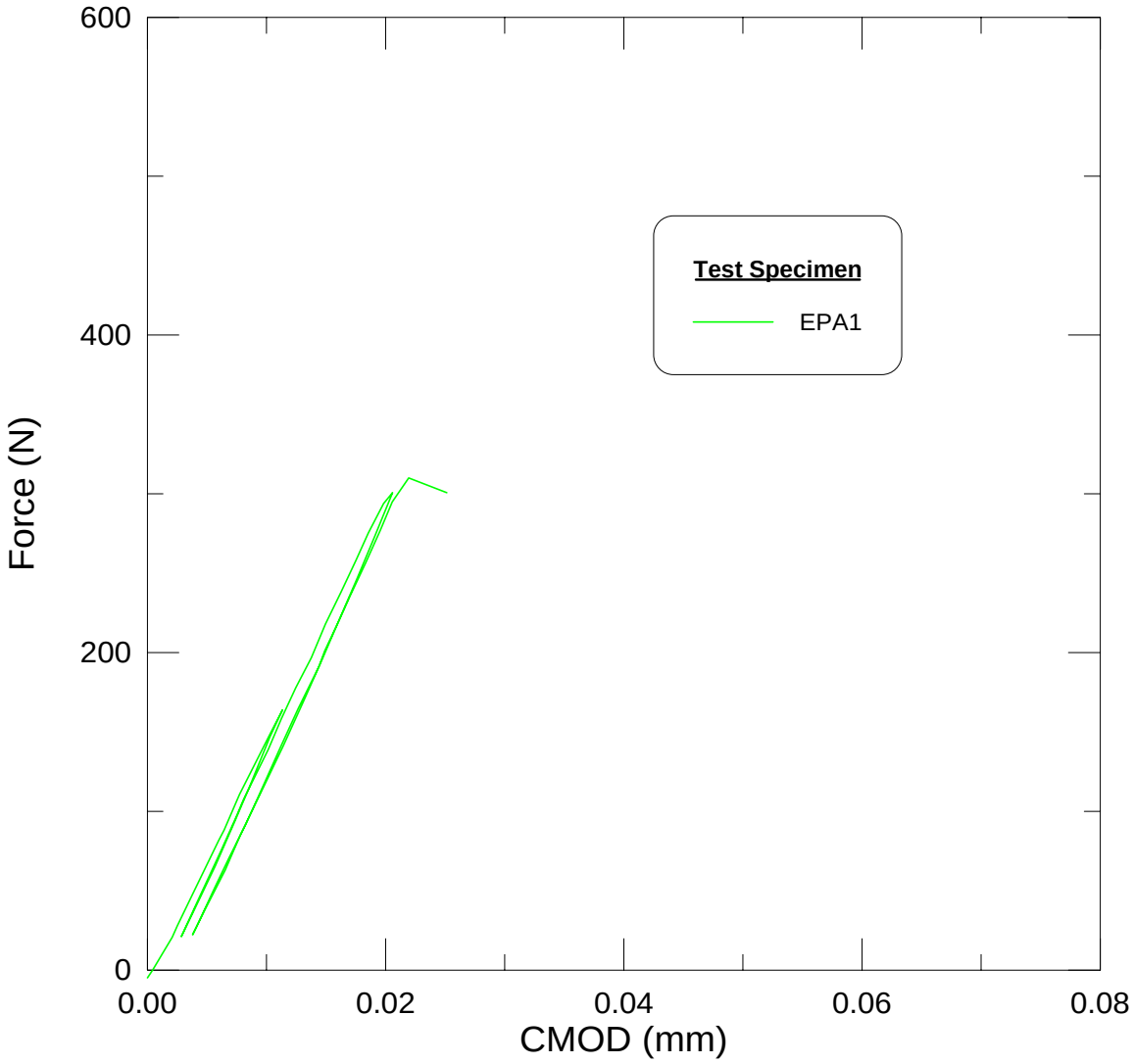
600
400
200
0
Force (N)
0.00
0.02
0.04
0.06
0.08
CMOD (mm)
Test Specimen
EPA1

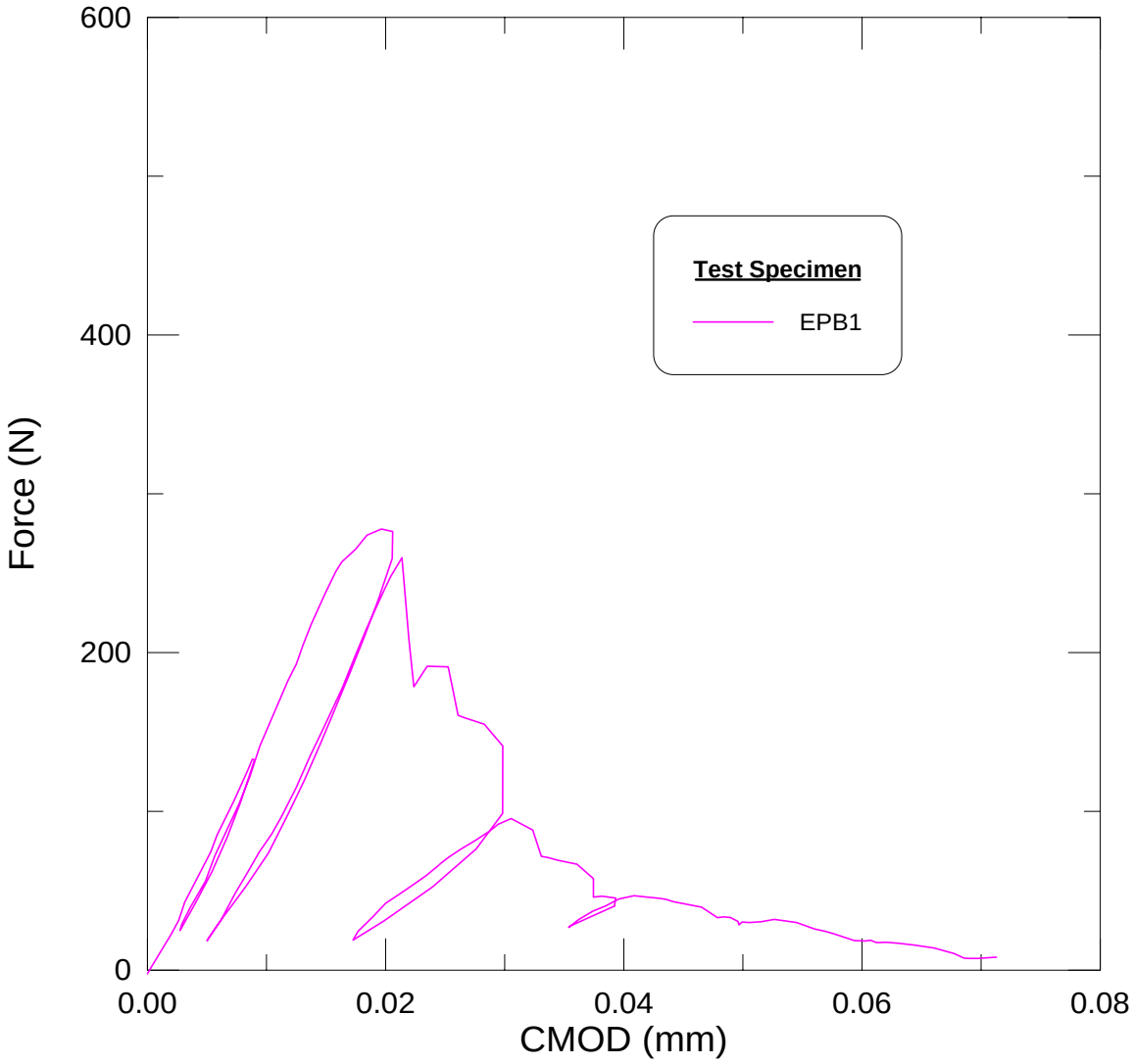
600
400
200
0
Force (N)
0.00
0.02
0.04
0.06
0.08
CMOD (mm)
Test Specimen
EPB1

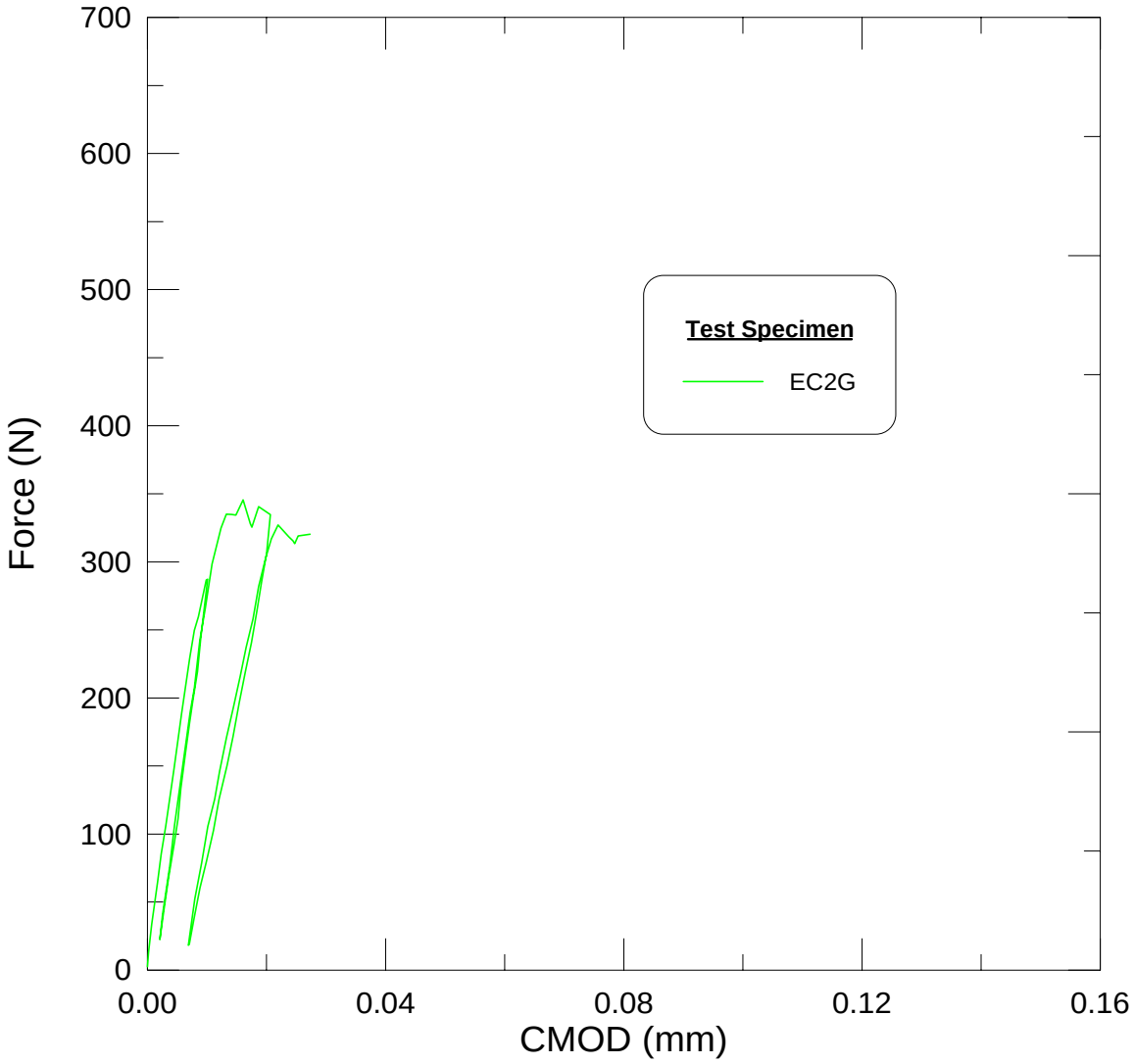
700
600
500
400
300
200
100
0
Force (N)
0.00
0.04
0.08
0.12
0.16
CMOD (mm)
Test Specimen
EC2G

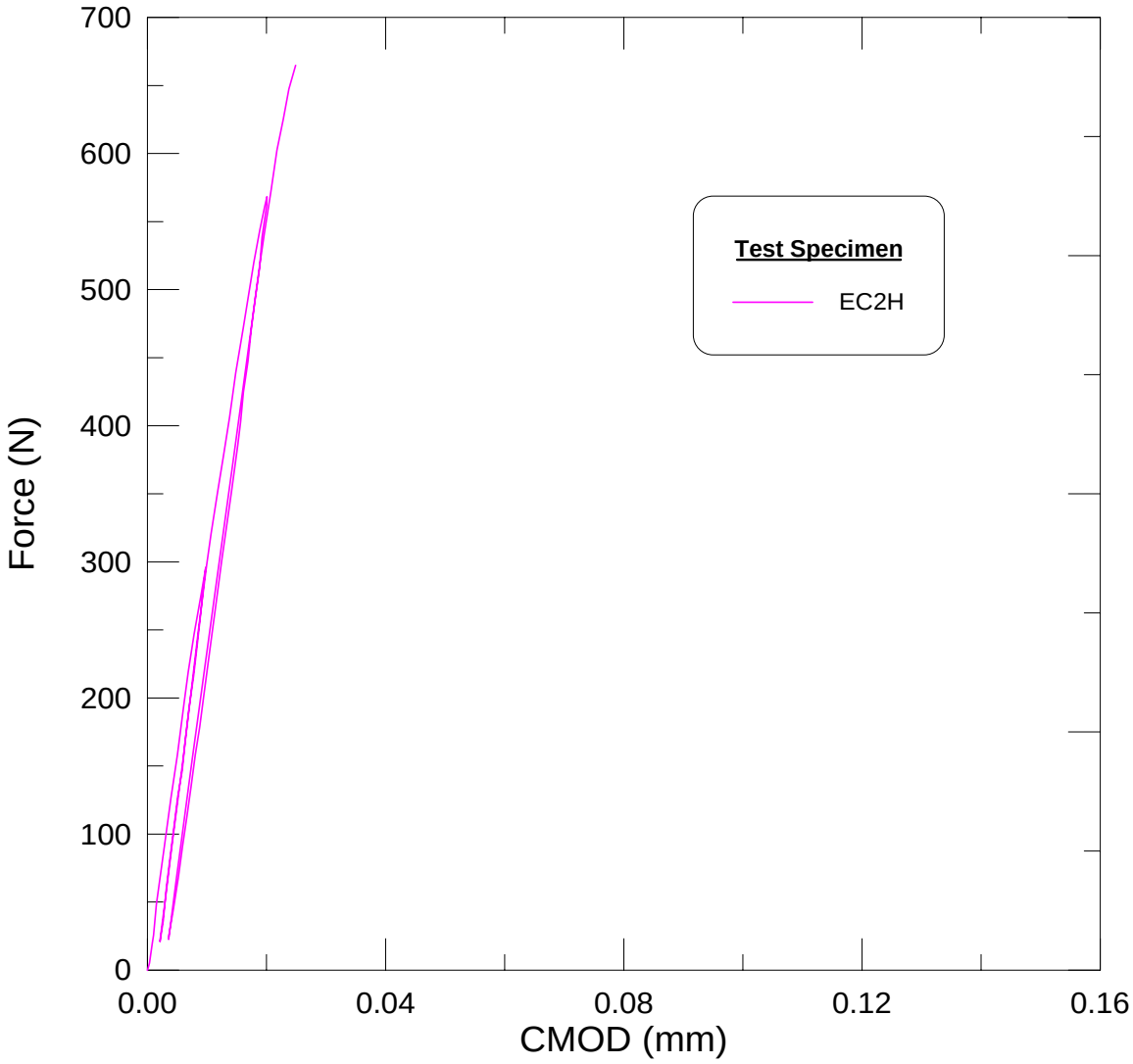
700
600
500
400
300
200
100
0
Force (N)
0.00
0.04
0.08
0.12
0.16
CMOD (mm)
Test Specimen
EC2H

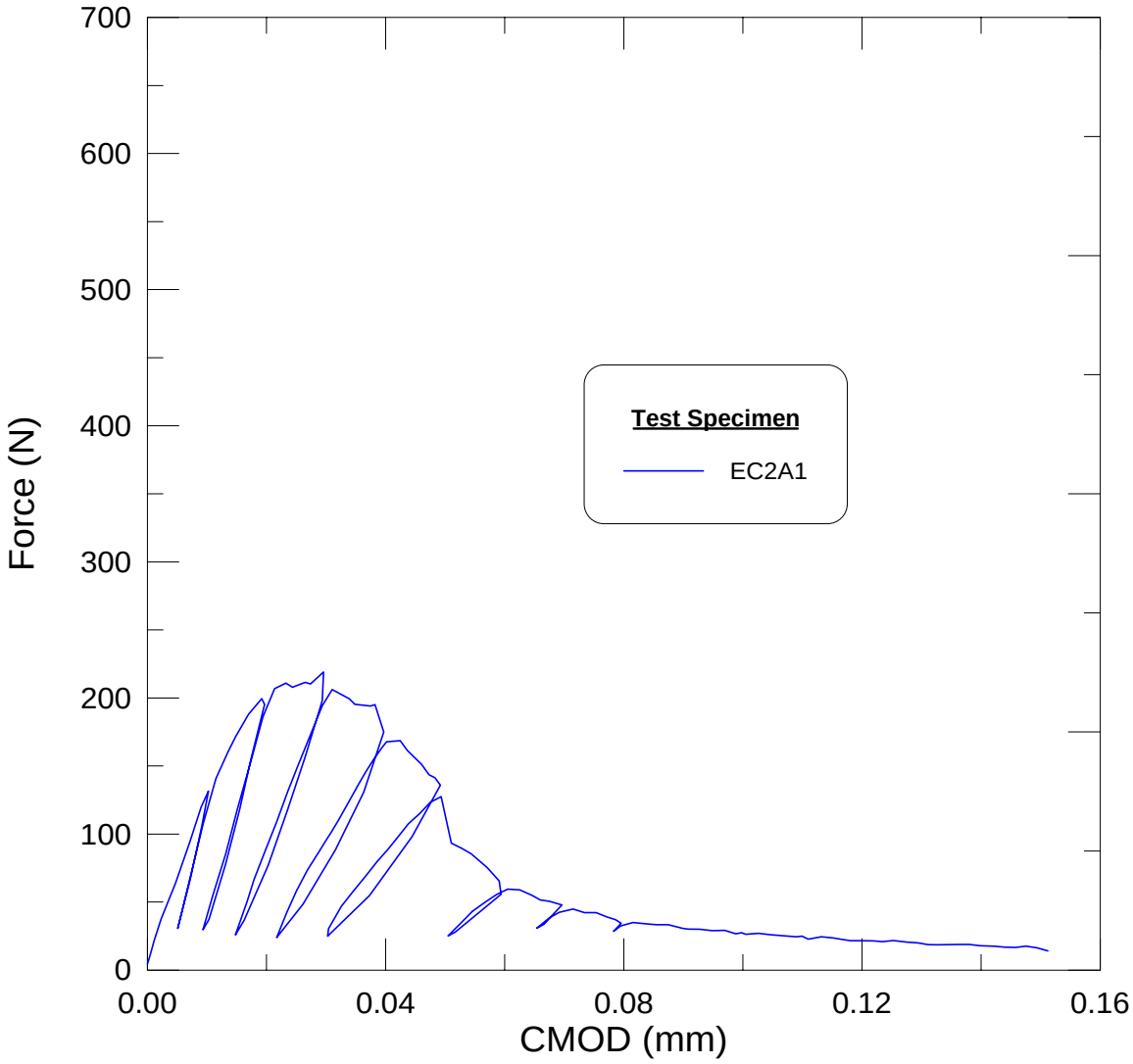
700
600
500
400
300
200
100
0
Force (N)
0.00
0.04
0.08
0.12
0.16
CMOD (mm)
Test Specimen
EC2A1

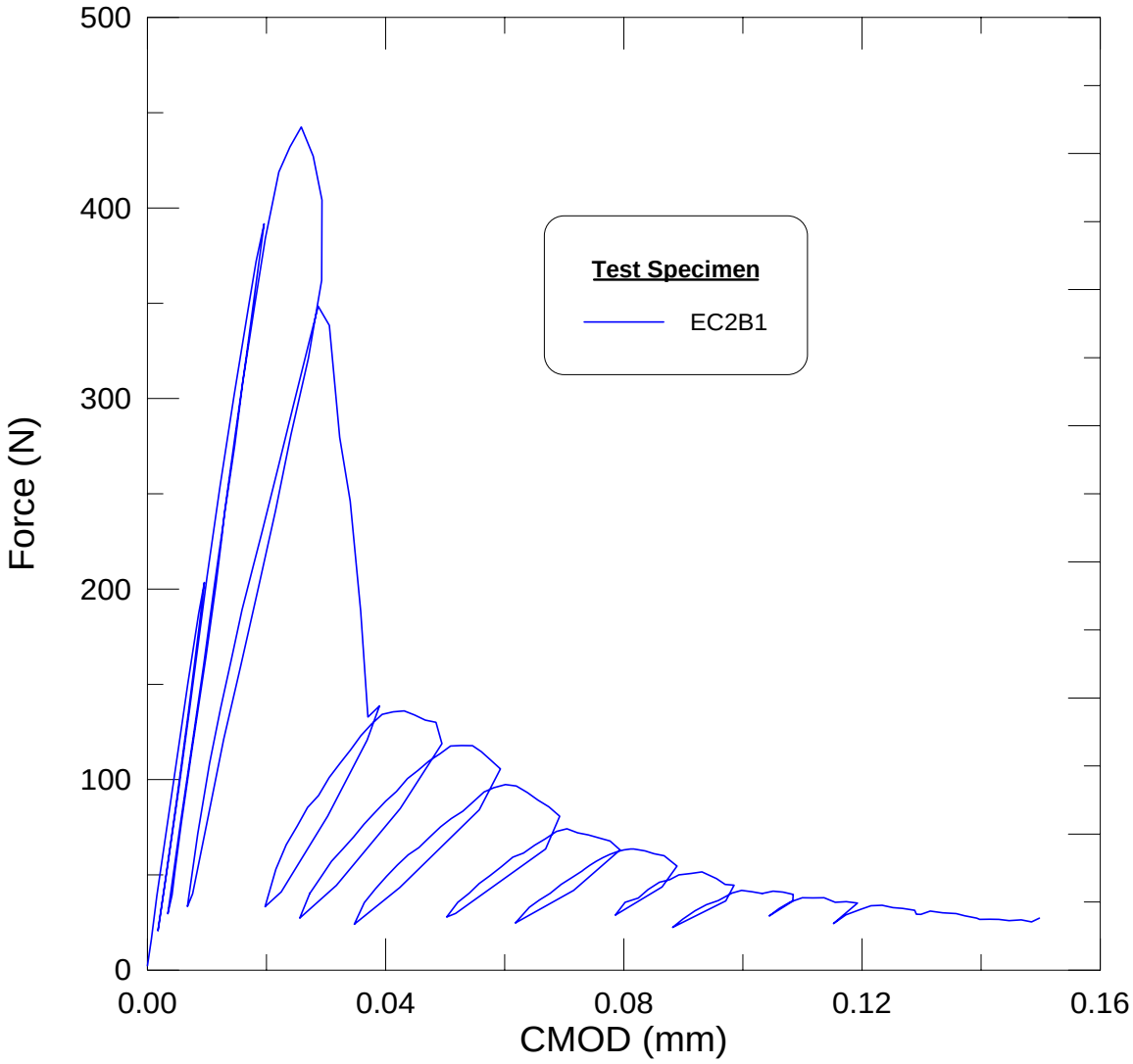
500
400
300
200
100
0
Force (N)
0.00
0.04
0.08
0.12
0.16
CMOD (mm)
Test Specimen
EC2B1

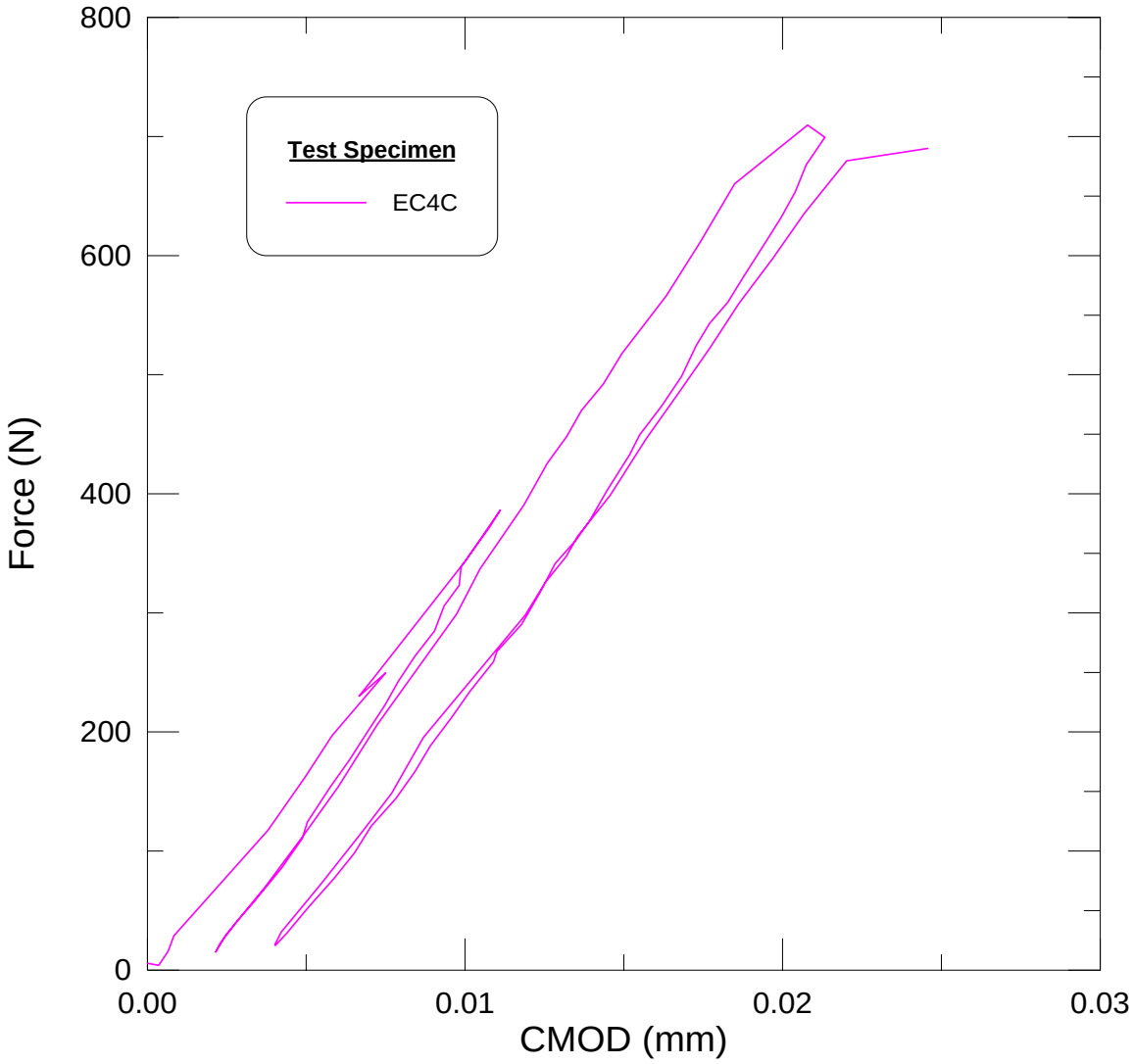
Test Specimen
EC4C
800
600
400
200
0
Force (N)
0.00
0.01
0.02
0.03
CMOD (mm)

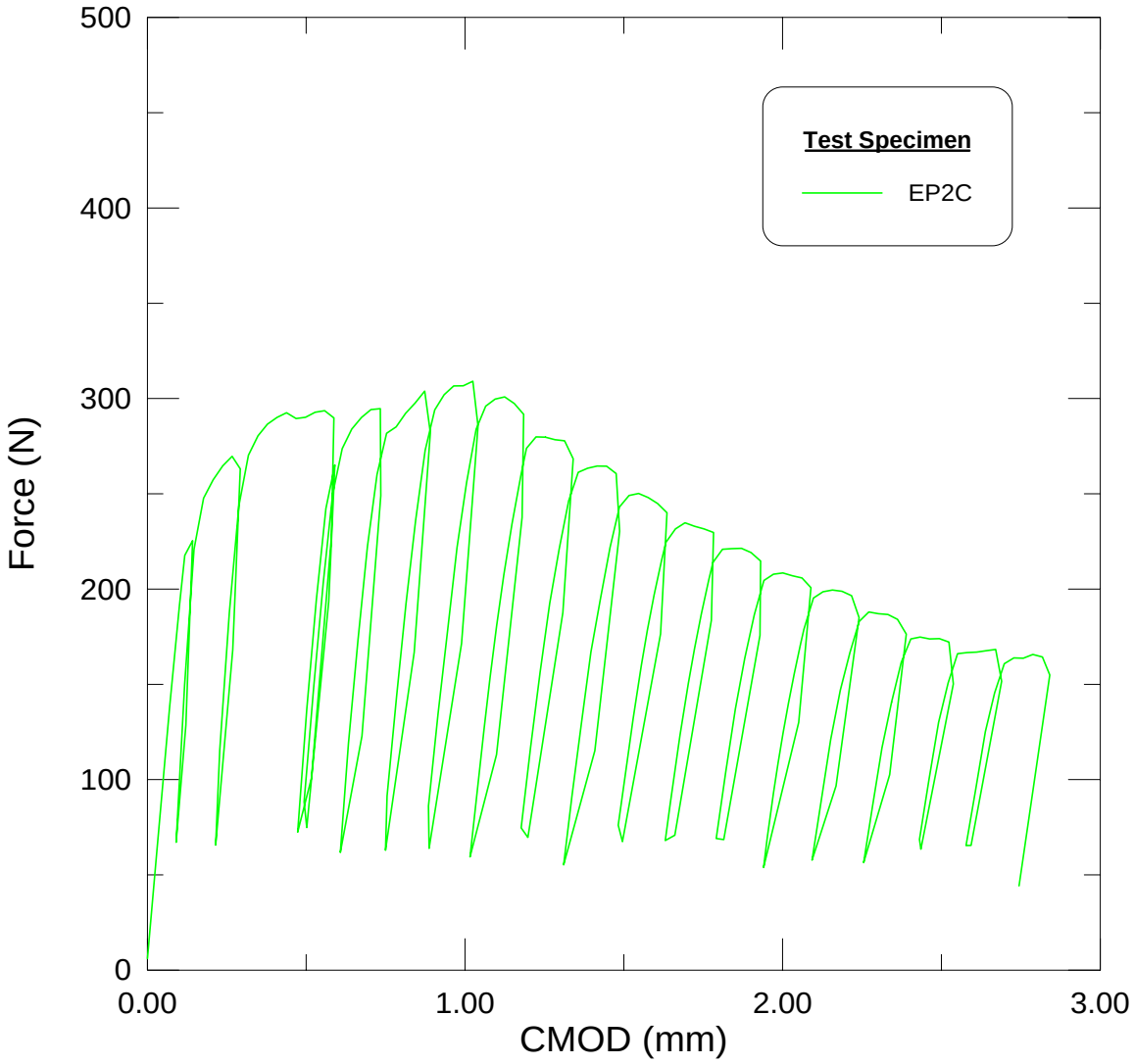
Test Specimen
EP2C
Force (N)
CMOD (mm)
0
100
200
300
400
500
0.00
1.00
2.00
3.00

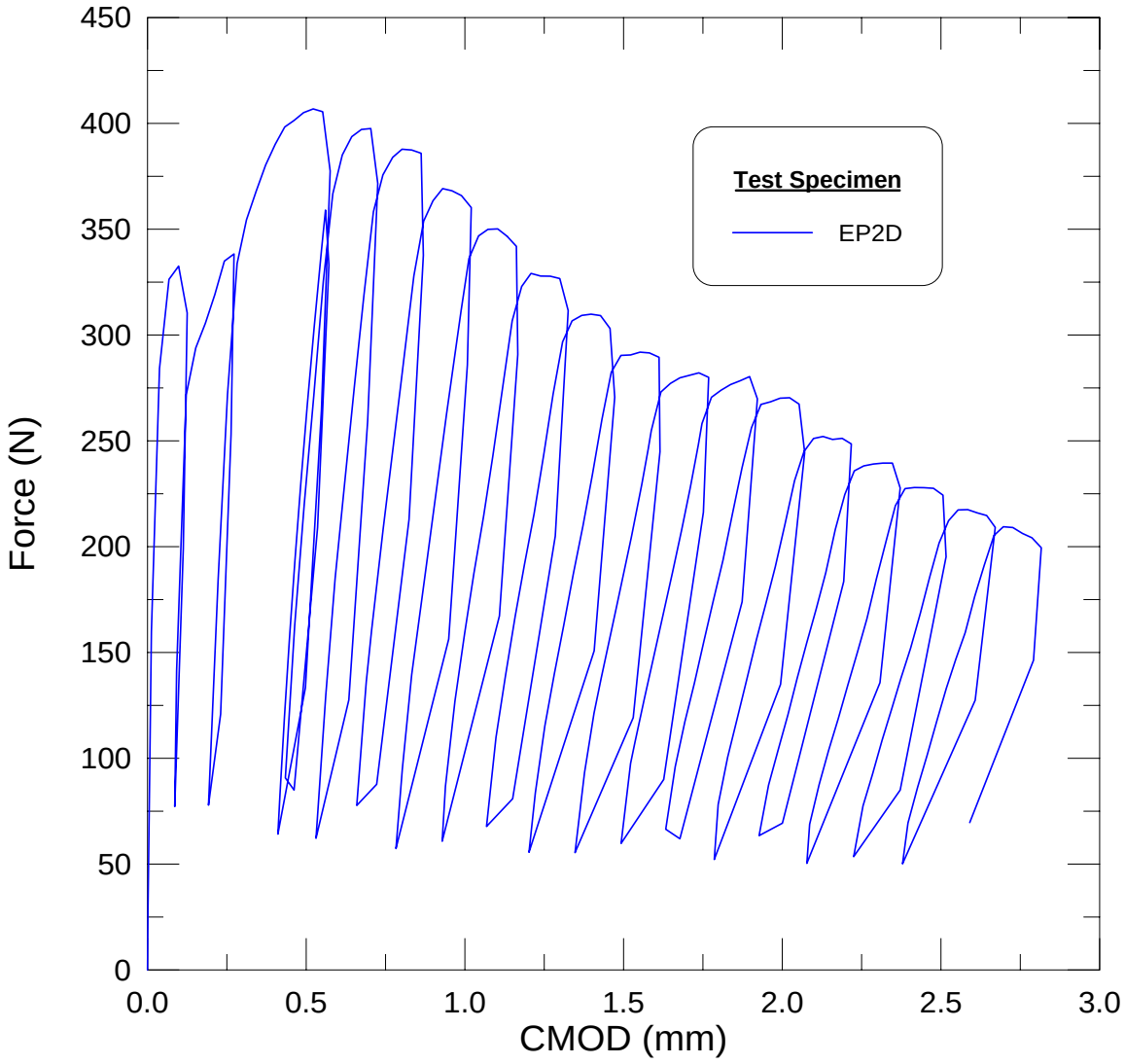
Test Specimen
EP2D
Force (N)
CMOD (mm)
0
50
100
150
200
250
300
350
400
450
0.0
0.5
1.0
1.5
2.0
2.5
3.0

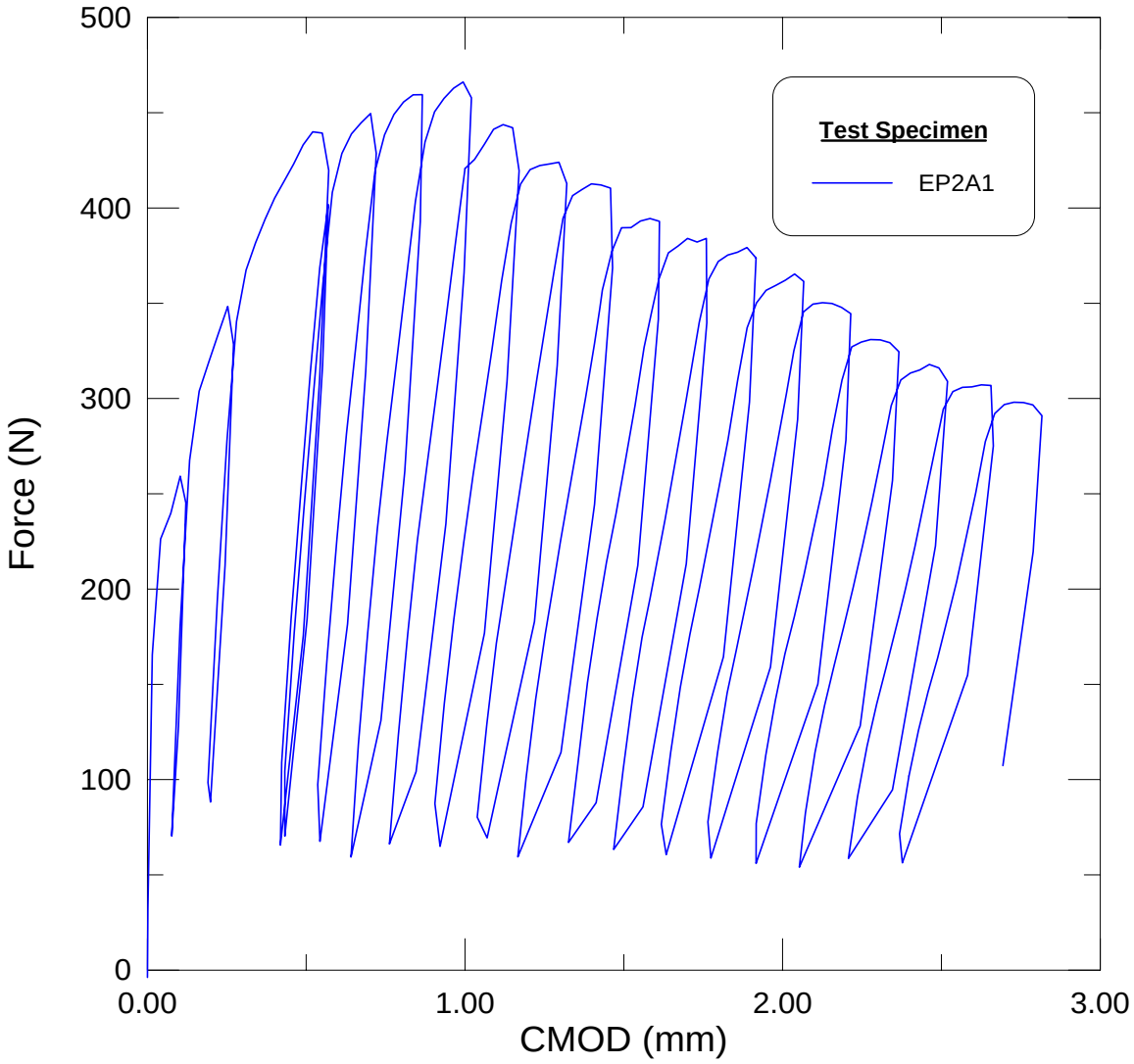
Test Specimen
EP2A1
Force (N)
CMOD (mm)
0
100
200
300
400
500
0.00
1.00
2.00
3.00

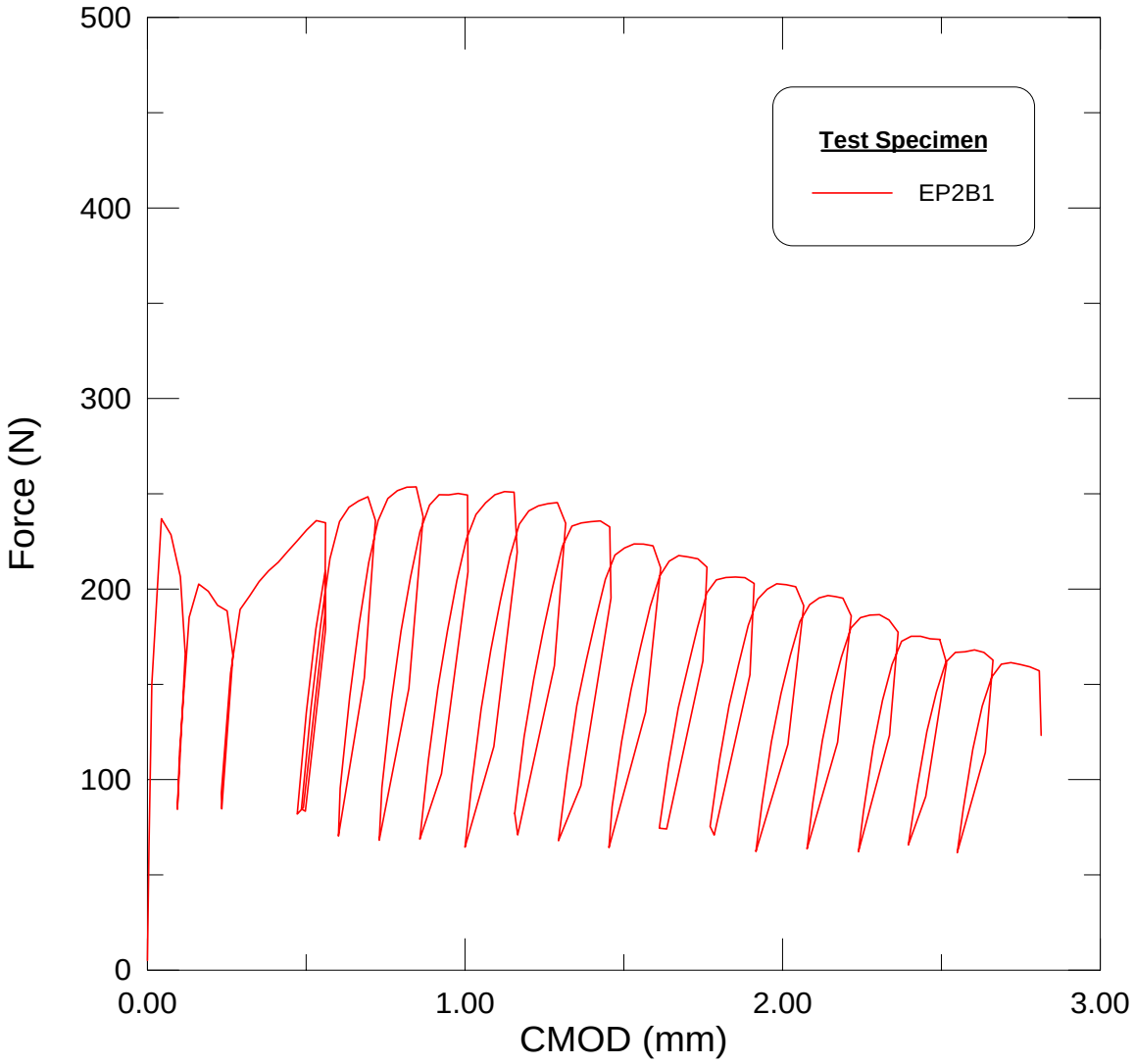
Test Specimen
EP2B1
Force (N)
CMOD (mm)
0
100
200
300
400
500
0.00
1.00
2.00
3.00

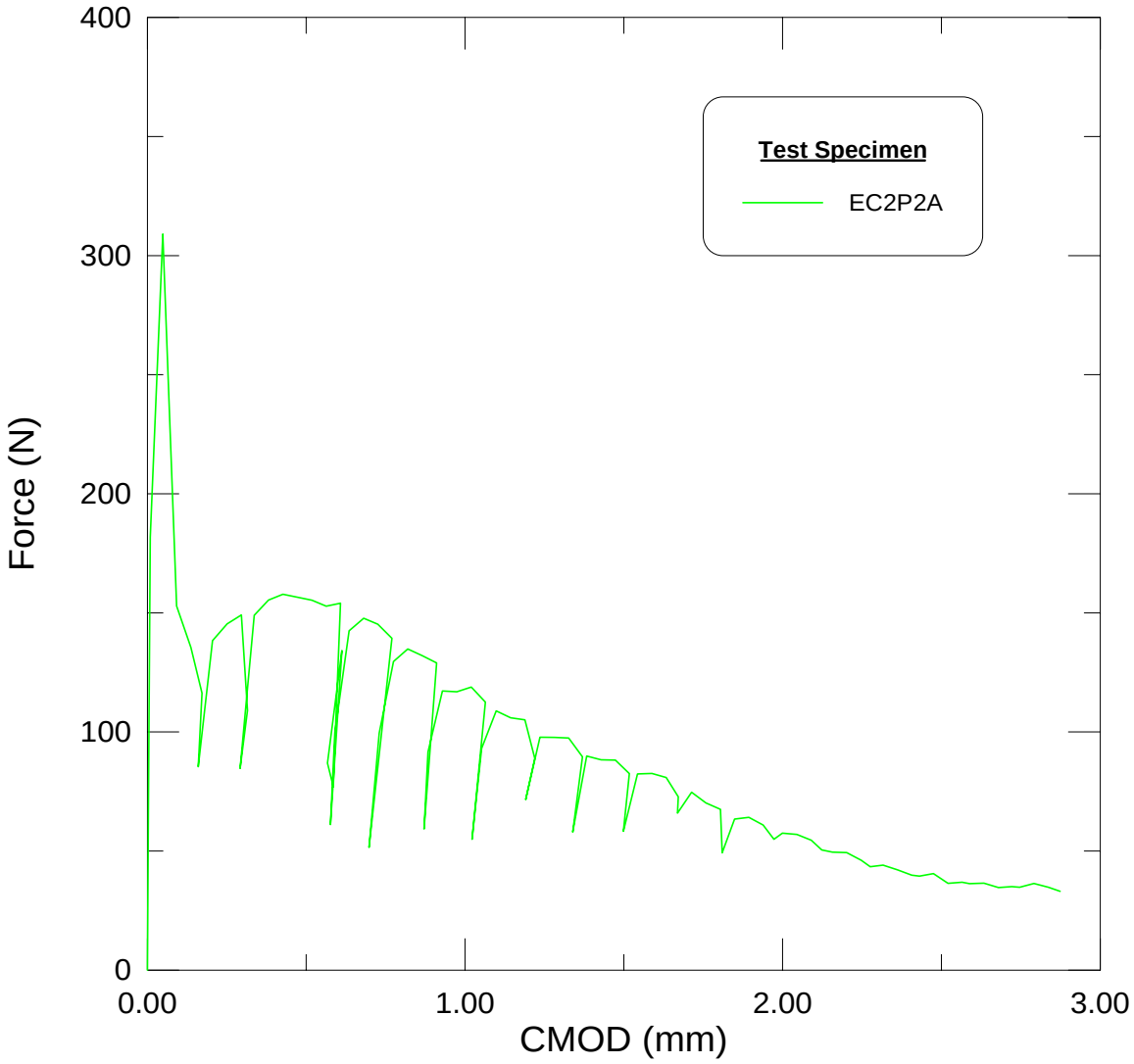
Test Specimen
EC2P2A
Force (N)
CMOD (mm)
0
100
200
300
400
0.00
1.00
2.00
3.00

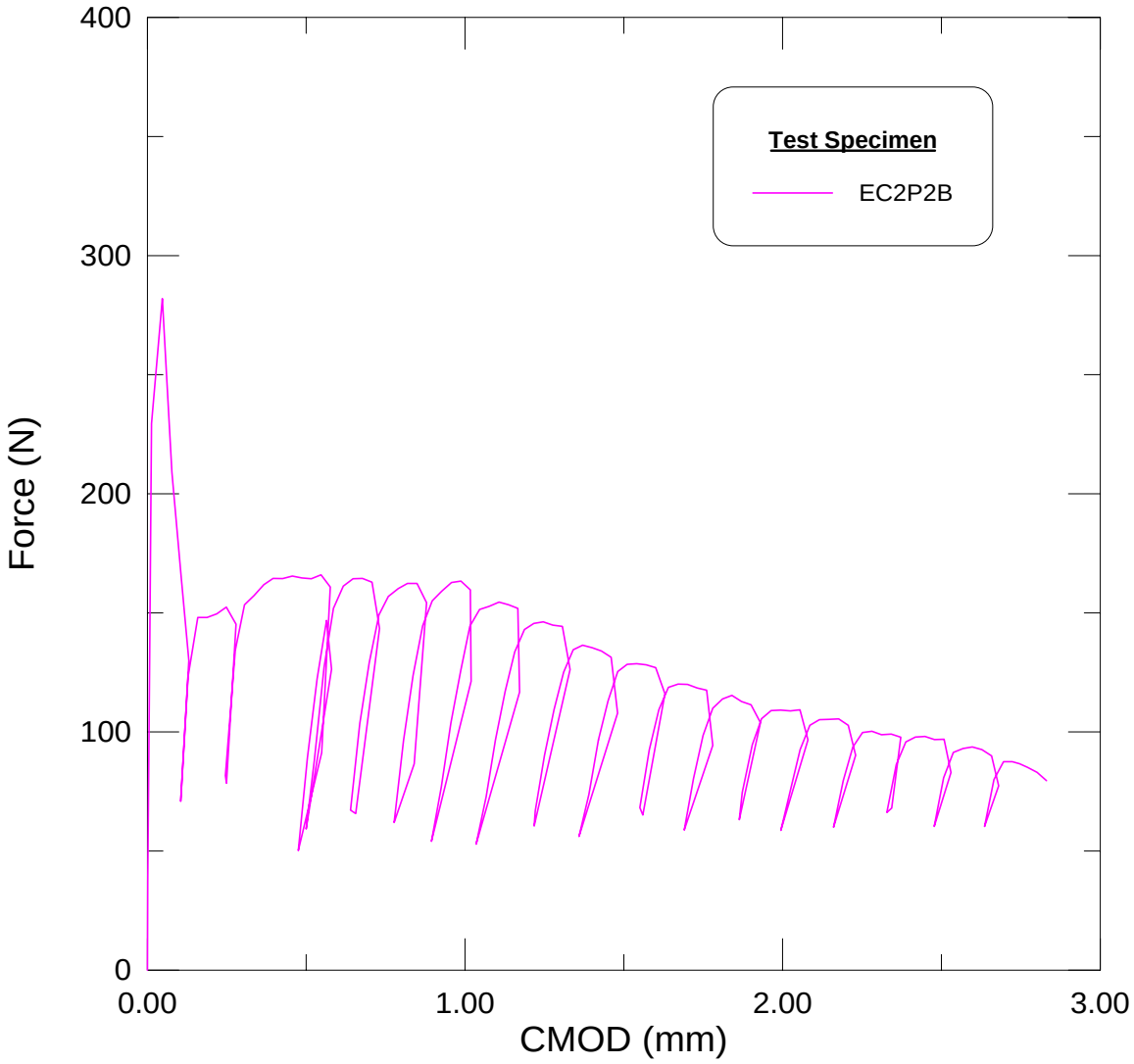
Test Specimen
EC2P2B
Force (N)
CMOD (mm)
0
100
200
300
400
0.00
1.00
2.00
3.00

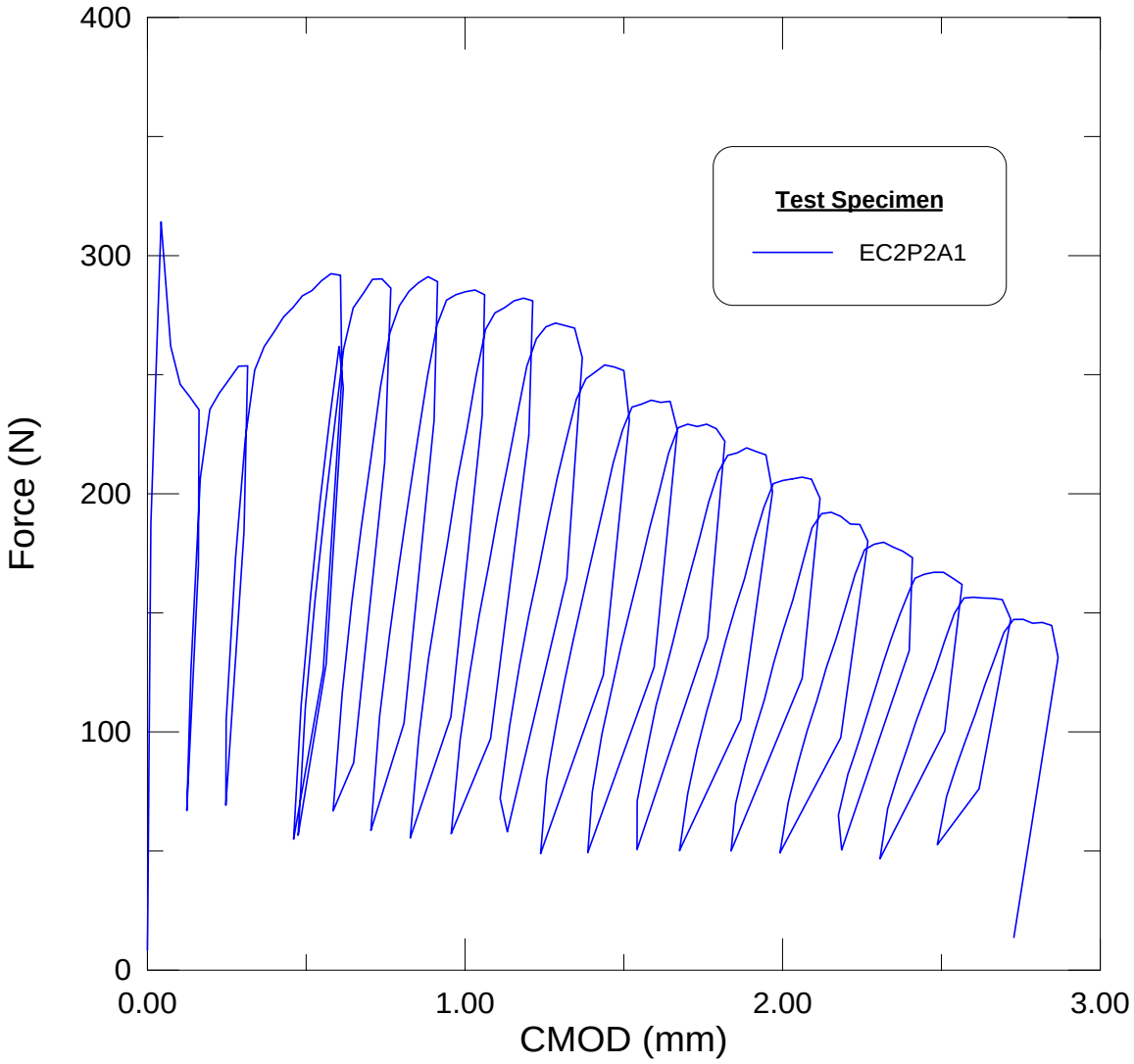
400
300
200
100
0
Force (N)
0.00
1.00
2.00
3.00
CMOD (mm)
Test Specimen
EC2P2A1

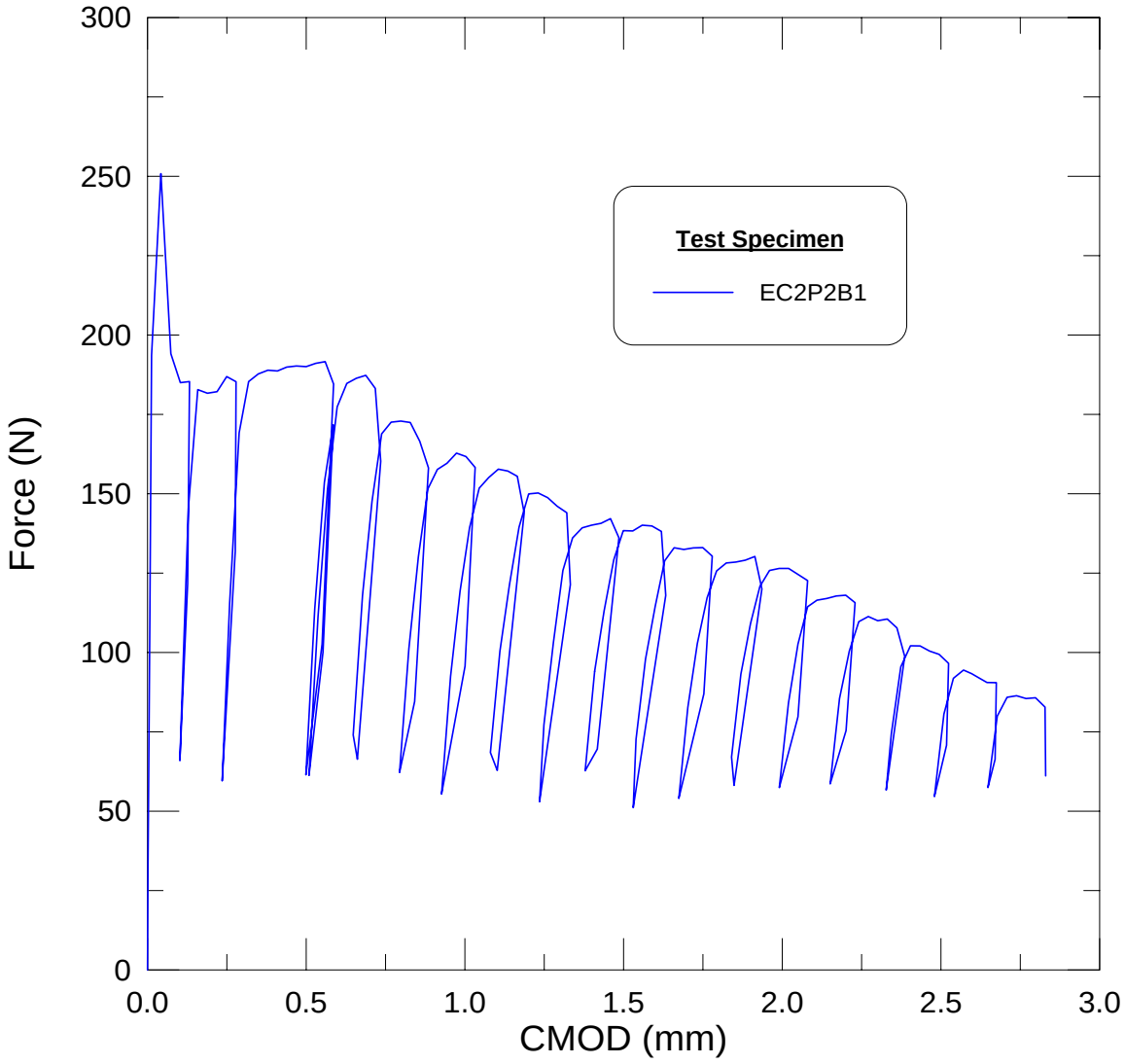
Test Specimen
EC2P2B1
Force (N)
CMOD (mm)
0
50
100
150
200
250
300
0.0
0.5
1.0
1.5
2.0
2.5
3.0

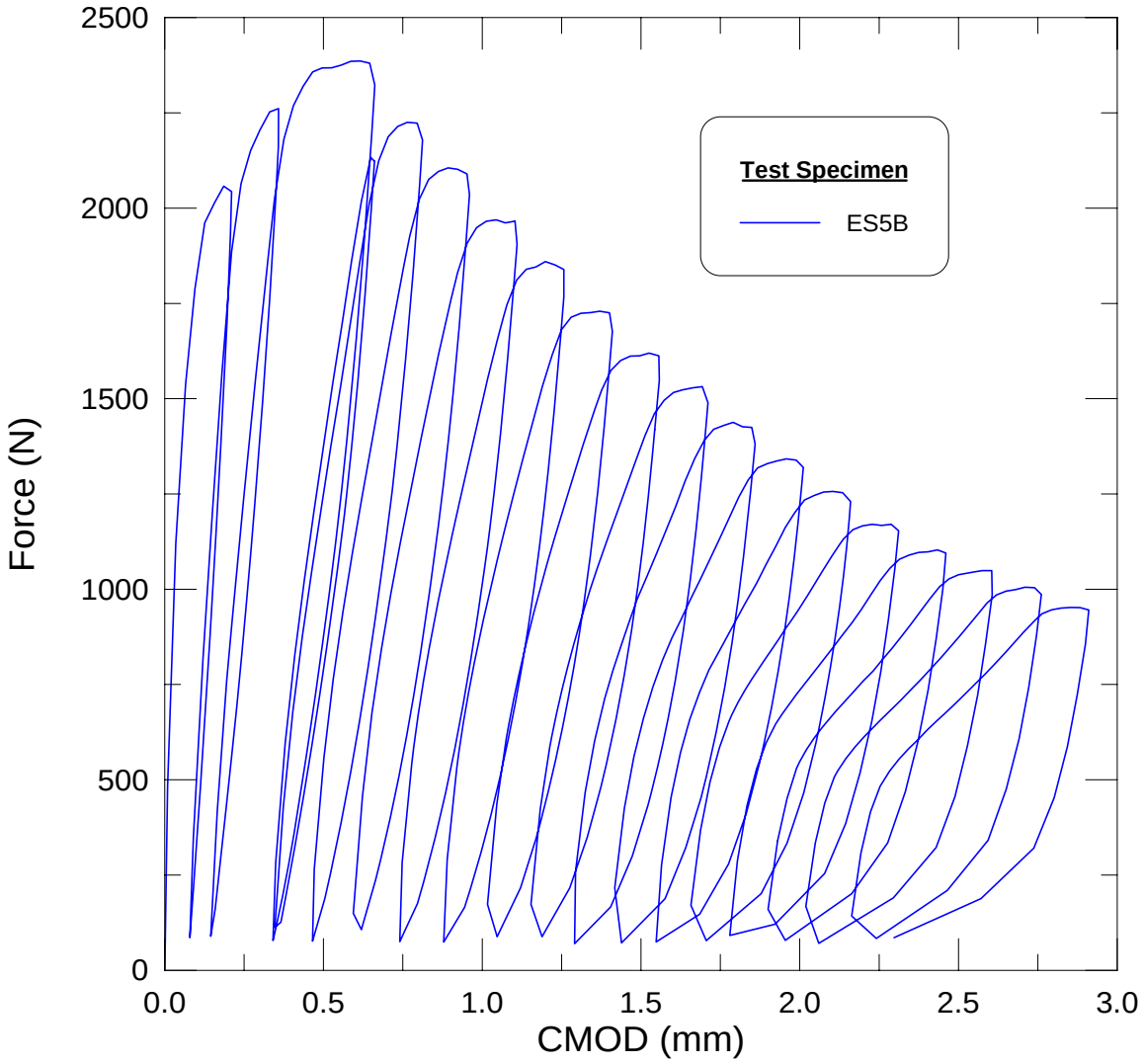
Test Specimen
ES5B
Force (N)
CMOD (mm)
0
500
1000
1500
2000
2500
0.0
0.5
1.0
1.5
2.0
2.5
3.0

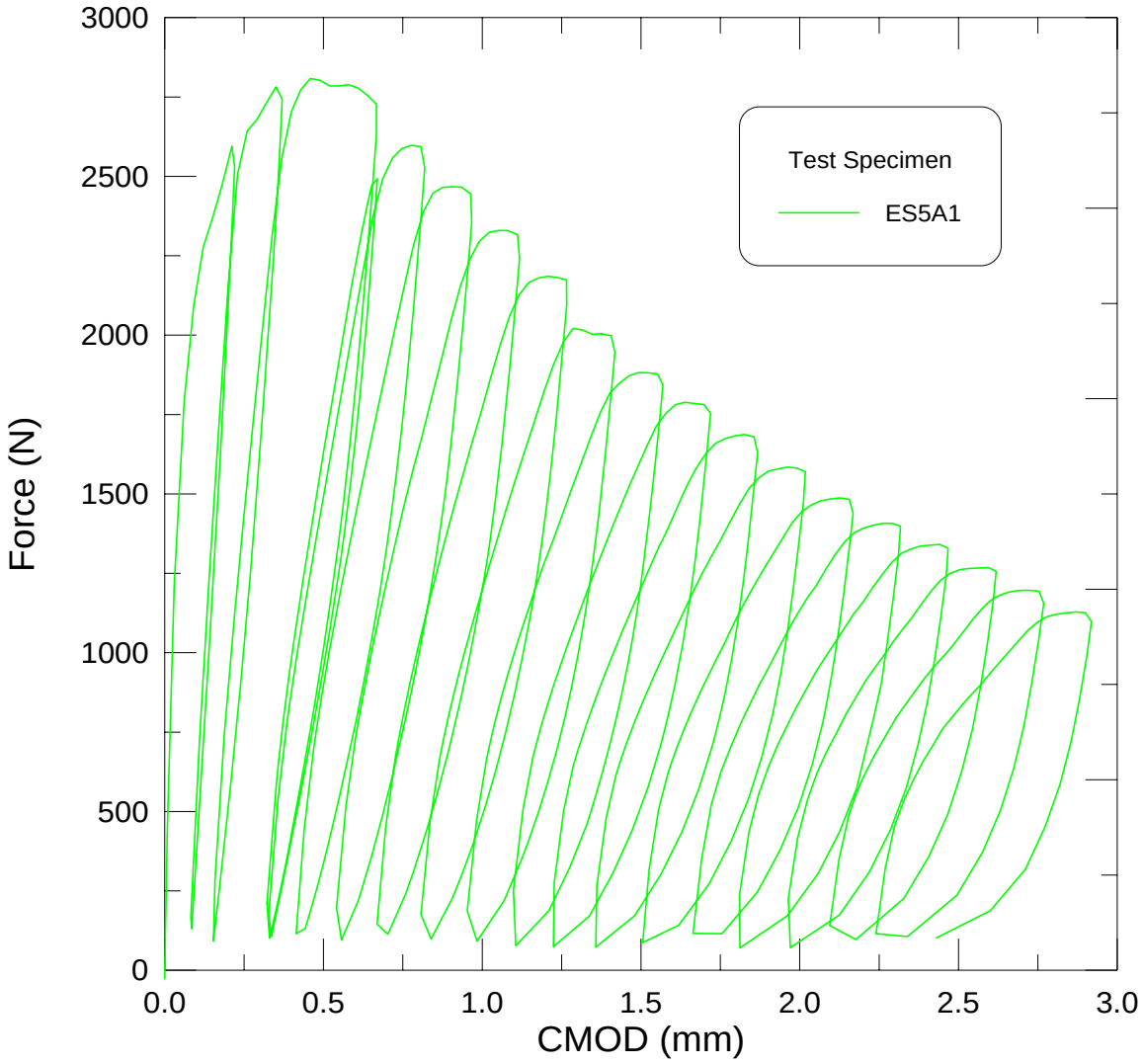
Test Specimen
ES5A1
Force (N)
CMOD (mm)
0
500
1000
1500
2000
2500
3000
0.0
0.5
1.0
1.5
2.0
2.5
3.0

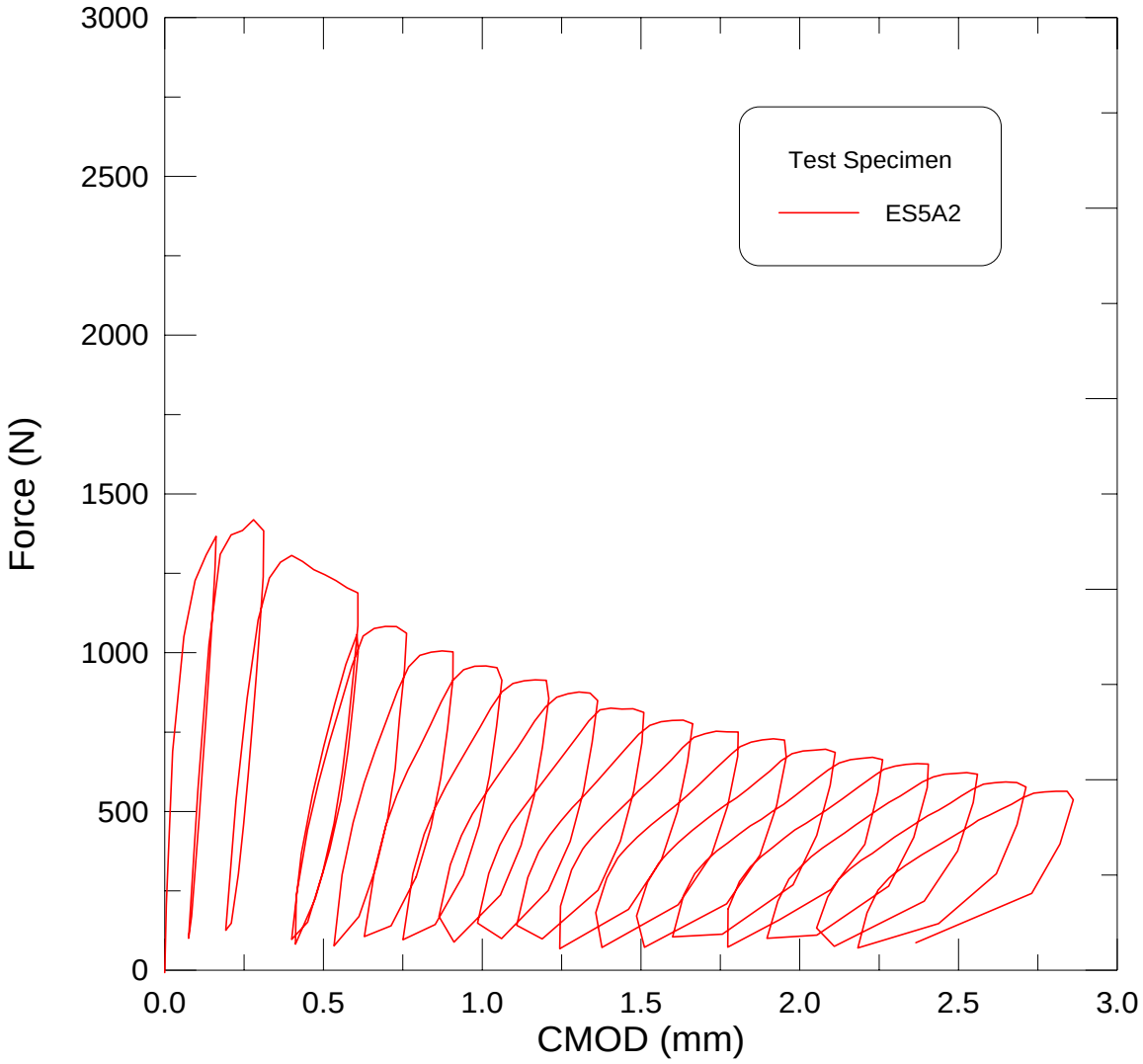
Test Specimen
ES5A2
Force (N)
CMOD (mm)
0
500
1000
1500
2000
2500
3000
0.0
0.5
1.0
1.5
2.0
2.5
3.0

APPENDIX B

Shear test results

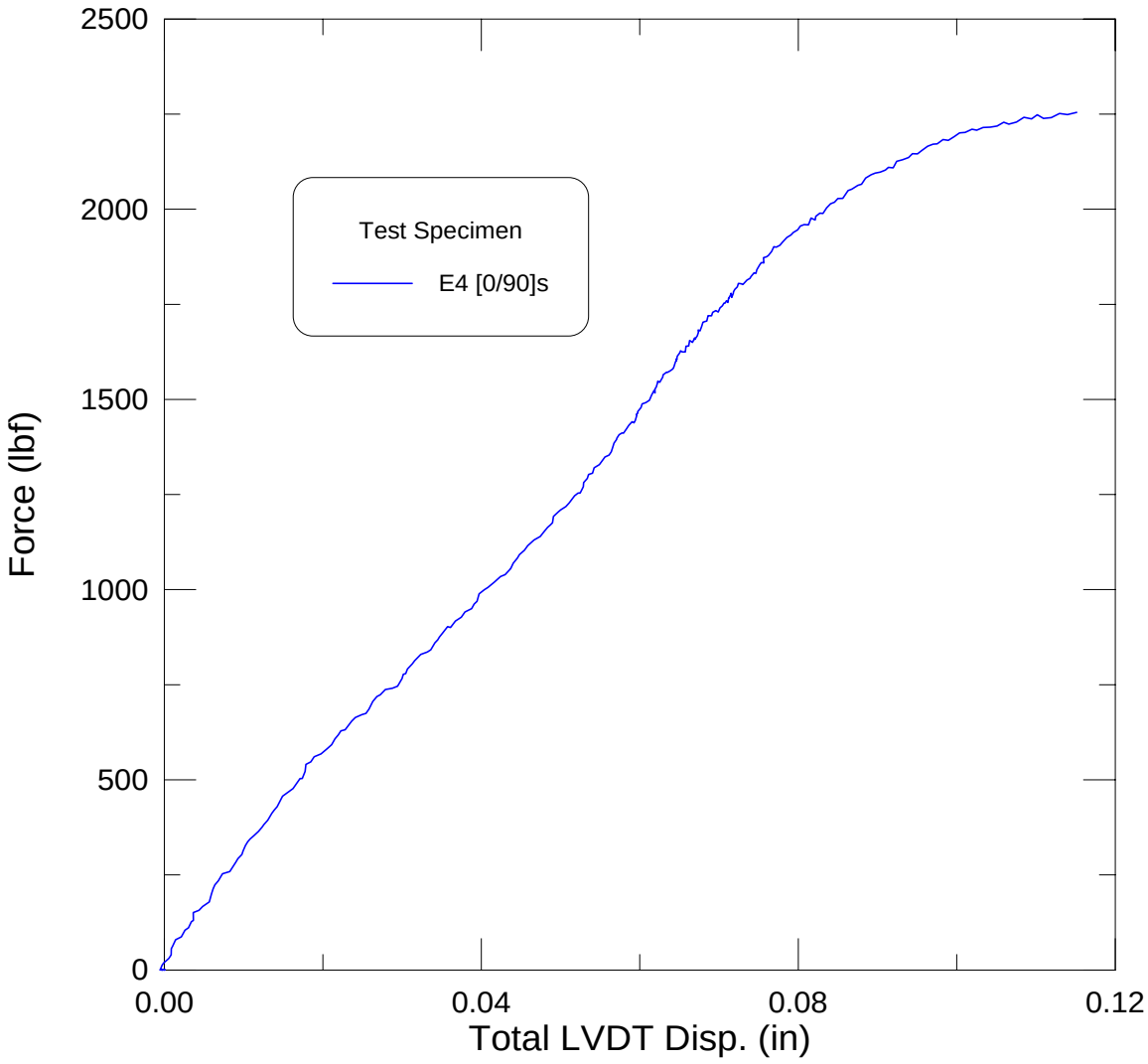
2500
2000
1500
1000
500
0
Force (lbf)
0.00
0.04
0.08
0.12
Total LVDT Disp. (in)
Test Specimen
E4 [0/90]s

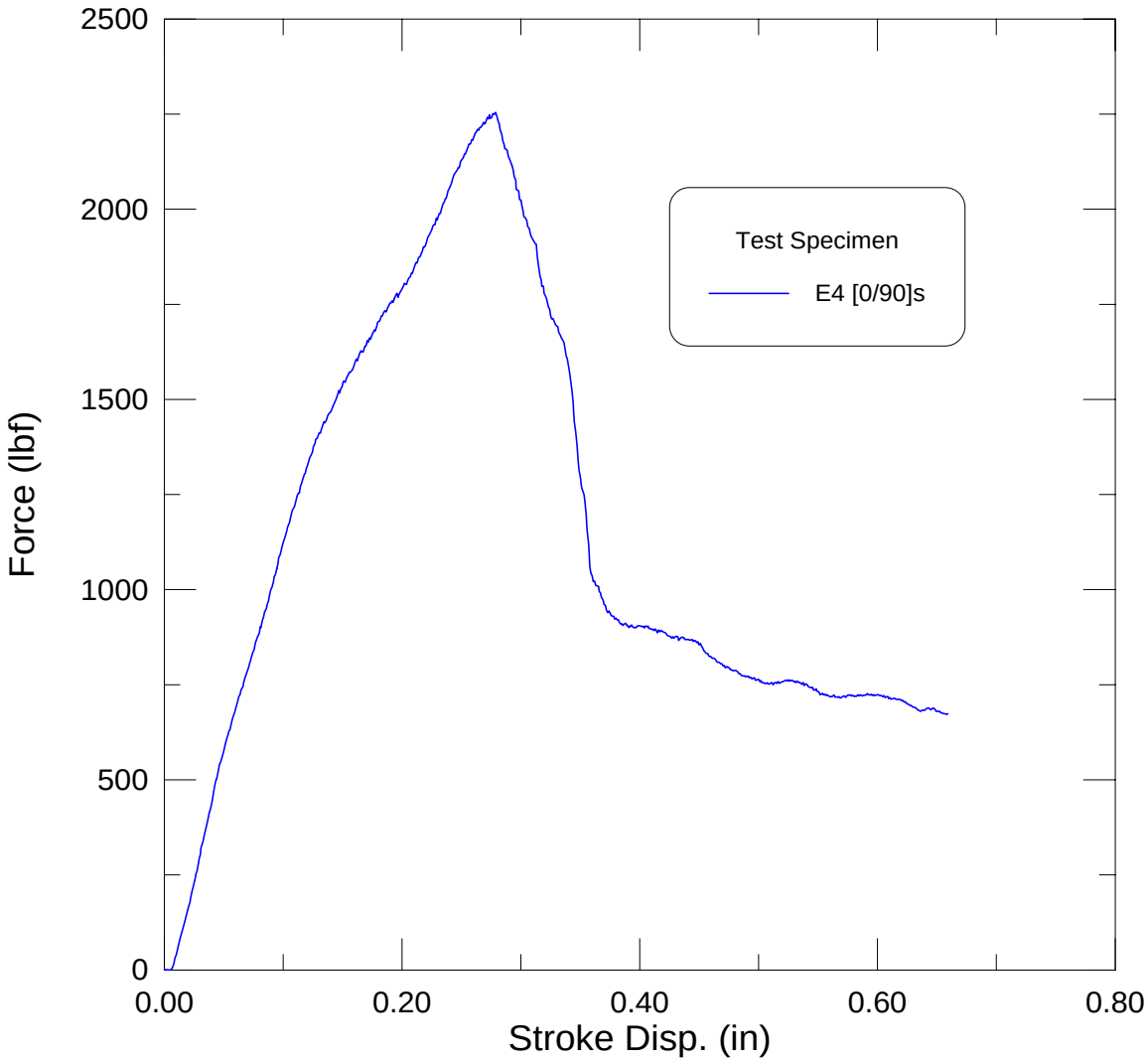
2500
2000
1500
1000
500
0
Force (lbf)
0.00
0.20
0.40
0.60
0.80
Stroke Disp. (in)
Test Specimen
E4 [0/90]s

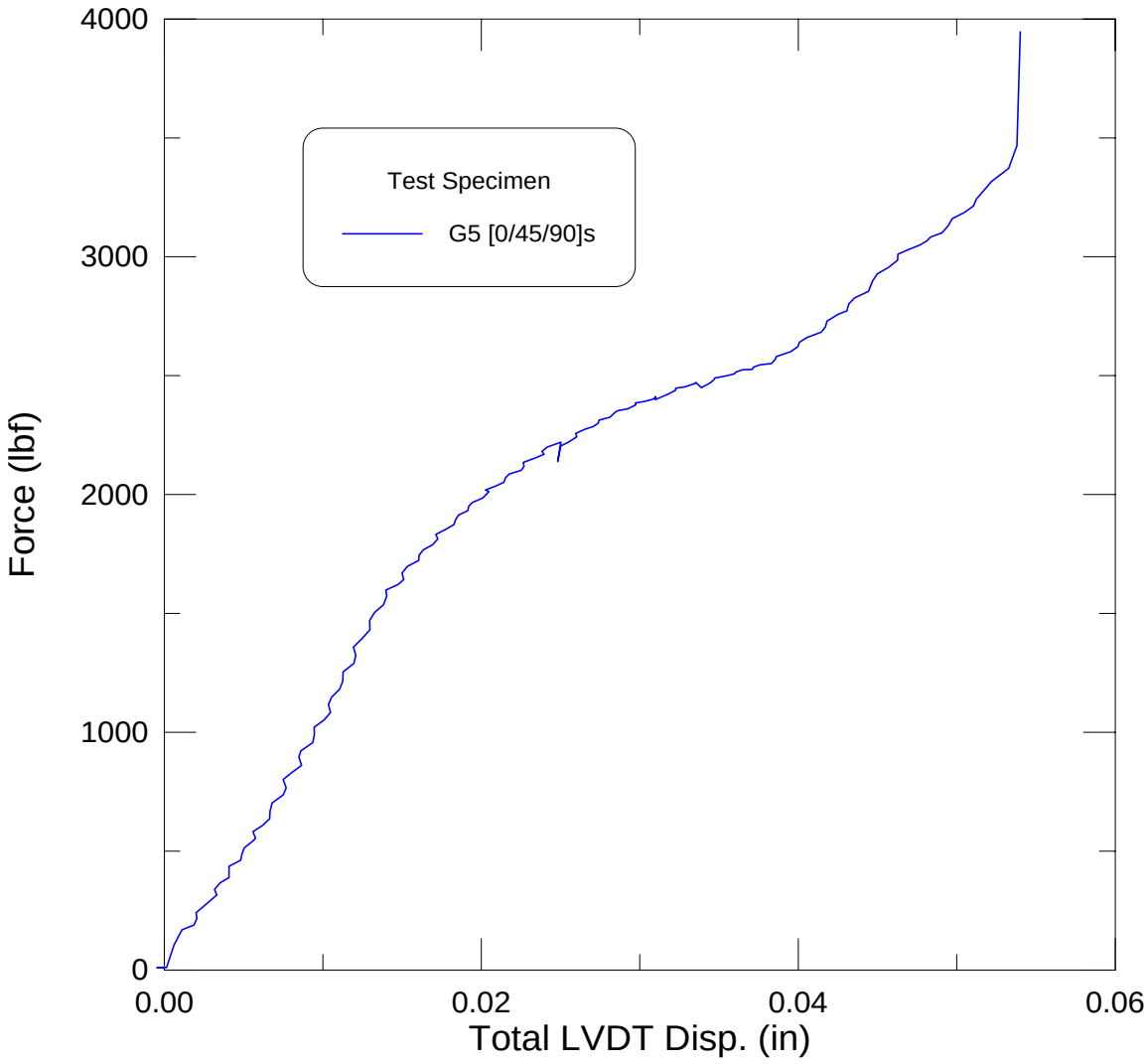
4000
3000
2000
1000
0
Force (lbf)
0.00
0.02
0.04
0.06
Total LVDT Disp. (in)
Test Specimen
G5 [0/45/90]s

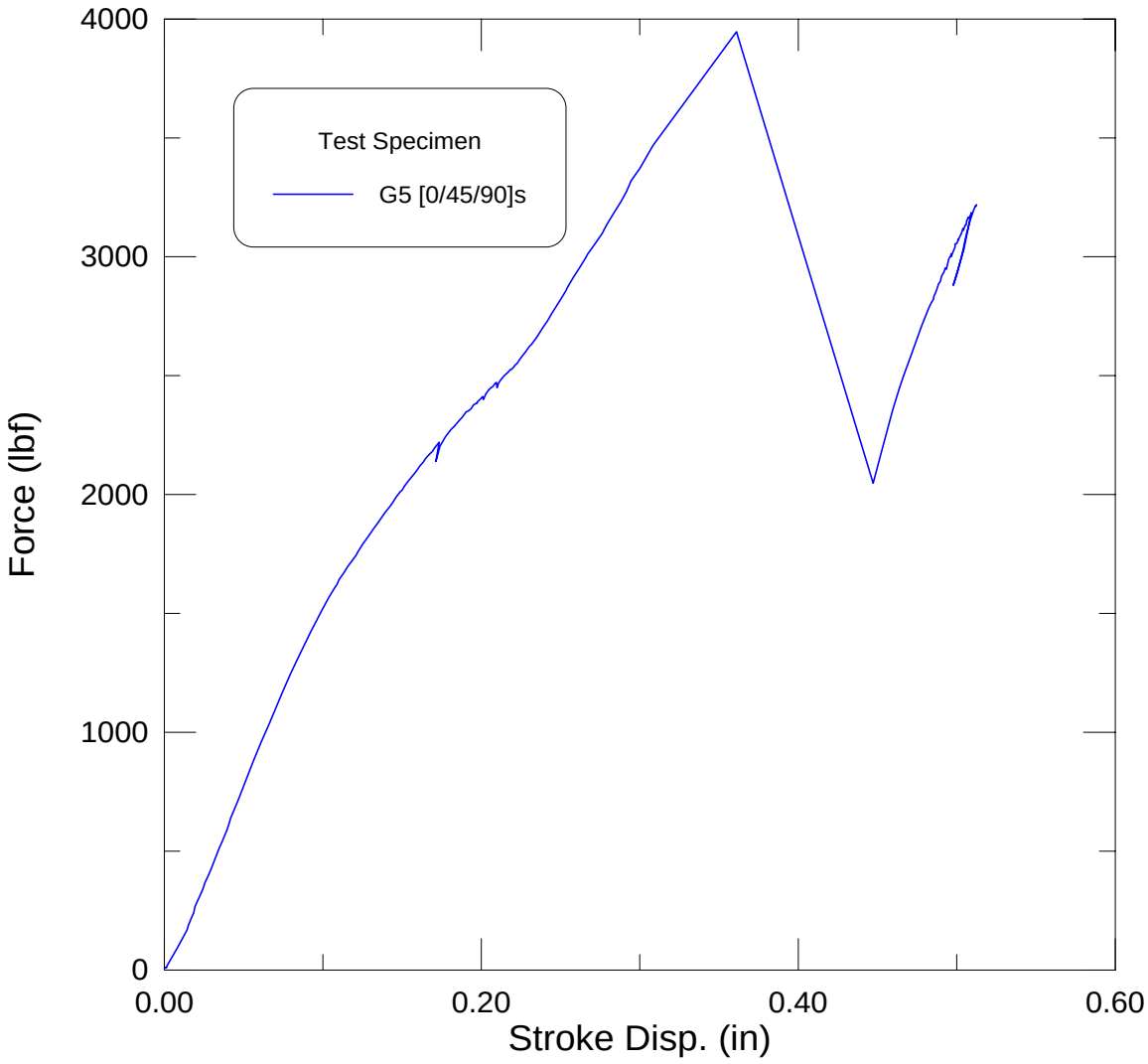
Test Specimen
G5 [0/45/90]s
Force (lbf)
Stroke Disp. (in)
4000
3000
2000
1000
0
0.00
0.20
0.40
0.60

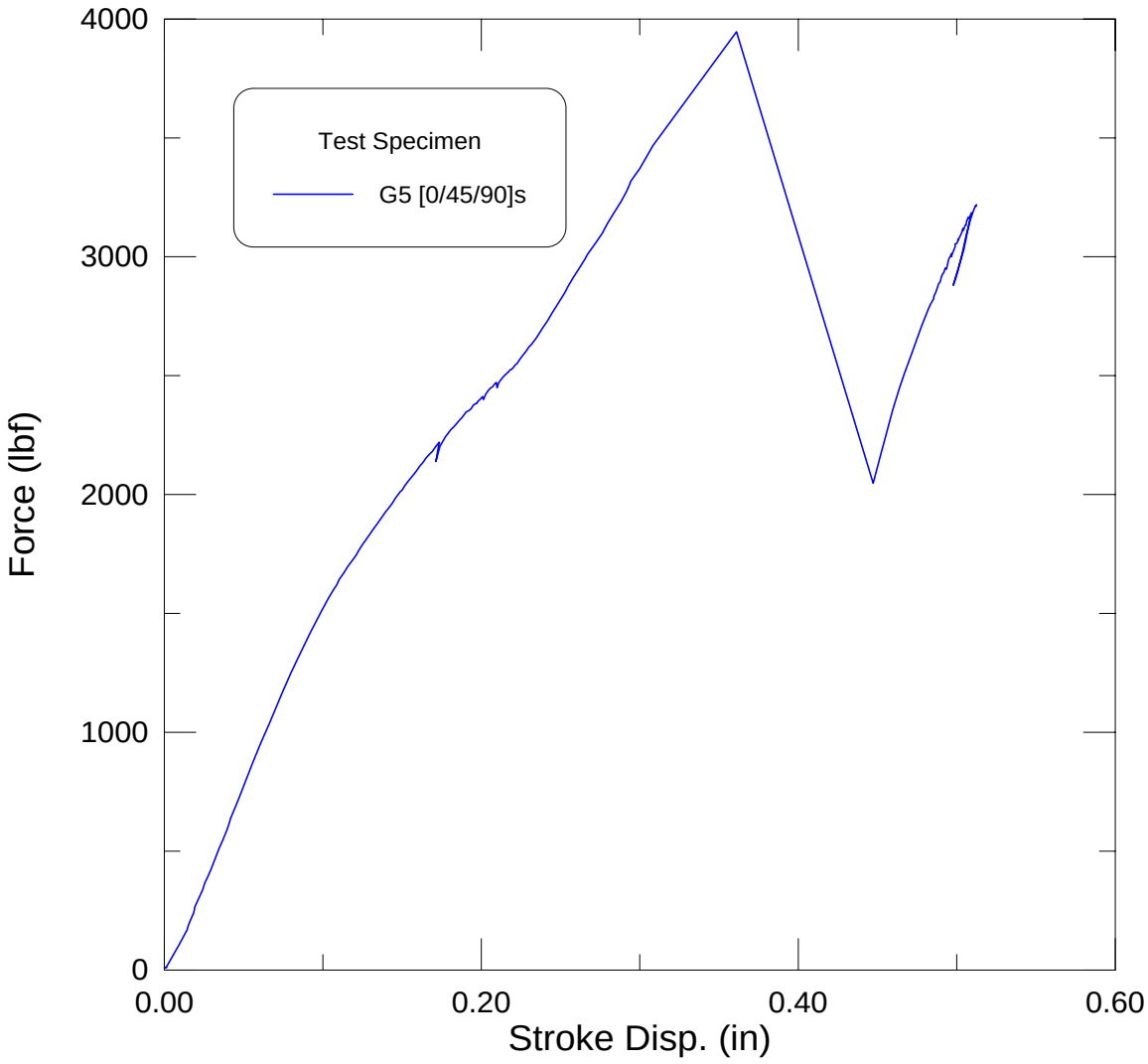
Test Specimen
G5 [0/45/90]s
Force (lbf)
Stroke Disp. (in)
4000
3000
2000
1000
0
0.00
0.20
0.40
0.60

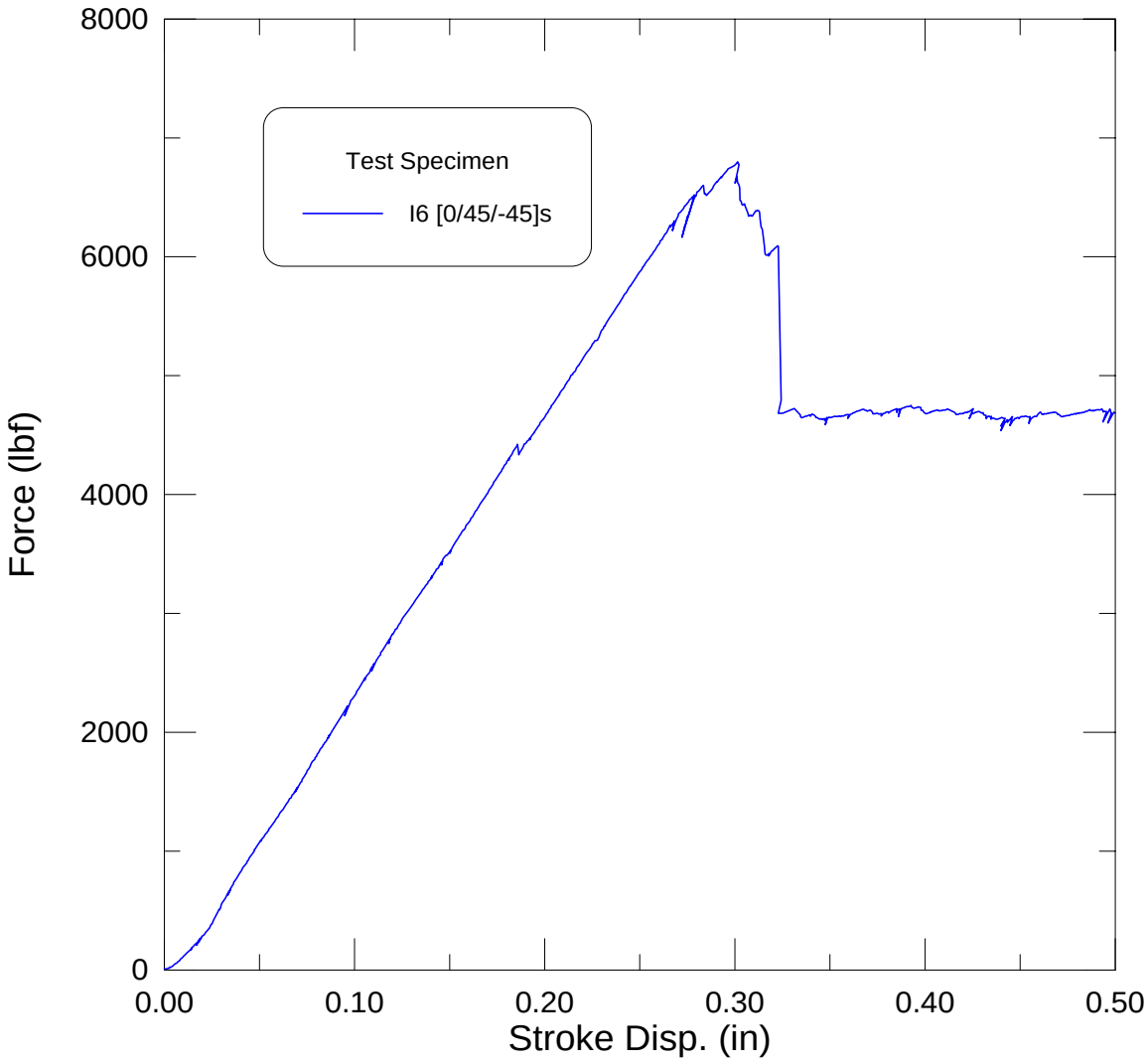
8000
6000
4000
2000
0
Force (lbf)
0.00
0.10
0.20
0.30
0.40
0.50
Stroke Disp. (in)
Test Specimen
I6 [0/45/-45]s

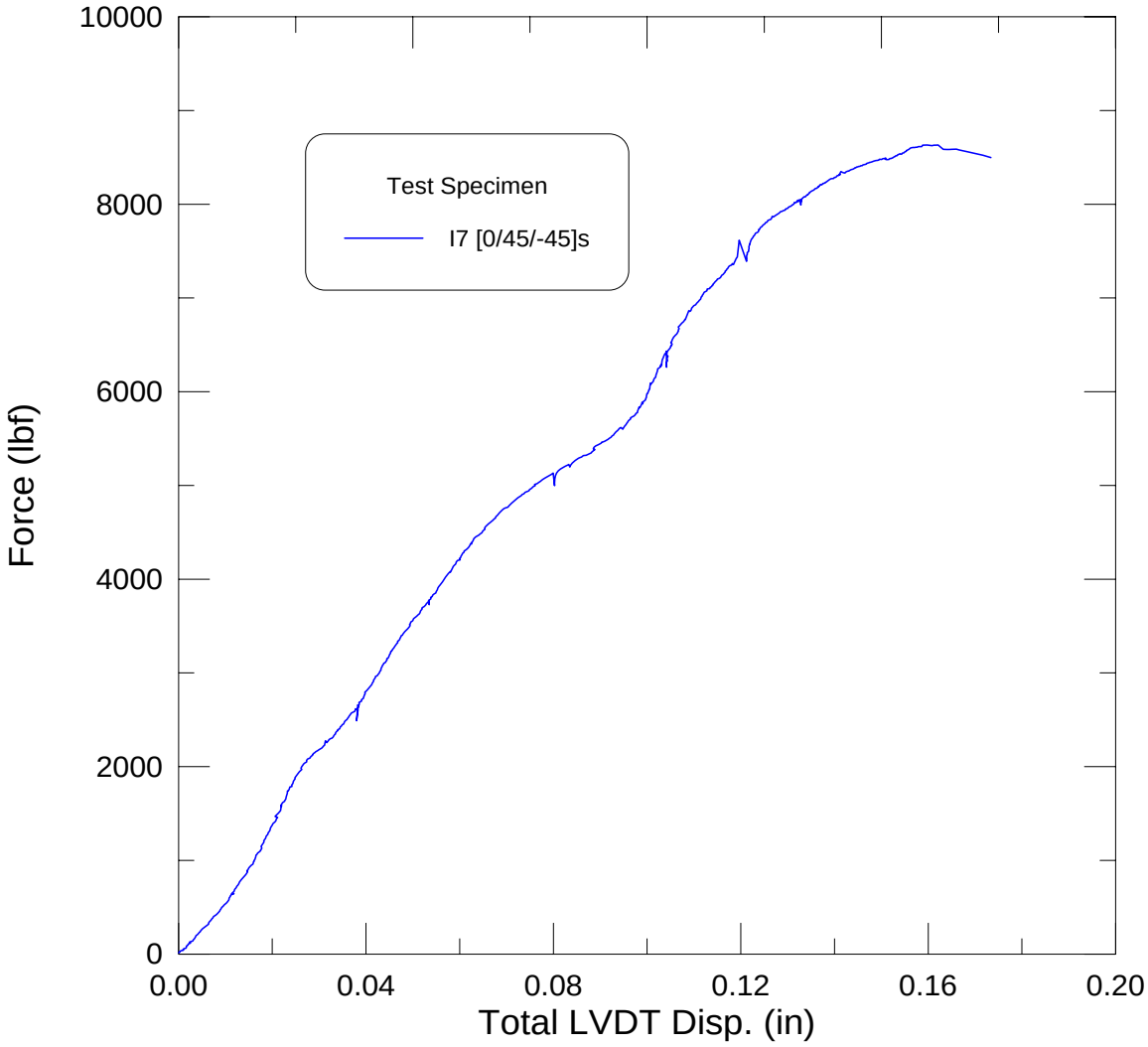
10000
8000
6000
4000
2000
0
Force (lbf)
0.00
0.04
0.08
0.12
0.16
0.20
Total LVDT Disp. (in)
Test Specimen
I7 [0/45/-45]s

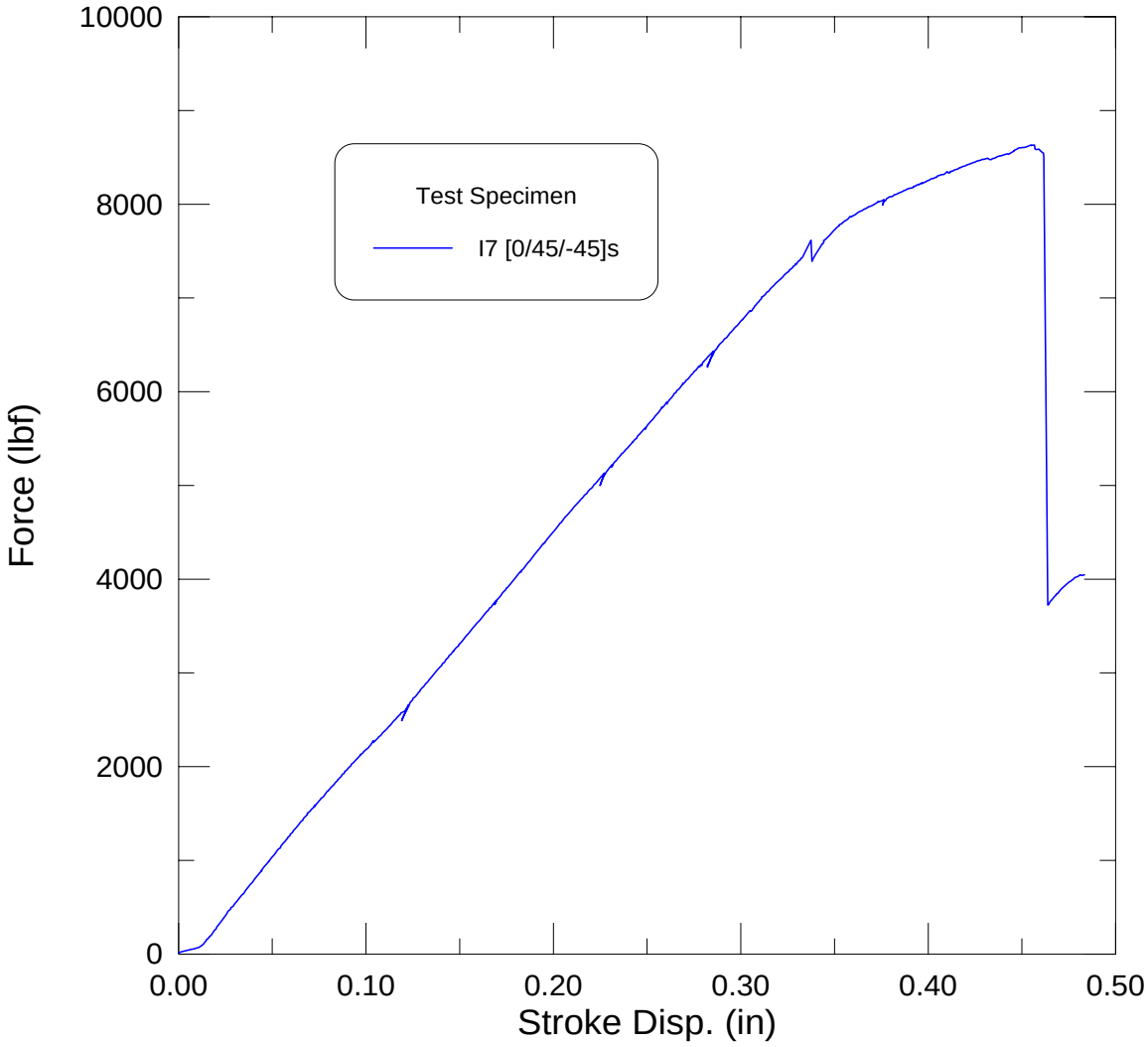
10000
8000
6000
4000
2000
0
Force (lbf)
0.00
0.10
0.20
0.30
0.40
0.50
Stroke Disp. (in)
Test Specimen
I7 [0/45/-45]s

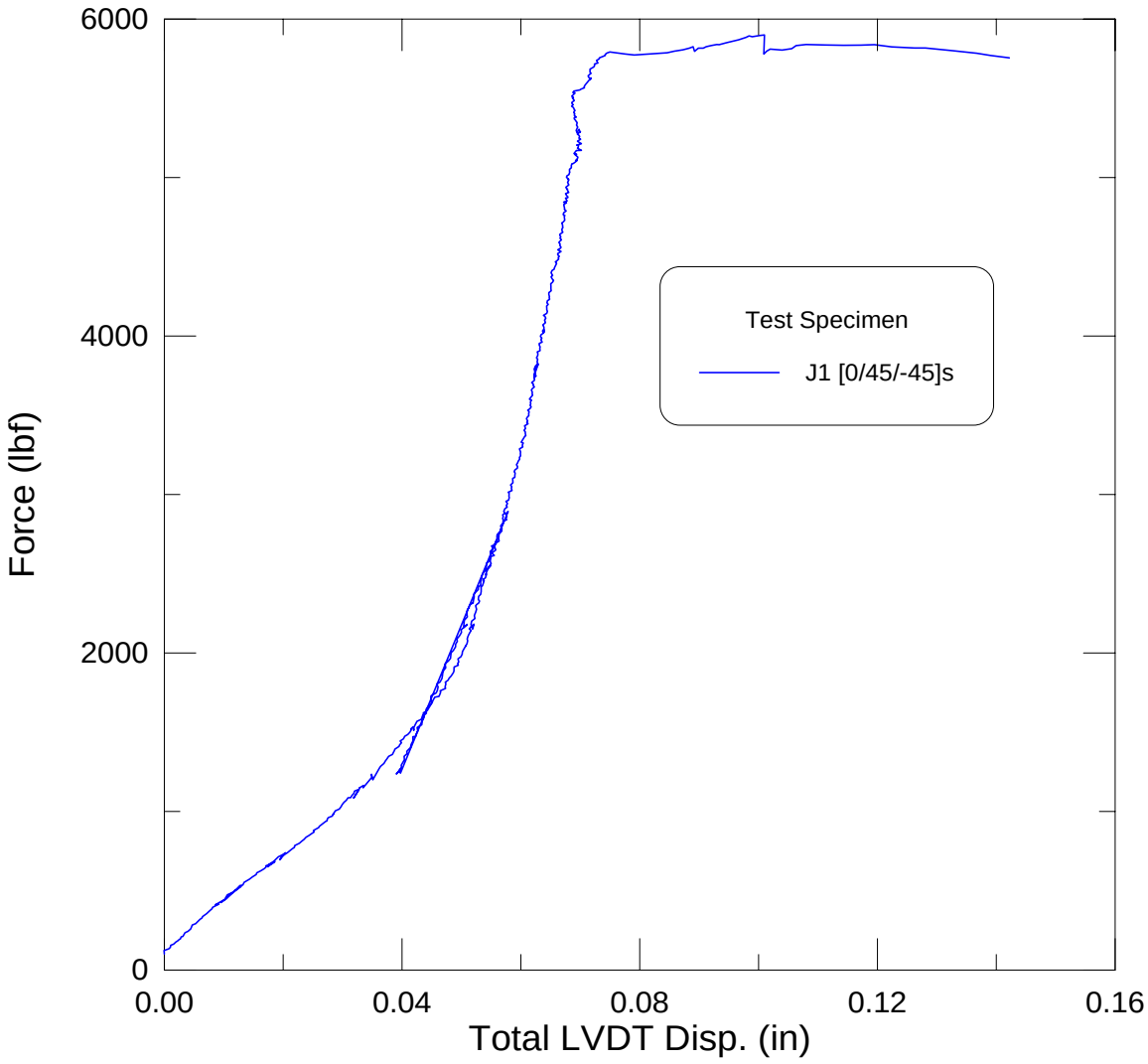
6000
4000
2000
0
Force (lbf)
0.00
0.04
0.08
0.12
0.16
Total LVDT Disp. (in)
Test Specimen
J1 [0/45/-45]s

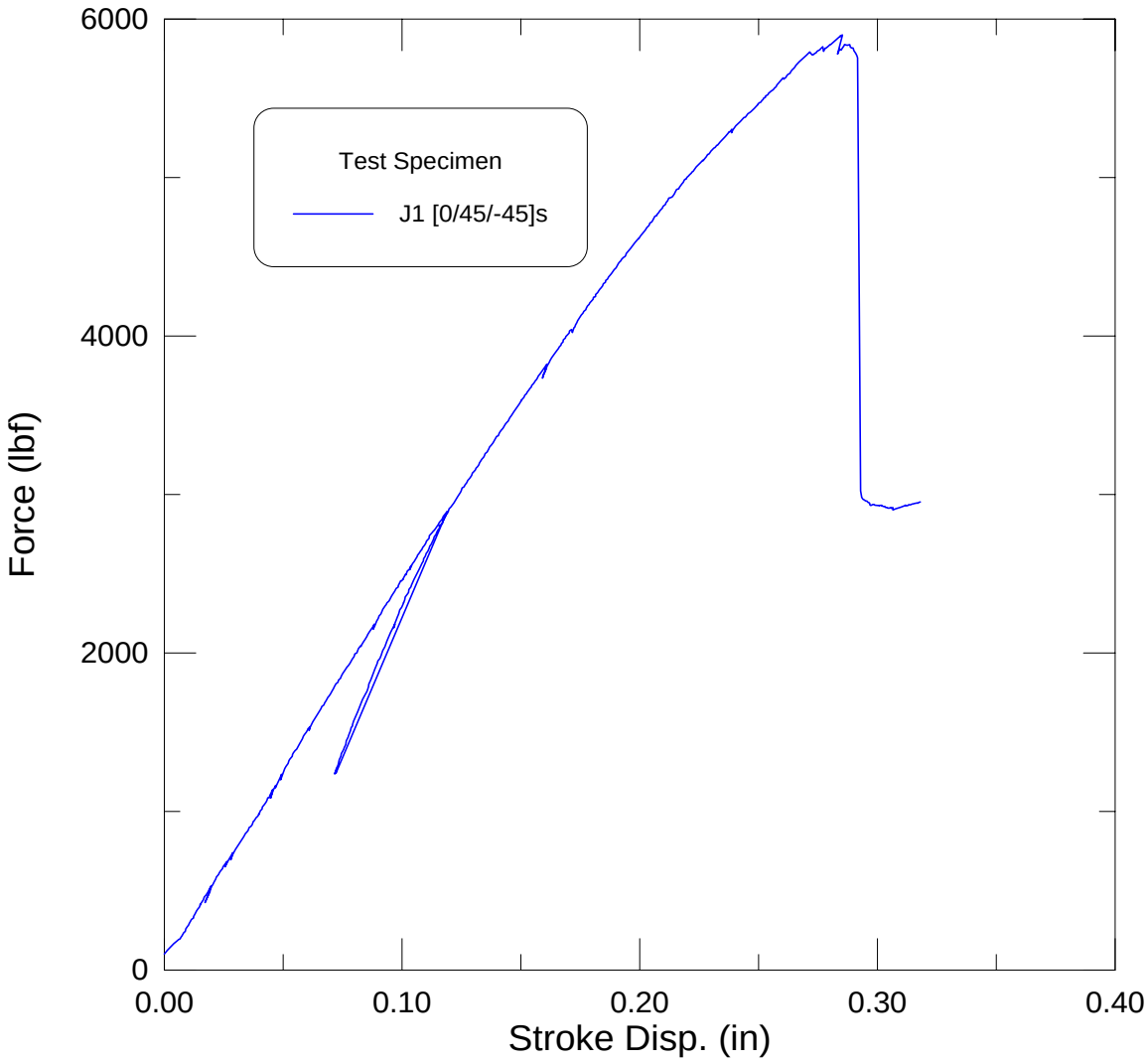
Test Specimen
J1 [0/45/-45]s
Force (lbf)
Stroke Disp. (in)
6000
4000
2000
0
0.00
0.10
0.20
0.30
0.40

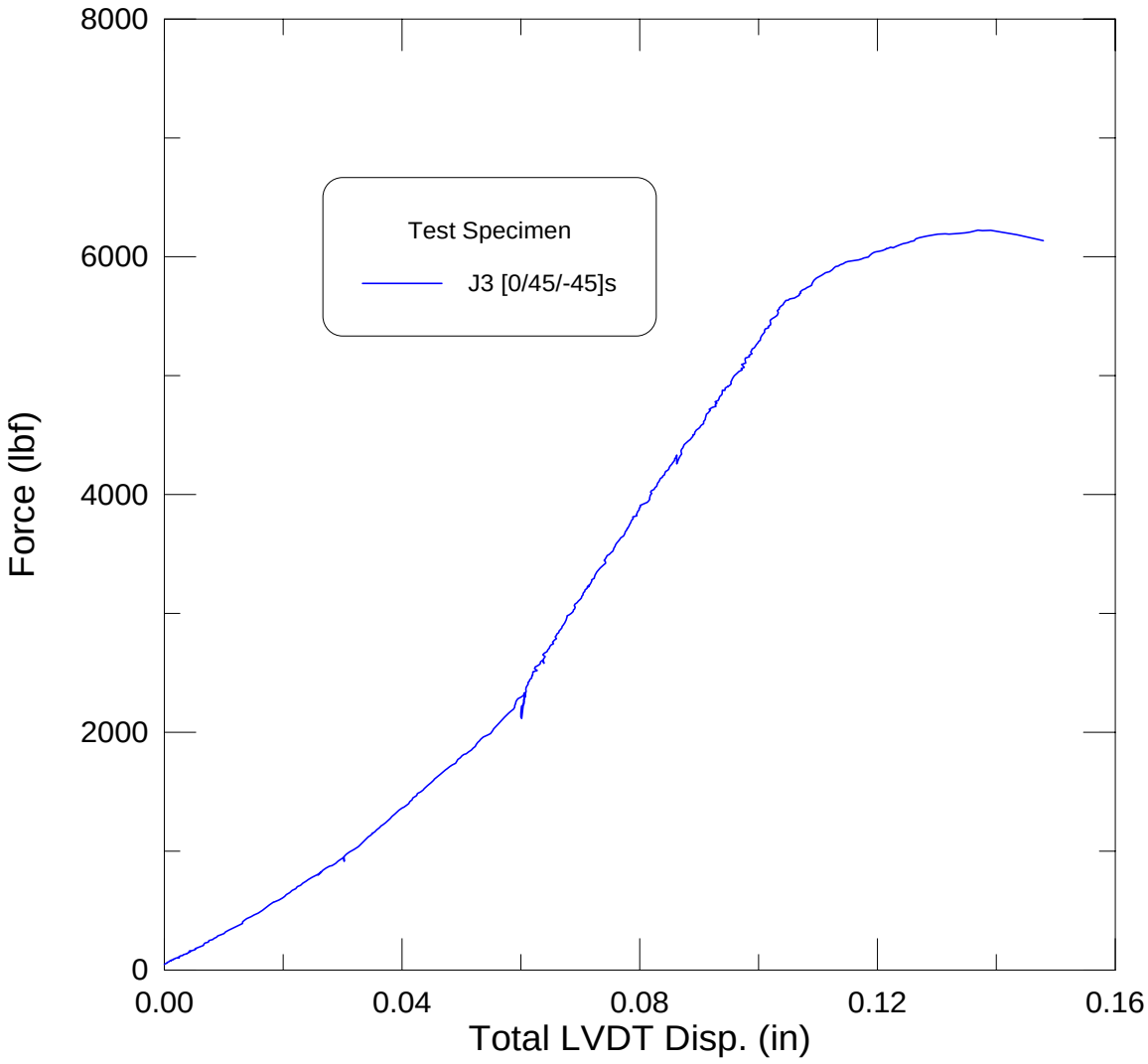
8000
6000
4000
2000
0
Force (lbf)
0.00
0.04
0.08
0.12
0.16
Total LVDT Disp. (in)
Test Specimen
J3 [0/45/-45]s

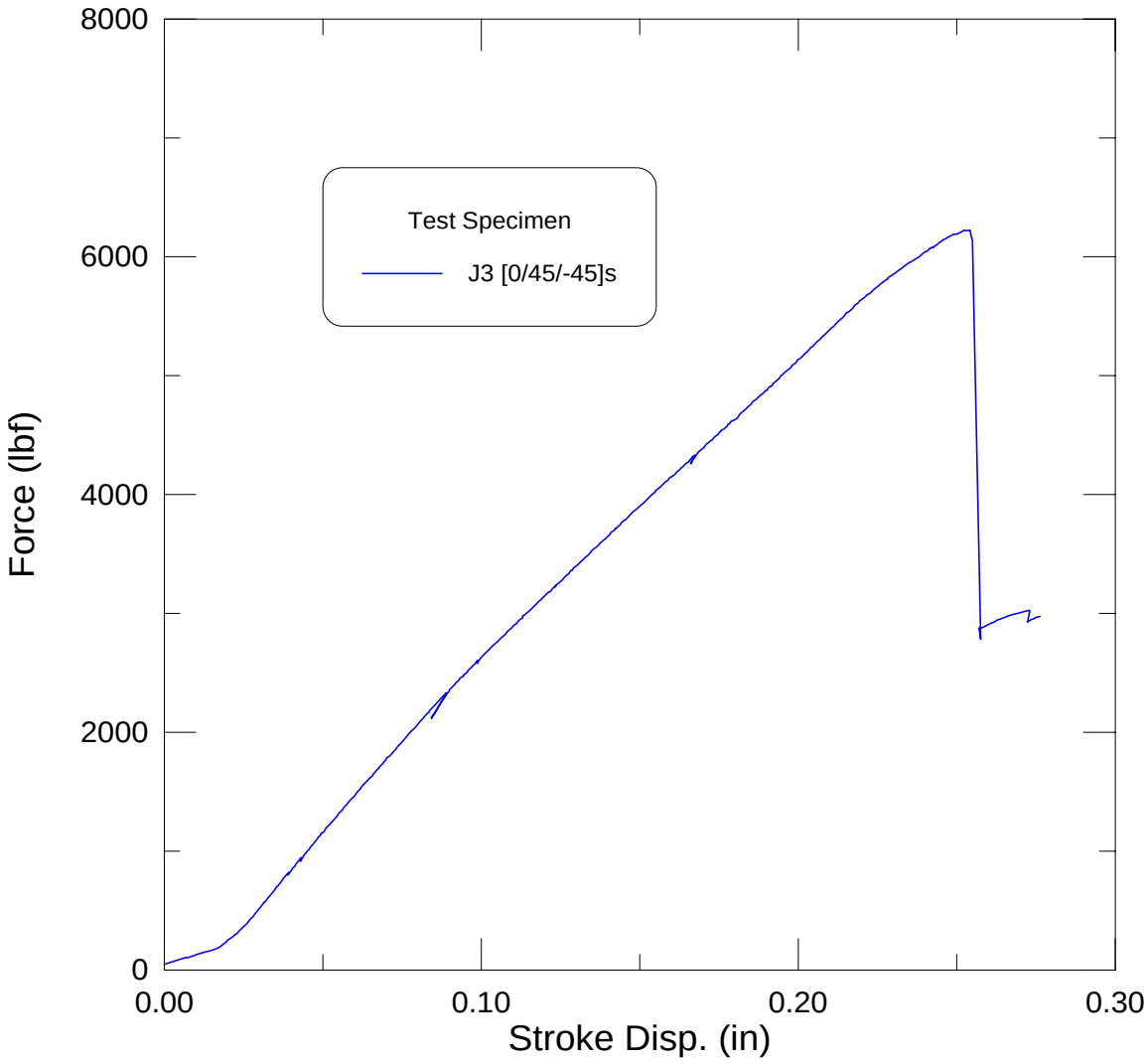
8000
6000
4000
2000
0
Force (lbf)
0.00
0.10
0.20
0.30
Stroke Disp. (in)
Test Specimen
J3 [0/45/-45]s

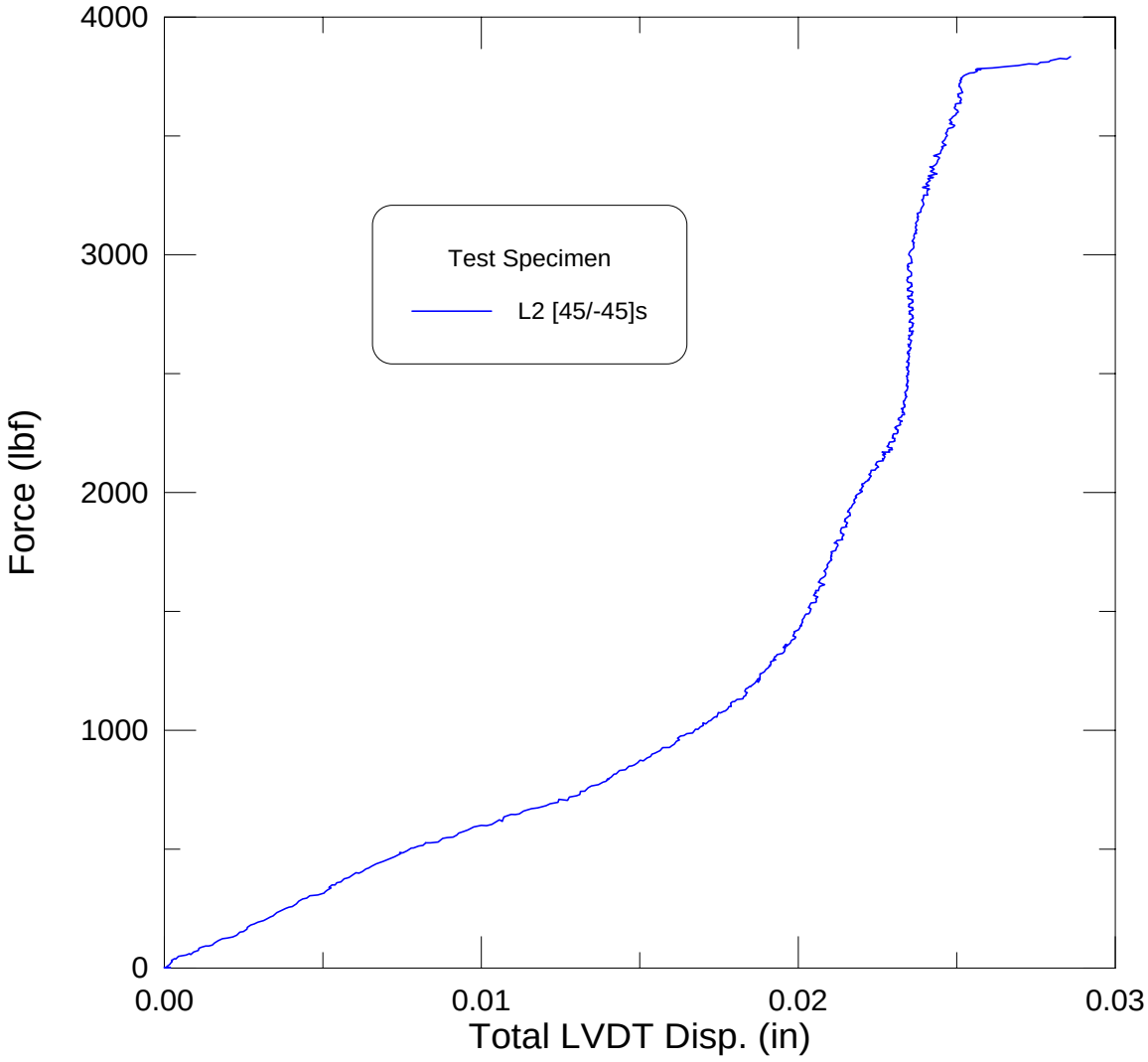
4000
3000
2000
1000
0
Force (lbf)
0.00
0.01
0.02
0.03
Total LVDT Disp. (in)
Test Specimen
L2 [45/-45]s

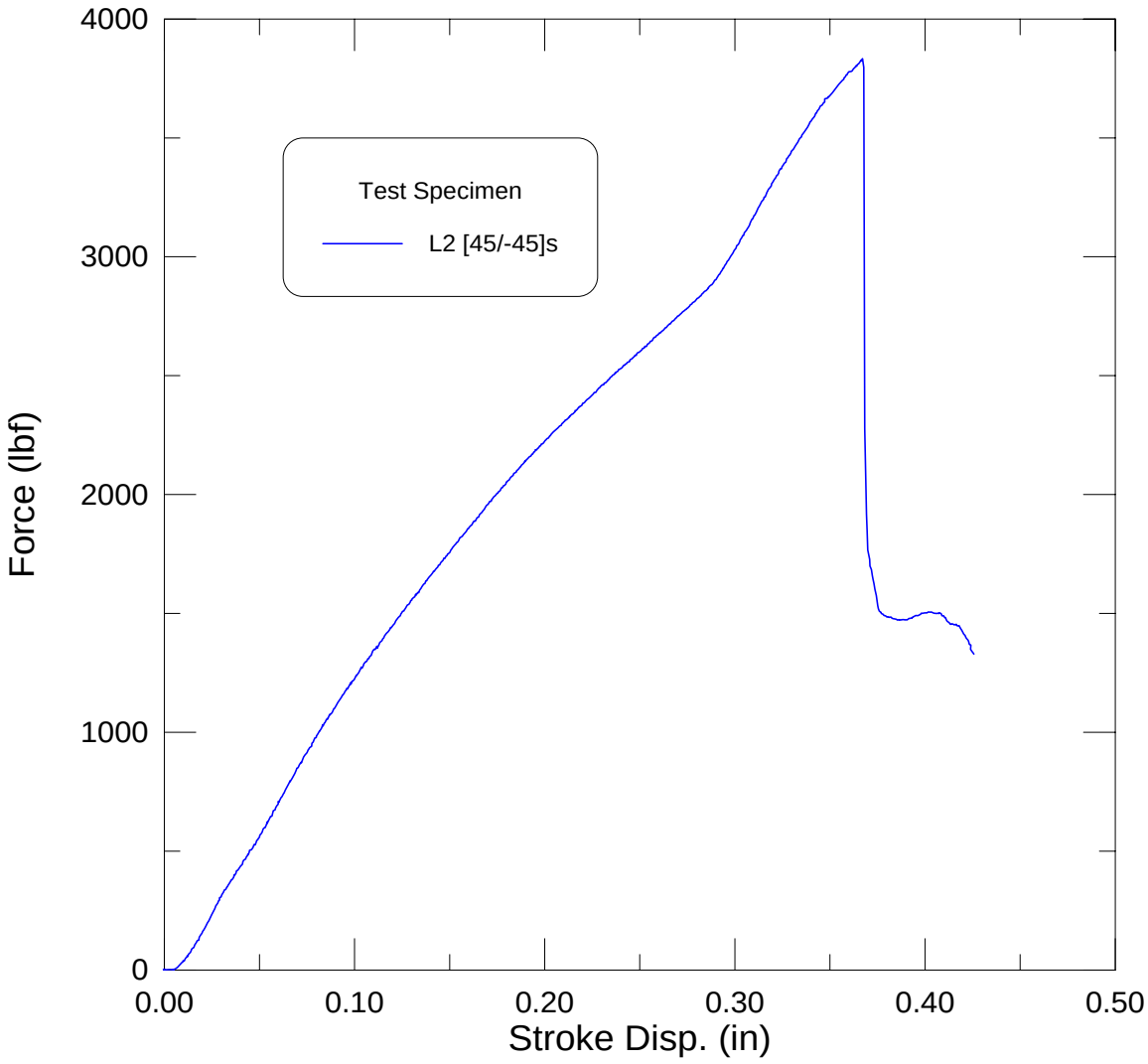
Test Specimen
L2 [45/-45]s
Force (lbf)
Stroke Disp. (in)
4000
3000
2000
1000
0
0.00
0.10
0.20
0.30
0.40
0.50

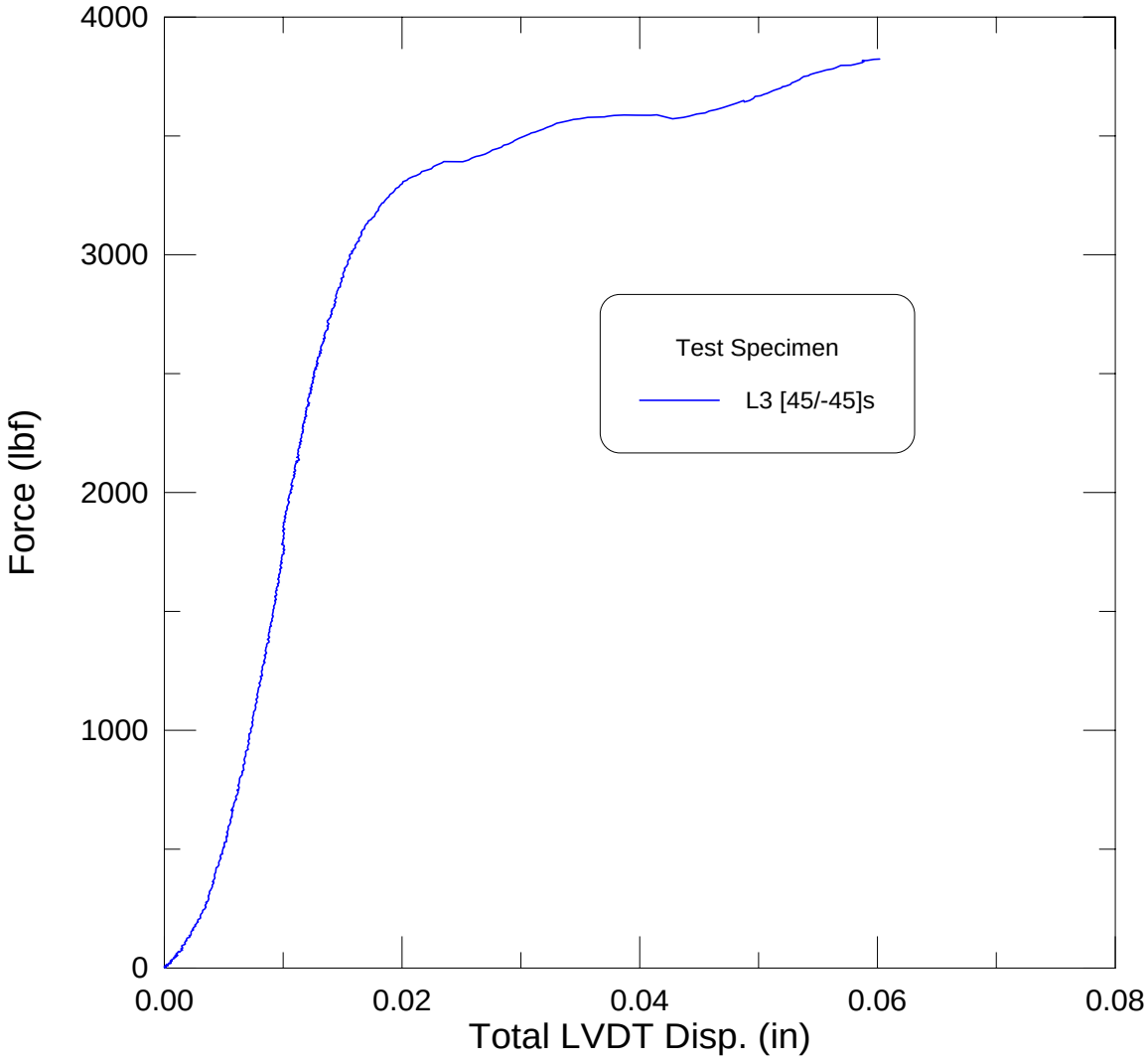
4000
3000
2000
1000
0
Force (lbf)
0.00
0.02
0.04
0.06
0.08
Total LVDT Disp. (in)
Test Specimen
L3 [45/-45]s

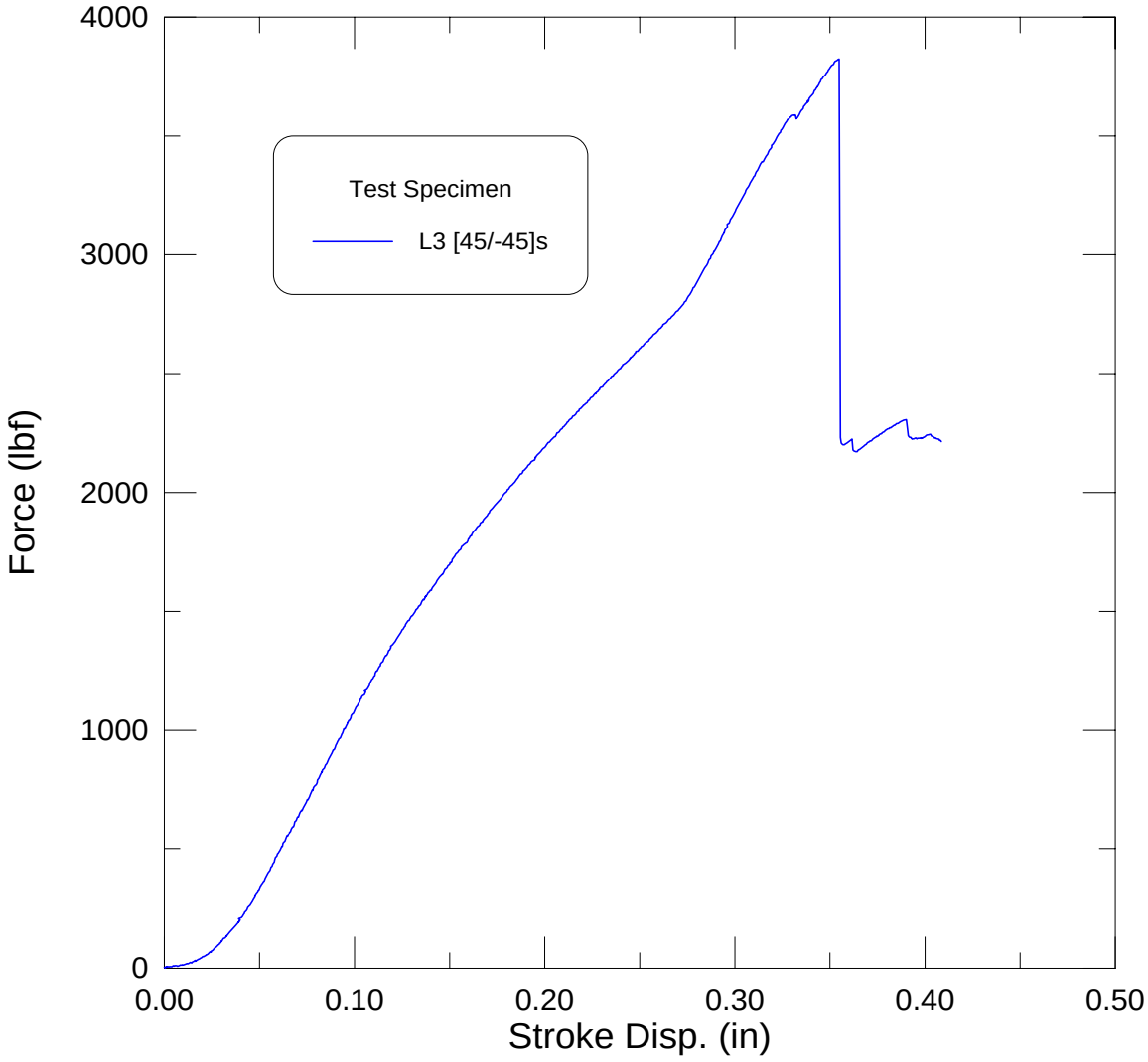
Test Specimen
L3 [45/-45]s
Force (lbf)
Stroke Disp. (in)
4000
3000
2000
1000
0
0.00
0.10
0.20
0.30
0.40
0.50

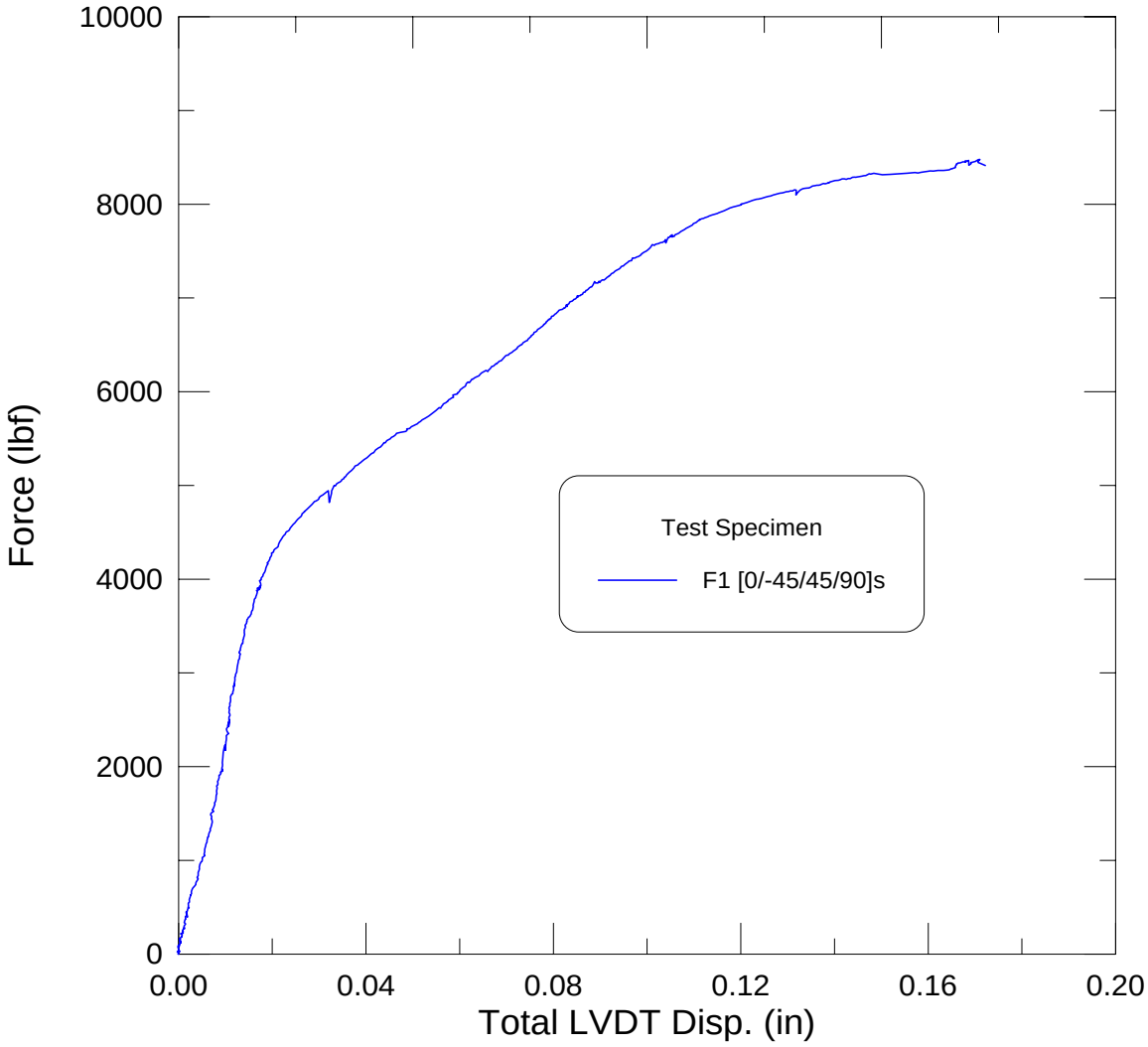
10000
8000
6000
4000
2000
0
Force (lbf)
0.00
0.04
0.08
0.12
0.16
0.20
Total LVDT Disp. (in)
Test Specimen
F1 [0/-45/45/90]s

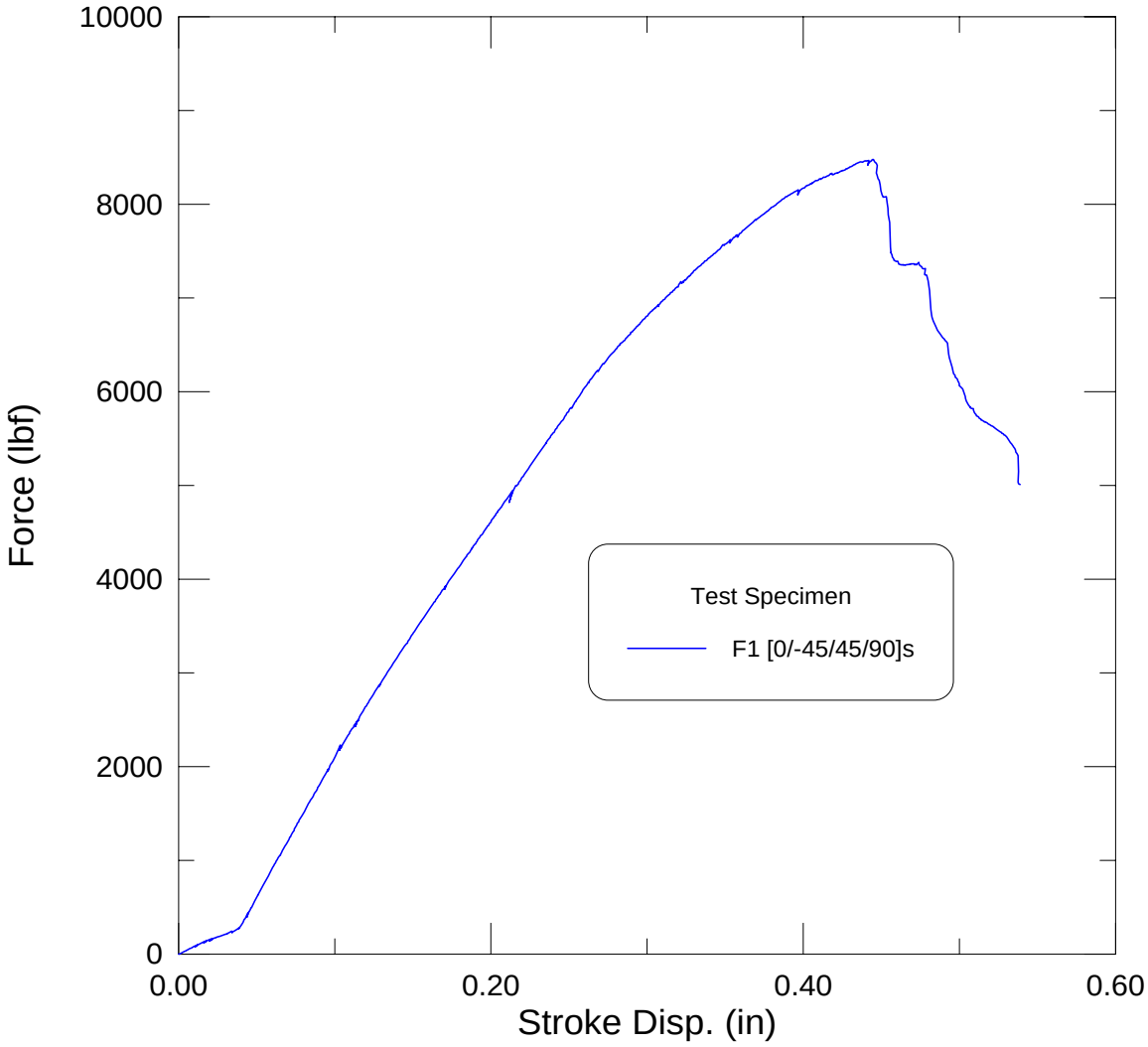
10000
8000
6000
4000
2000
0
Force (lbf)
0.00
0.20
0.40
0.60
Stroke Disp. (in)
Test Specimen
F1 [0/-45/45/90]s

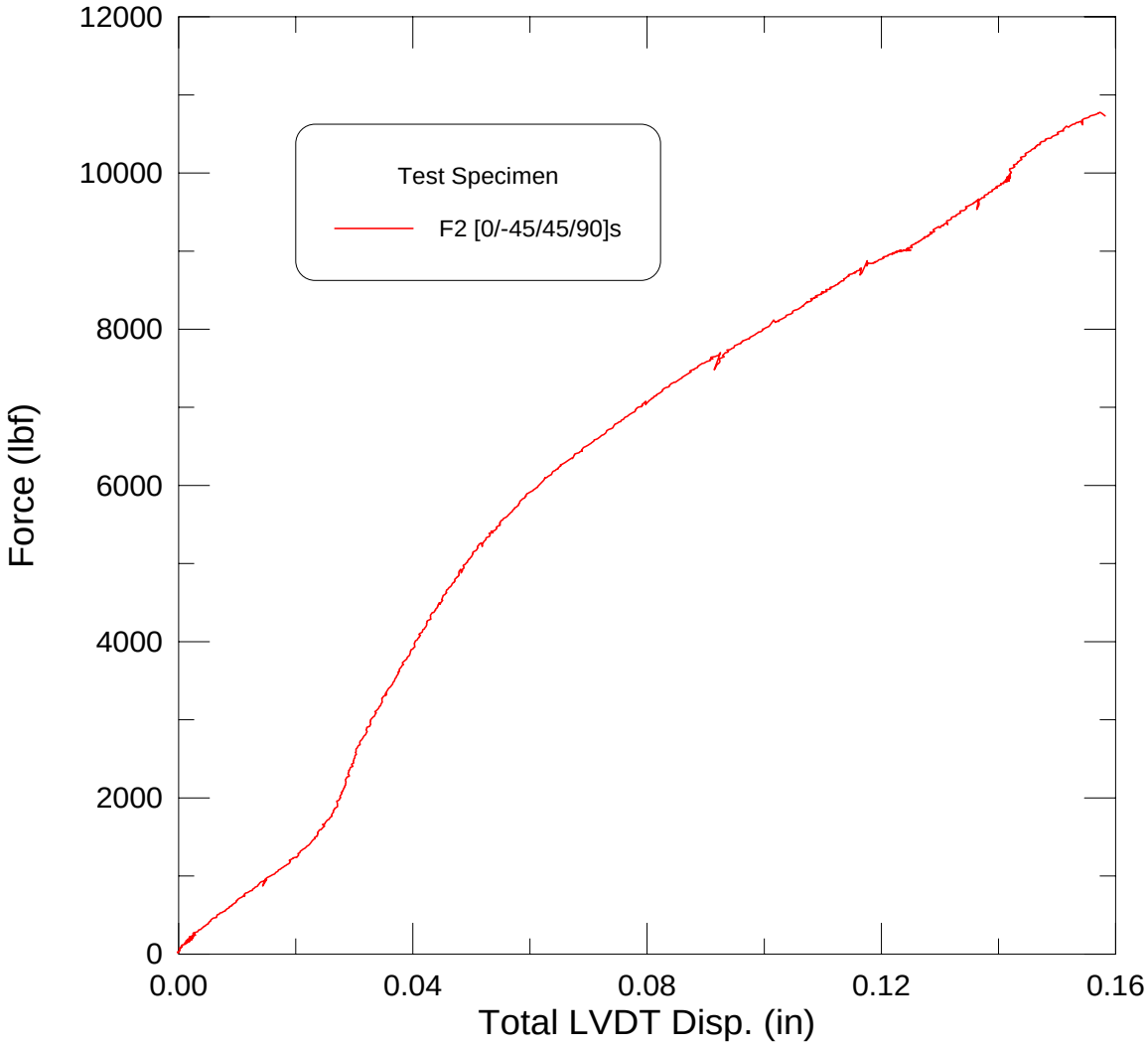
12000
10000
8000
6000
4000
2000
0
Force (lbf)
0.00
0.04
0.08
0.12
0.16
Total LVDT Disp. (in)
Test Specimen
F2 [0/-45/45/90]s

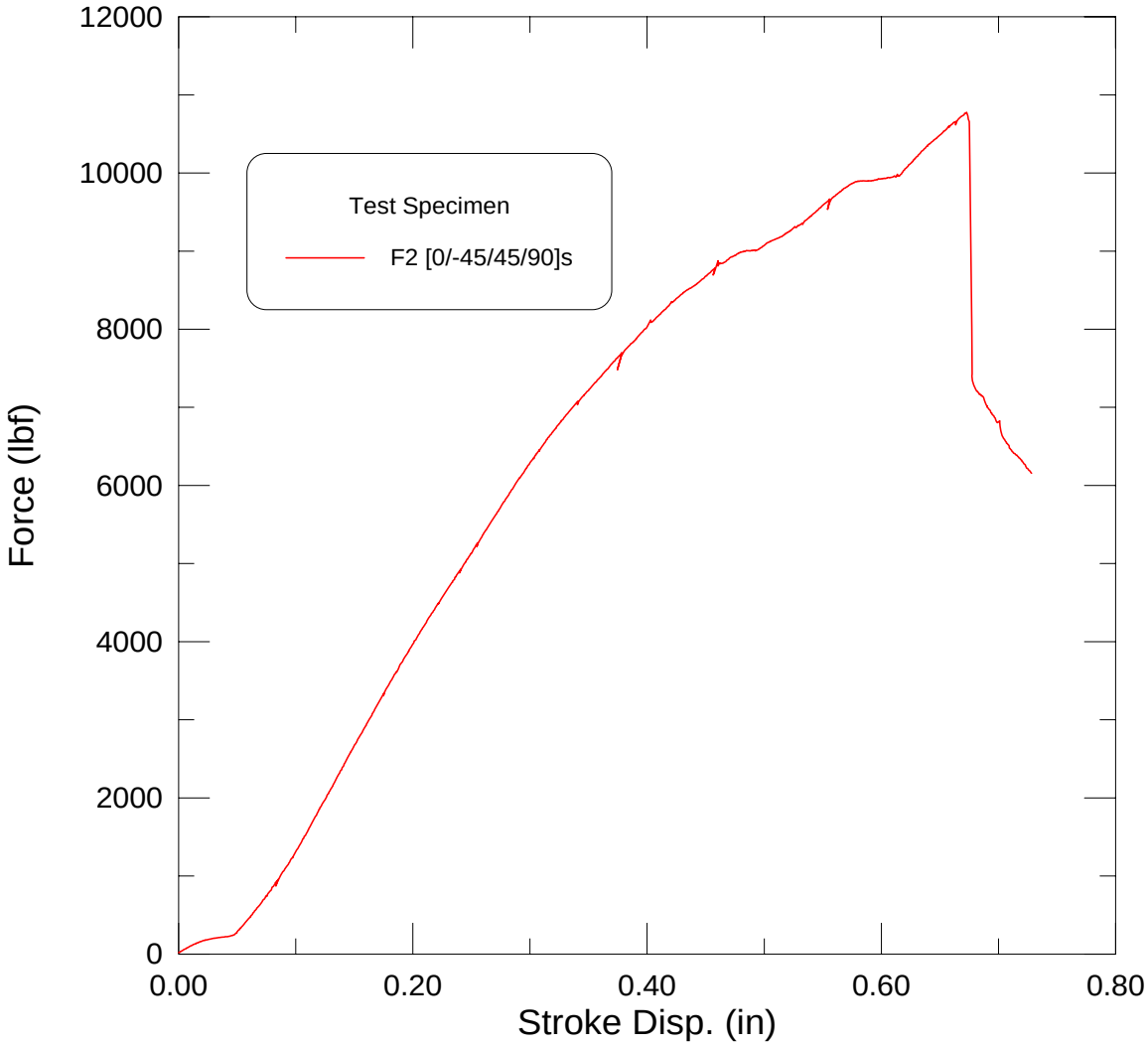
12000
10000
8000
6000
4000
2000
0
Force (lbf)
0.00
0.20
0.40
0.60
0.80
Stroke Disp. (in)
Test Specimen
F2 [0/-45/45/90]s

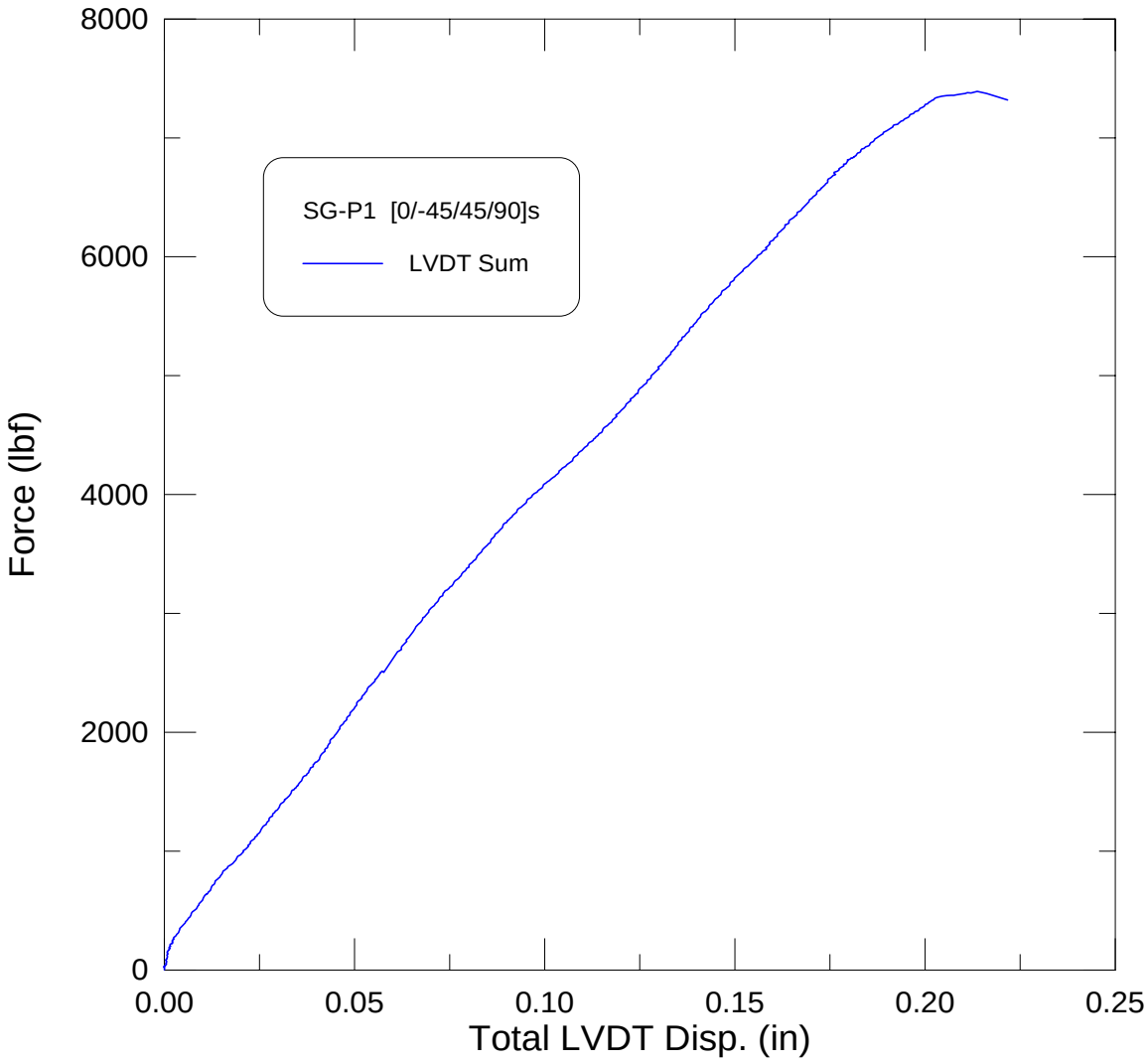
SG-P1 [0/-45/45/90]s
LVDT Sum
Force (lbf)
Total LVDT Disp. (in)
8000
6000
4000
2000
0
0.00
0.05
0.10
0.15
0.20
0.25

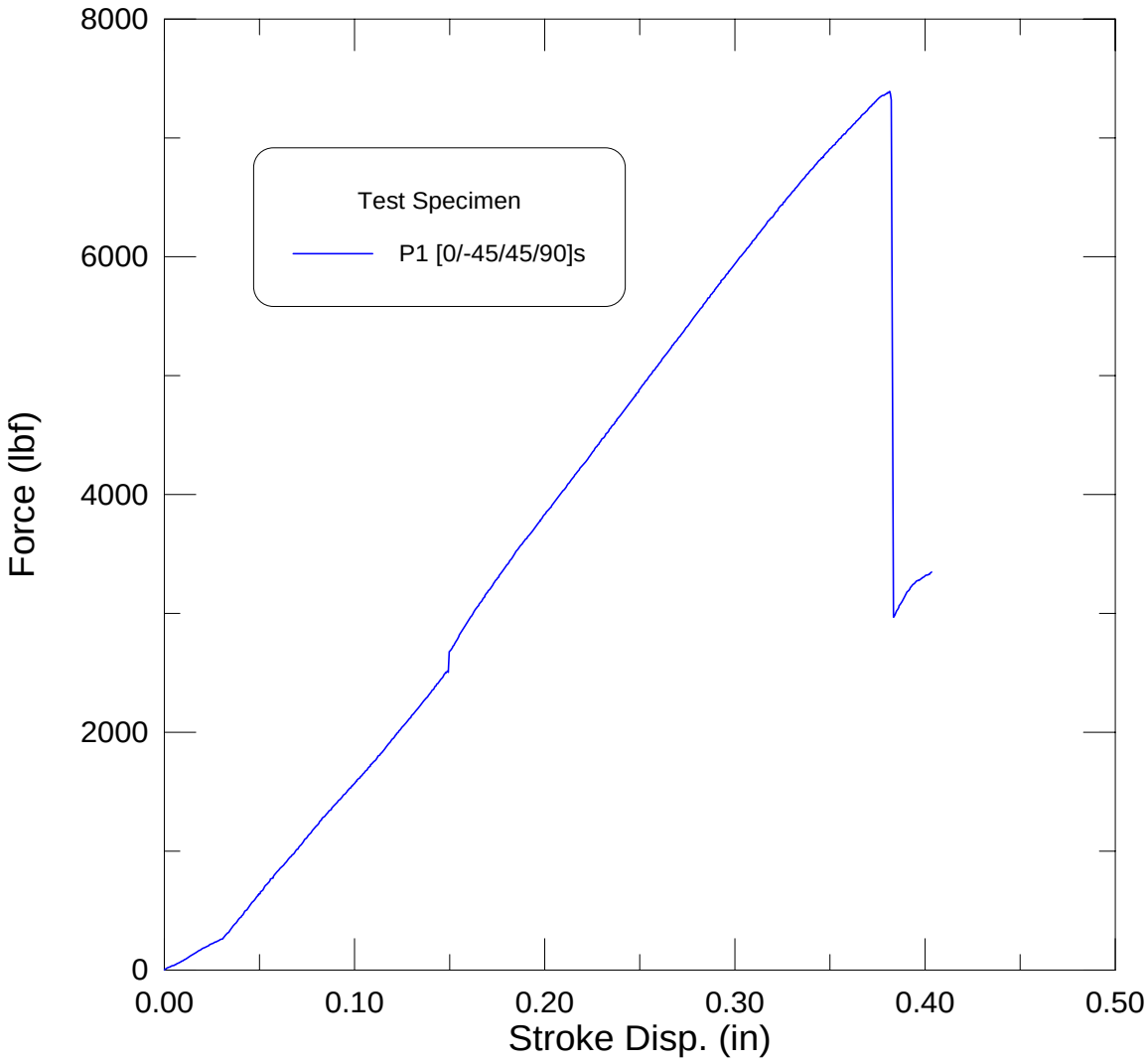
8000
6000
4000
2000
0
Force (lbf)
0.00
0.10
0.20
0.30
0.40
0.50
Stroke Disp. (in)
Test Specimen
P1 [0/-45/45/90]s

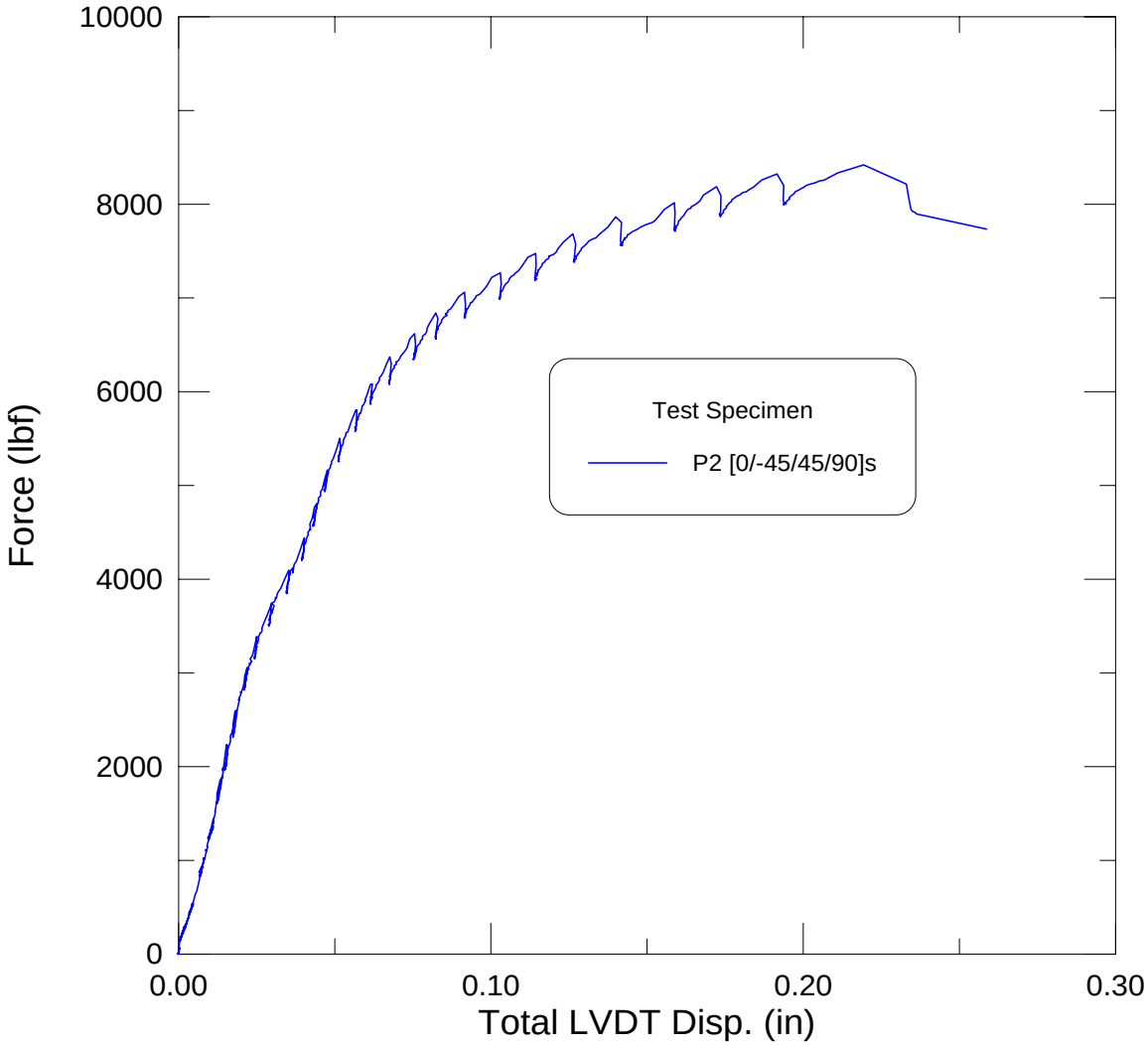
10000
8000
6000
4000
2000
0
Force (lbf)
0.00
0.10
0.20
0.30
Total LVDT Disp. (in)
Test Specimen
P2 [0/-45/45/90]s

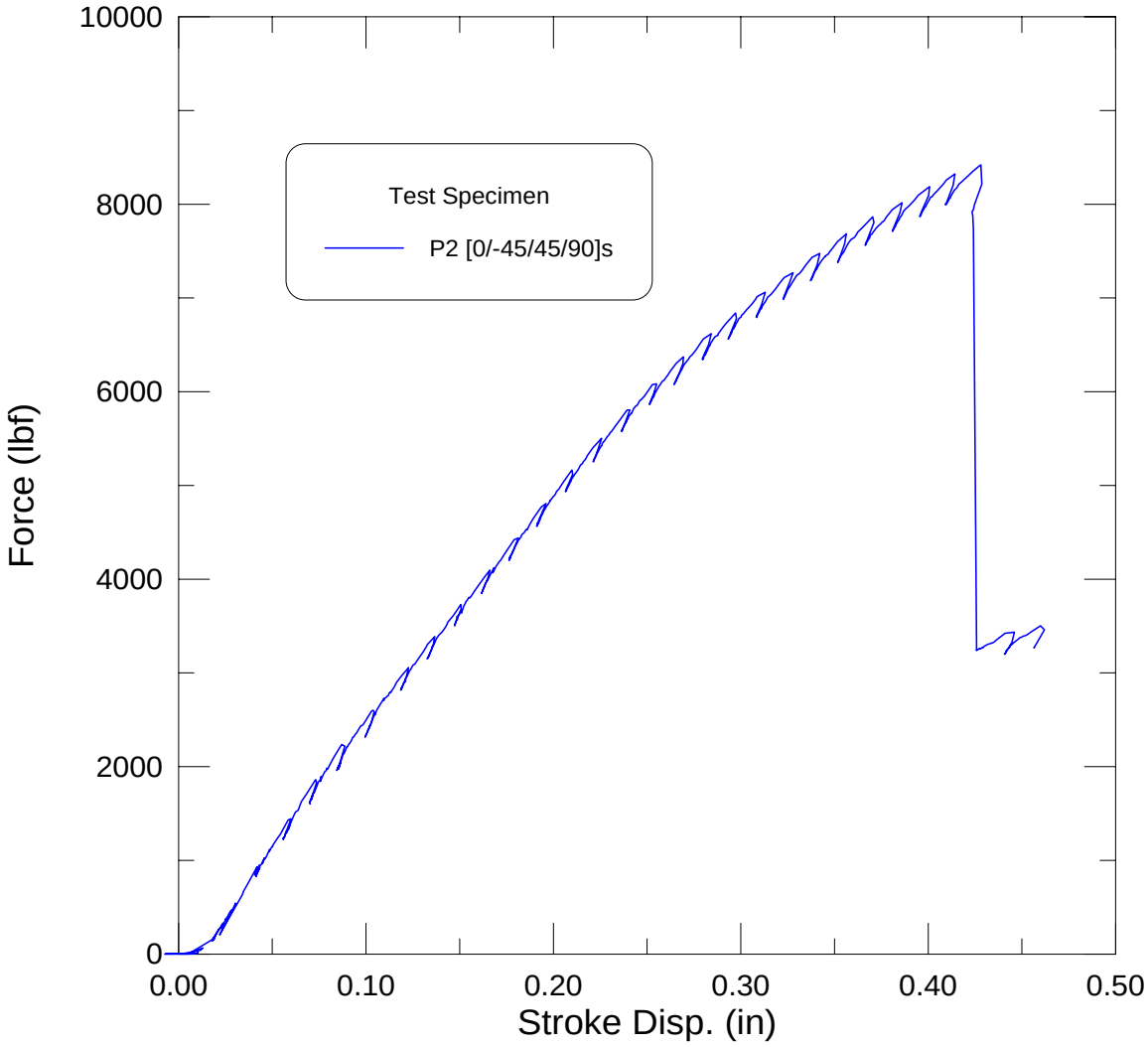
Test Specimen
P2 [0/-45/45/90]s
Force (lbf)
Stroke Disp. (in)
10000
8000
6000
4000
2000
0
0.00
0.10
0.20
0.30
0.40
0.50

APPENDIX C

Digital pictures

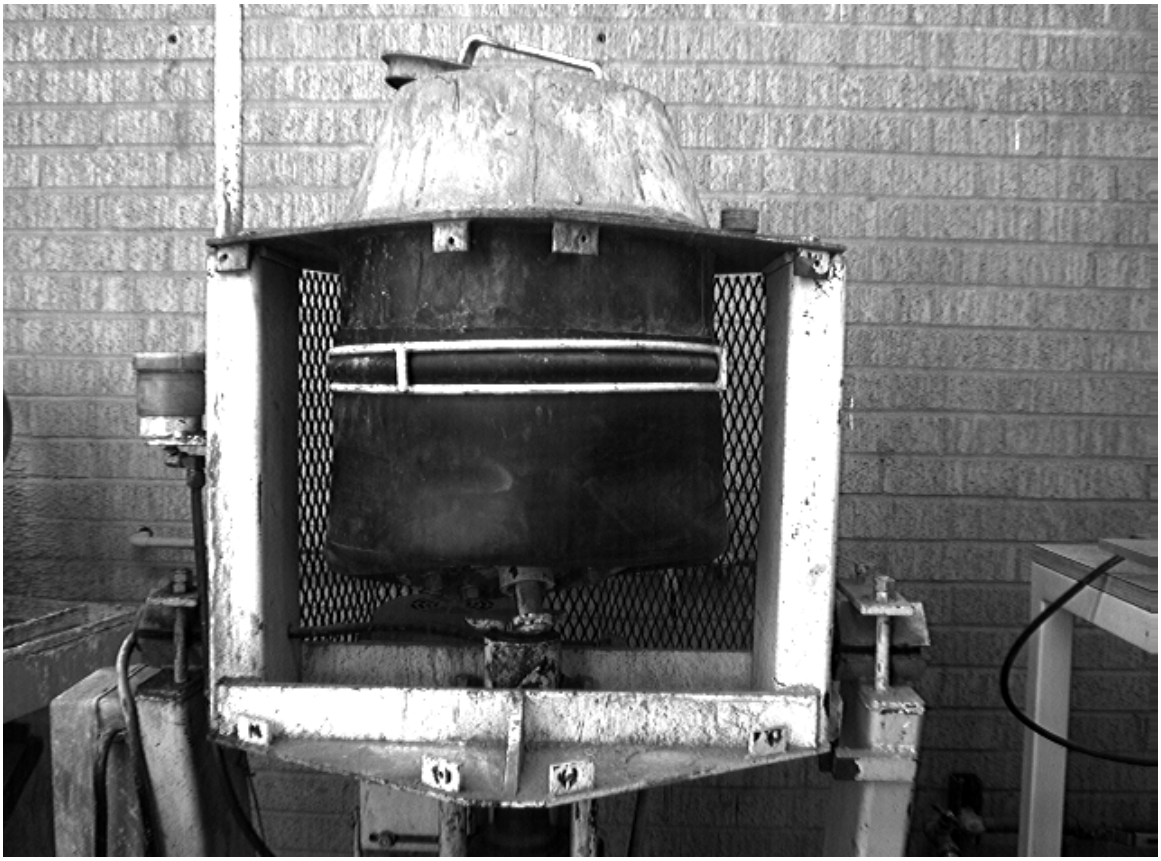

Picture 1 Omnie mixer.

Picture 2 Wobble plate inside Omni mixer.

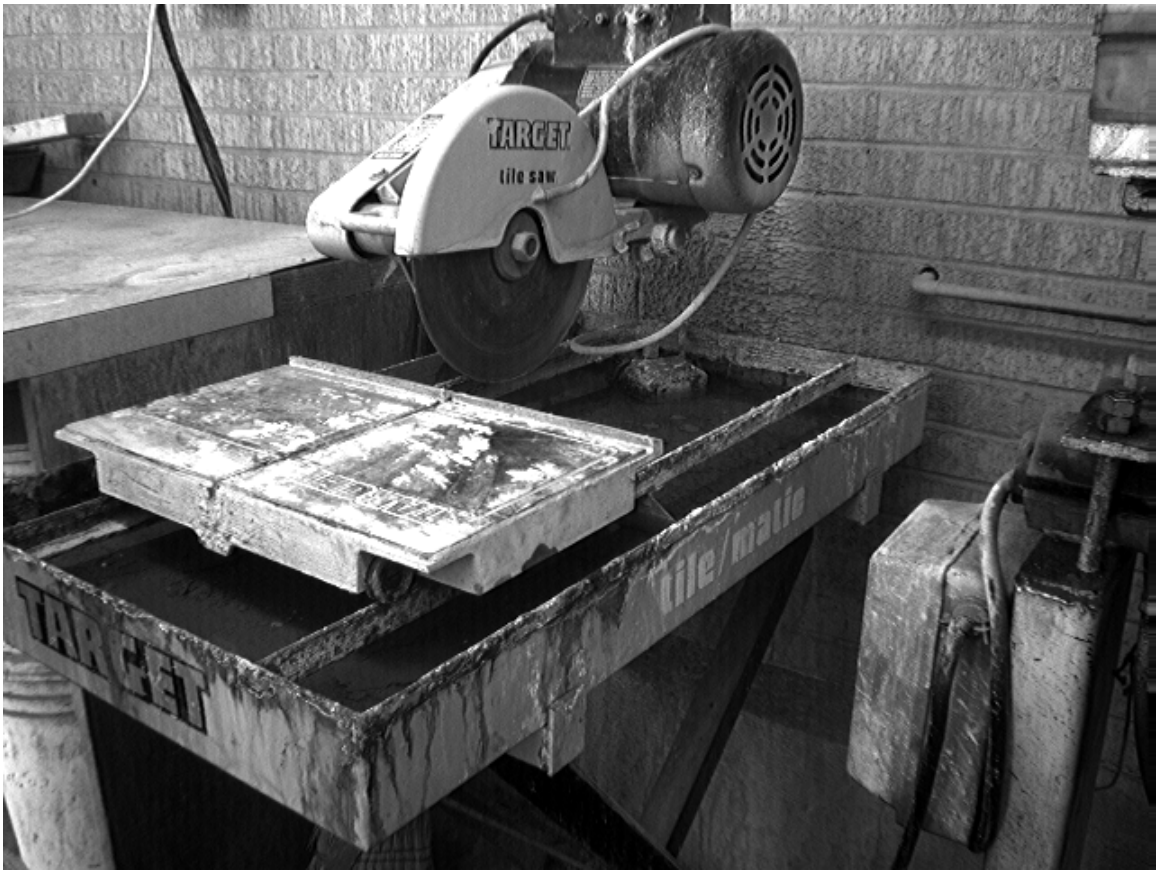

Picture 3 Tile saw.

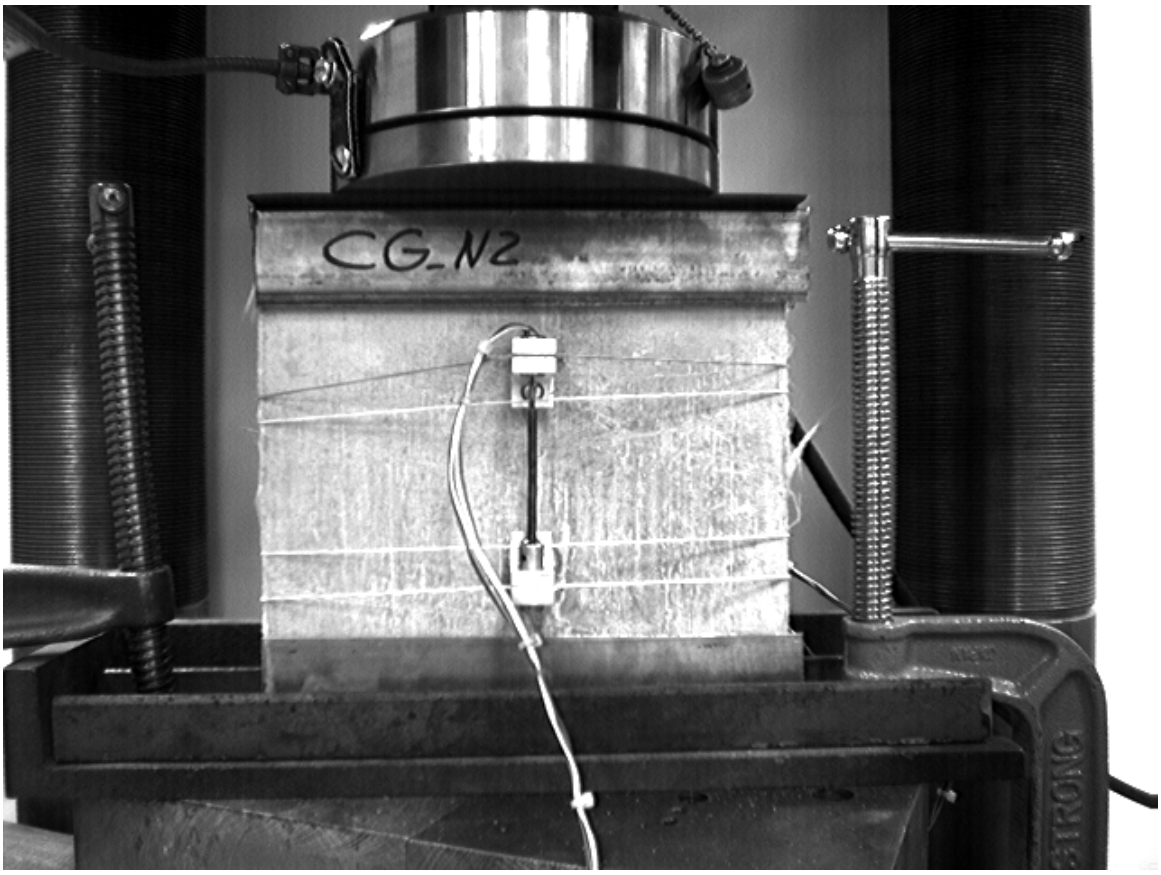

Picture 4 Compression test setup.

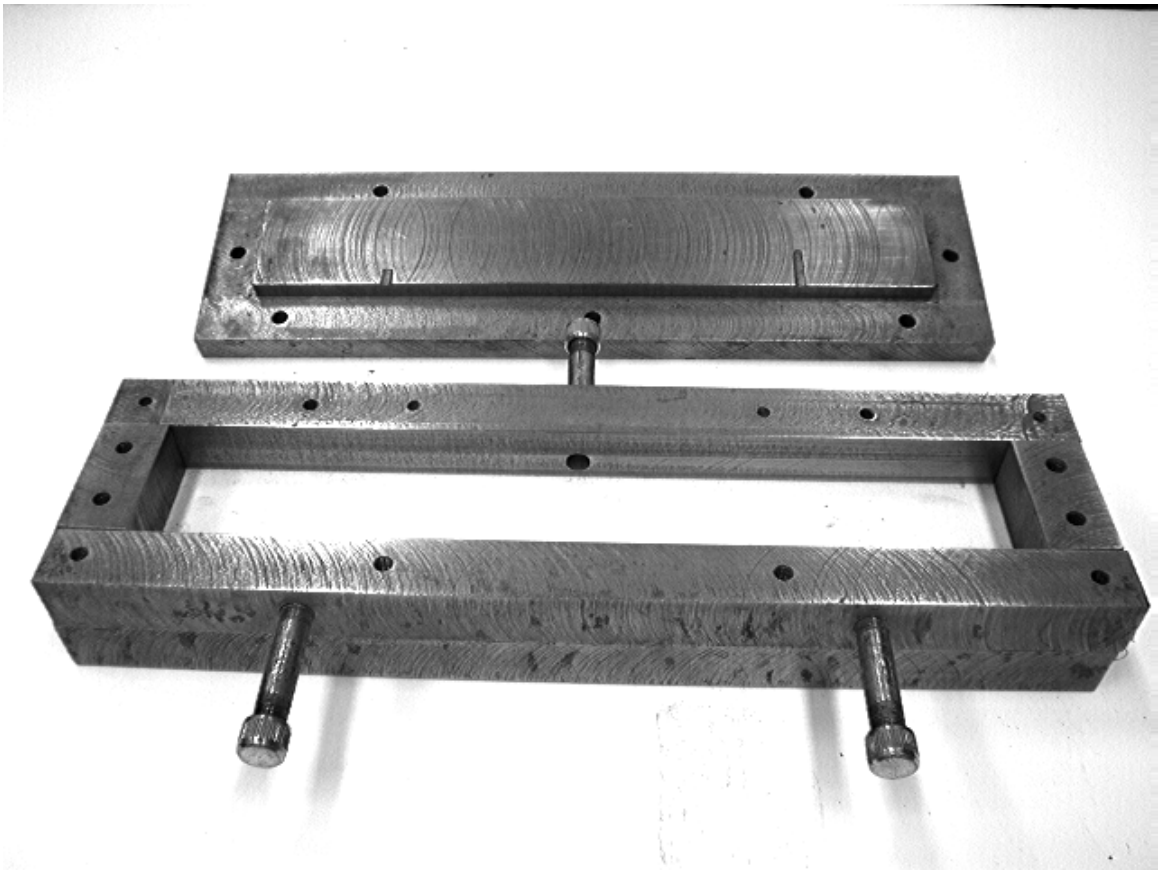

Picture 5 Compression molding.

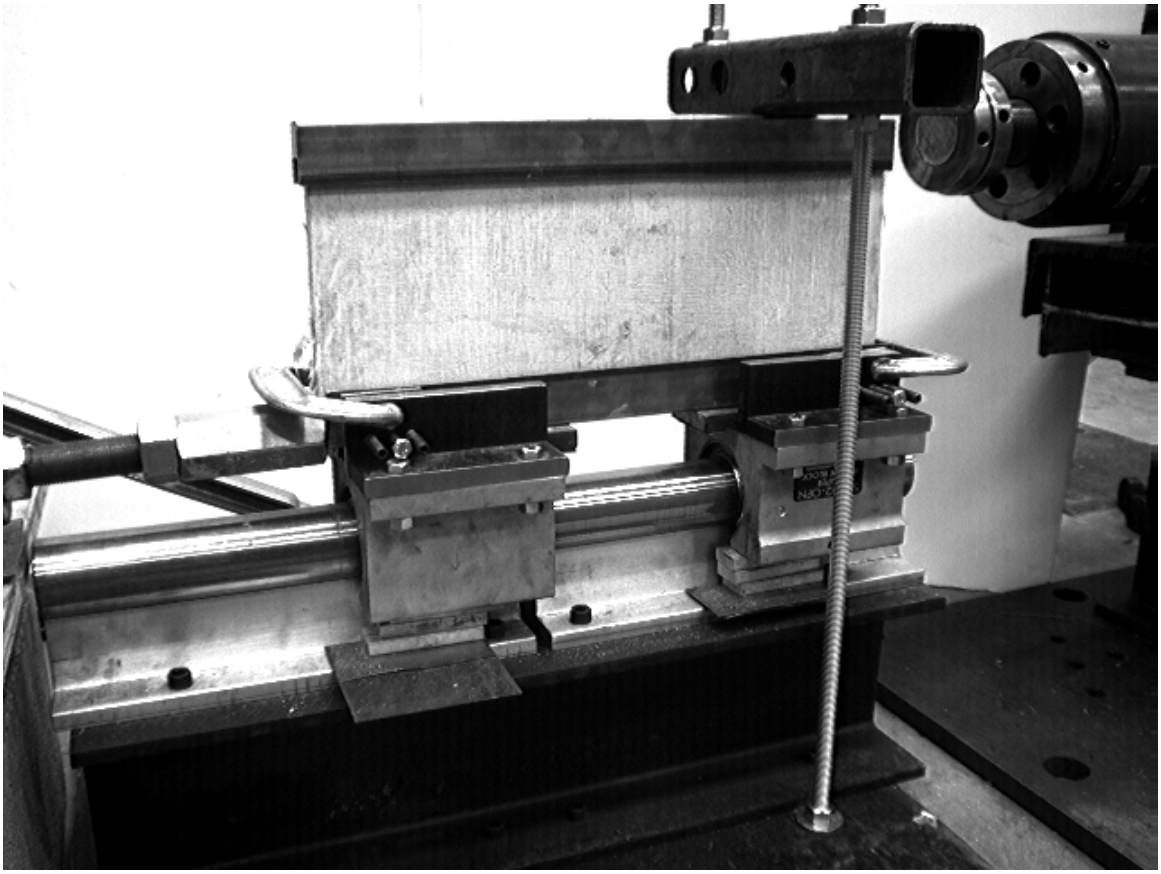

Picture 6 Shear test apparatus.

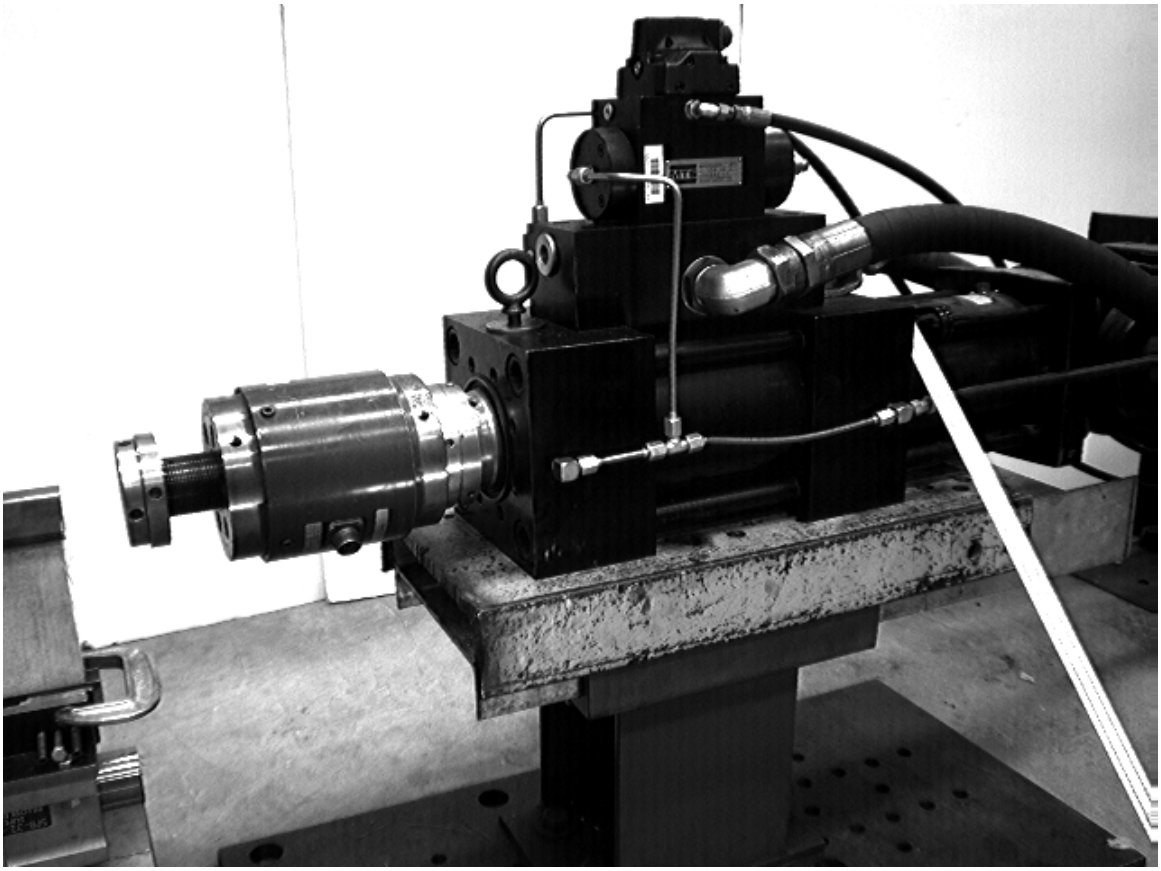

Picture 7 110 kip hydraulic ram used for shear tests.

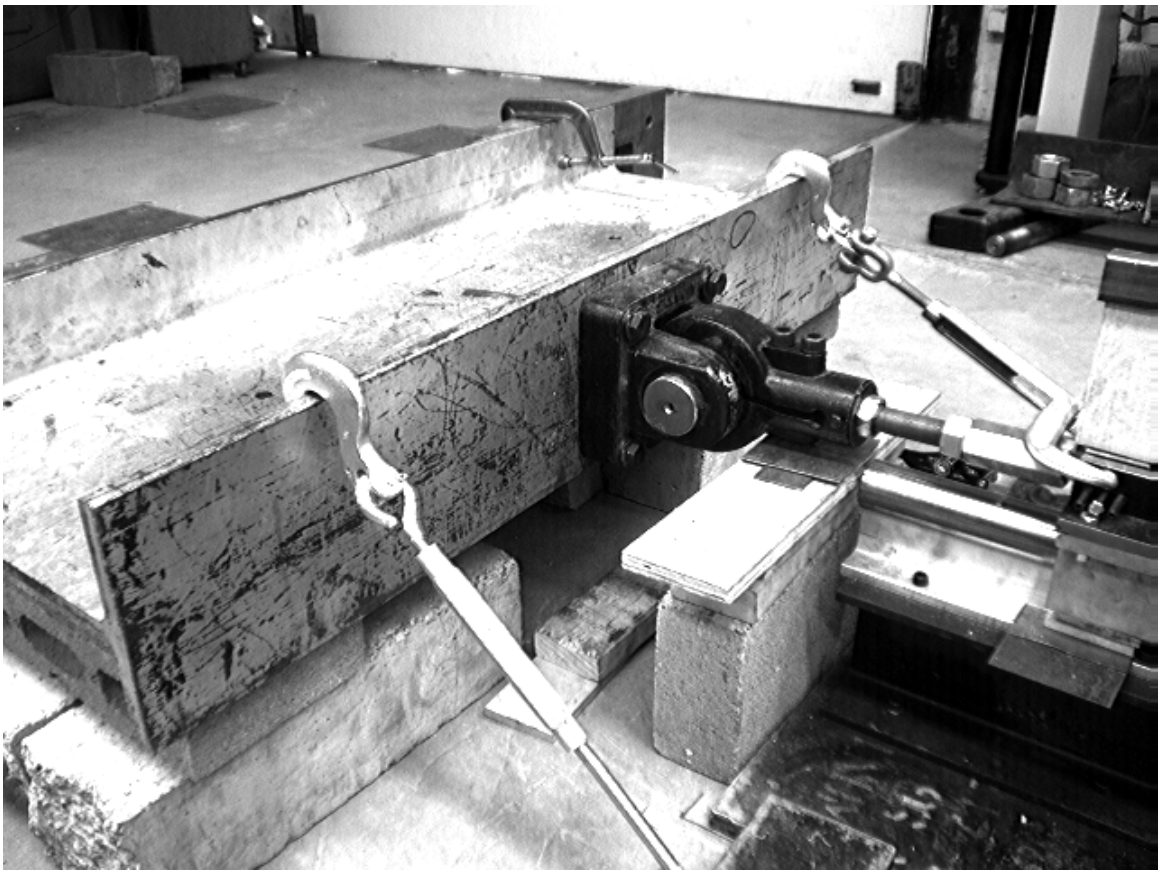

Picture 8 Resistance for shear test.

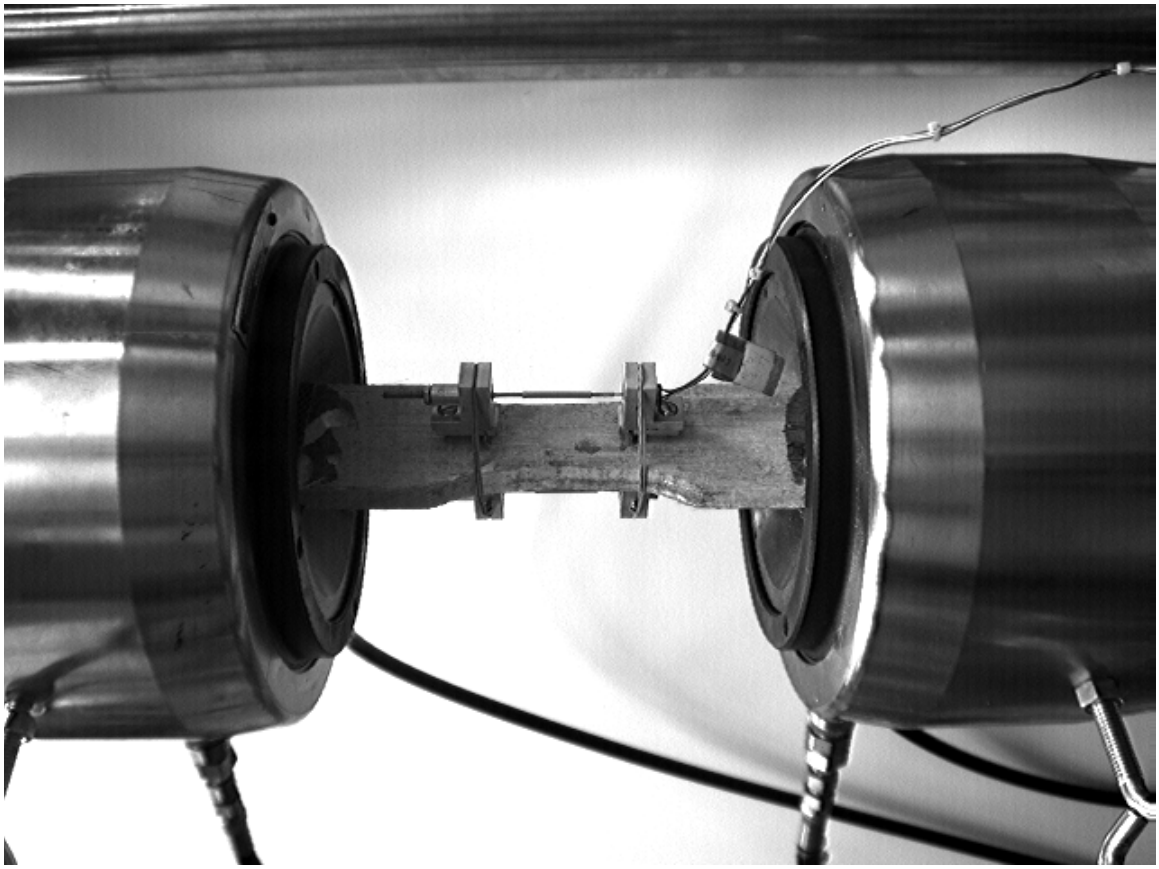

Picture 9 Hydraulic grips for tension test.